MULTICELLULAR REGULATION OF THE PANCREATIC ISLET IN DIABETES

by

NICHOLAS HUGH FRANCIS FINE

A thesis submitted to the University of Birmingham for the degree of

DOCTOR OF PHILOSOPHY

Institute of Metabolism and Systems Research

College of Medical and Dental Sciences

University of Birmingham

April 2022

ABSTRACT

Since the discovery of insulin-secreting beta cells and their role in glucose homeostasis, there has been an incredible focus on these cells and how they interact with other cells within the pancreatic islet to respond to increased blood glucose levels. This regulation requires both individual effort on the part of beta cells, as well as cooperative communication across the population. Until recently, all beta cells were considered equal, possessing a single programme of cell processes that enable them to function as required. In reality, there is a startling degree of variation within the beta cell population, and this variation, or heterogeneity, is required to maintain normoglycemia. For instance, some niche subpopulations of beta cells coordinate Ca^{2+} fluxes across the islet via gap junctions, while others possess the capacity to proliferate to restore beta cell numbers after an assault by immune or metabolic factors. Here, we aim to show that heterogeneity is vital for pancreatic function. We use a variety of cell and molecular techniques to interrogate functional changes in the islet after perturbating the islet's normal heterogeneity by overexpressing beta cell identity genes or using exogenous steroids to alter gene expression.

ACKNOWLEDGMENTS

Thanks to Professor David Hodson for being a mentor and ever-present looming threat, without which I knew I would never be able to complete this PhD.

All the members of the Islet Biology Group that have made my time in the lab bearable. As well as those members of the IMSR that helped me both scientifically and socially.

Professor Gareth Lavery for providing the HSD11 knockout mouse line and being my second supervisor.

Dr Ildem Akerman of her assistance with all aspects of the RNA sequencing, including all the analysis.

All electrophysiology was kindly performed by Dr Nicholas Vierra and Dr David Jacobson from the University of California, Davis.

I am grateful to the European Consortium for Islet Transplantation (ECIT), which was supported by JDRF award 31-2008-416 (ECIT Islet for Basic Research program). This project was supported by a Diabetes UK R.D. Lawrence (12/0004431) Fellowship, a Wellcome Trust Institutional Support Award, and MRC (MR/N00275X/1 and MR/S025618/1) and Diabetes UK (17/0005681) Project Grants. This project has received funding from the European Research Council (ERC) under the European Union's Horizon 2020 research and innovation program (Starting Grant 715884).

My parents for forbidding me from pursuing a career as an architect, probably making me much happier and poorer.

Finally, I would like to thank Becky for always believing in me, even when I didn't believe in myself, and for not letting me fall at the final hurdle.

TABLE OF CONTENTS

LIST OF FIGURES

LIST OF TABLES

LIST OF ABBREVIATIONS

11-DHC	11-dihydrocorticosterone
Acetyl-CoA	Acetyl-coenzyme A
ACTH	Adrenocorticotrophic hormone
ADP	Adenosine diphosphate
AKT	Protein kinase B
ARX	Aristaless Related Homeobox
ATP	Adenosine triphosphate
AUC	Area under the curve
BSA	Bovine serum albumin
cAMP	Cyclic adenosine monophosphate
CBG	Cortisol binding globulin
cDNA	Complementary deoxyribonucleic acid
Cort	Corticosterone
CO_2	Carbon dioxide
CRH	Corticotrophin releasing hormone
DHP	Dihydropyridines
Dox	Doxycycline
EDTA	Ethylenediaminetetraacetic acid
ER	Endoplasmic reticulum
FAD	Flavin adenine dinucleotide
FADH	Flavin adenine dinucleotide (reduced)
FBS	Foetal bovine serum
G	Glucose
G6DPH	Glucose-6-phosphate dehydrogenase

G6P	Glucose-6-phosphate
GATA	Globin transcription factor 1
GC	Glucocorticoid
GCK	Glucokinase
GFP	Green fluorescent protein
GIP	Glucose-dependent insulinotropic polypeptide
GLP-1	Glucagon-like peptide 1
GLP-1R	GLP-1 receptor
GLUT	Glucose transporter
GPCR	G-protein coupled receptor
GR	Glucocorticoid receptor
GSIS	Glucose-stimulated insulin secretion
HCl	Hydrochloric acid
HPA	Hypothalamic-pituitary-adrenal
HSD11B1	11β-hydroxysteroid dehydrogenase type 1
HSD11B2	11β-hydroxysteroid dehydrogenase type 2
HTRF	Homogenous time resolved fluorescence
Hz	Hertz
IL1-β	Interleukin 1 beta
IL-6	Interleukin 6
IP	Inter-peritoneal
IP3	Inositol 1,4,5-trisphosphate
IPGTT	Inter-peritoneal glucose tolerance test
IR	Insulin receptor
IRS	Insulin receptor substrate

K_{ATP}	ATP-sensitive potassium
MAFB	MAF BZIP transcription factor B
MCT1	Monocarboxylate transporter 1
mg	Milligram
mL	Millilitre
mM	Millimolar
mmol	Millimole
mRNA	Messenger ribonucleic acid
ms	Millisecond
N	Normality
NAD	Nicotinamide adenine dinucleotide
NADH	Nicotinamide adenine dinucleotide (reduced)
NADP	Nicotinamide adenine dinucleotide phosphate
NADPH	Nicotinamide adenine dinucleotide phosphate (reduced)
NGN3	Neurogenin3
NKX6.1	Nk6 homeobox 1
nm	Nanometre
OGTT	Oral-glucose tolerance test
PBS	Phosphate buffered saline
PDX1	Pancreatic and duodenal homeobox 1
PN	Peripheral neuropathy
PFA	Paraformaldehyde
PKA	Protein kinase A
PKC	Protein kinase C
PP	Pancreatic polypeptide cell

PPY	Pancreatic polypeptide
Pred	Prednisolone
RIN	RNA integrity number
RIP7rtTA	Tetracycline trans-activator under the control of the *Ins2* promoter
RMPI	Roswell Park memorial institute 1640 medium
RNA	Ribonucleic acid
RNA-seq	RNA sequencing
rpm	Revolutions per minute
RT-qPCR	Reverse transcription quantitative PCR
SD	Standard deviation
SEM	Standard error of the mean
SSTR	Somatostatin receptor
SUR	Sulphonylurea receptor
T1D	Type 1 diabetes
T2D	Type 2 diabetes
U	Units
UCN3	Urocortin-3
VDCC	Voltage-dependent Ca^{2+} channel
w/v	Weigh per volume
µg	Microgram
µL	Microlitre
µm	Micrometre
µM	Micromolar
Ω	Ohms

1 CHAPTER ONE – INTRODUCTION

Diabetes mellitus is a disease which affects millions of people worldwide and occurs when the body is unable to reduce blood glucose levels through the appropriate production of insulin from pancreatic beta cells. Presented in this chapter is an overview of the processes that maintain blood glucose homeostasis under normal conditions, starting with the development of beta cell, production and secretion of insulin, and how glucose sensing occurs. It then goes on to describe how these processes go wrong in the disease state, and the effects of diabetes, and its comorbidities, on health and the global economy, thus highlighting its importance as a field of research. Additionally, it will introduce the role that glucocorticoids play in glucose metabolism and diabetes, and how the heterogenous nature of pancreatic beta cells is important for their function as both of these aspects of beta cell biology are central to the experimental chapters of this thesis.

1.1 Overview of pancreatic islets and their architecture

1.1.1 The pancreas

The organ responsible for the regulation of blood glucose is the pancreas. The pancreas is a complex multifunctional organ and has exocrine acinar cells which secrete enzymes into the digestive system, and hormone-secreting endocrine cells arranged in discrete areas known as the islets of Langerhans (Figure 1-1).

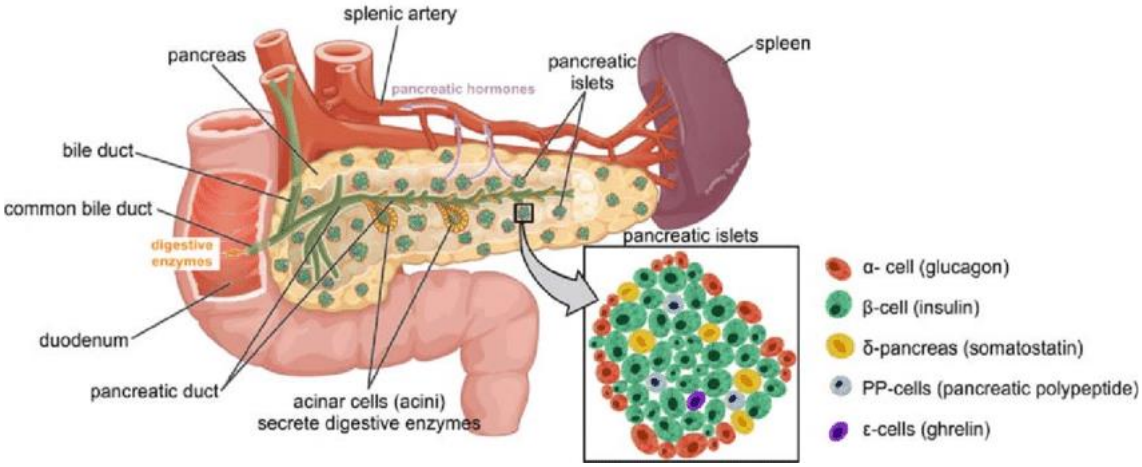

Figure 1-1 | Schematic overview of the pancreas showing its location relative to the small intestine and the spleen, along with its vasculature. Exocrine acinar cells secrete catalytic enzymes into the digestive system via the bile duct. Endocrine cells located within the islet of Langerhans secrete hormones into the circulatory system (Mühlemann, 2018).

During development, the pancreas starts to form from the foregut endoderm from day 22 post-conception in human, and embryonic stage 7.5 in the mouse. The notochord represses sonic hedgehog expression in the foregut endoderm, upregulating expression of the master pancreatic transcription factor, pancreatic and duodenal homeobox 1 (*PDX1*) (Hebrok, Kim and Melton, 1998). Expression of PDX1 in combination with globin transcription factor (*GATA*) 6 and Nk6 Homeobox 1 (*NKX6.1*) defines the transition from pancreatic-specified endoderm into pancreatic progenitor cells. Mice and humans who lack *PDX1* and humans without *GATA6* present with pancreatic agenesis (Offield *et al.*, 1996; Villamayor *et al.*, 2018). Subsequent *GATA4* expression drives the generation of tip progenitors which go on to become the exocrine acinar cells, whereas those cells without *GATA4* expression form the trunk progenitor cells. Trunk progenitor cells which maintain *PDX1* and Neurogenin3 (*NGN3*) expression form the most populous endocrine cell type, the beta cell. Cells that

do not express *PDX1* but do express *NGN3*, Aristaless Related Homeobox (*ARX*), and MAF BZIP Transcription Factor B (*MAFB*) differentiate into alpha cells. Those cells that show diminished *PDX1* expression go on to form duct cells (Jennings *et al.*, 2015). This process has been summarised in Figure 1-2, taken with permission from (Jennings *et al.*, 2015).

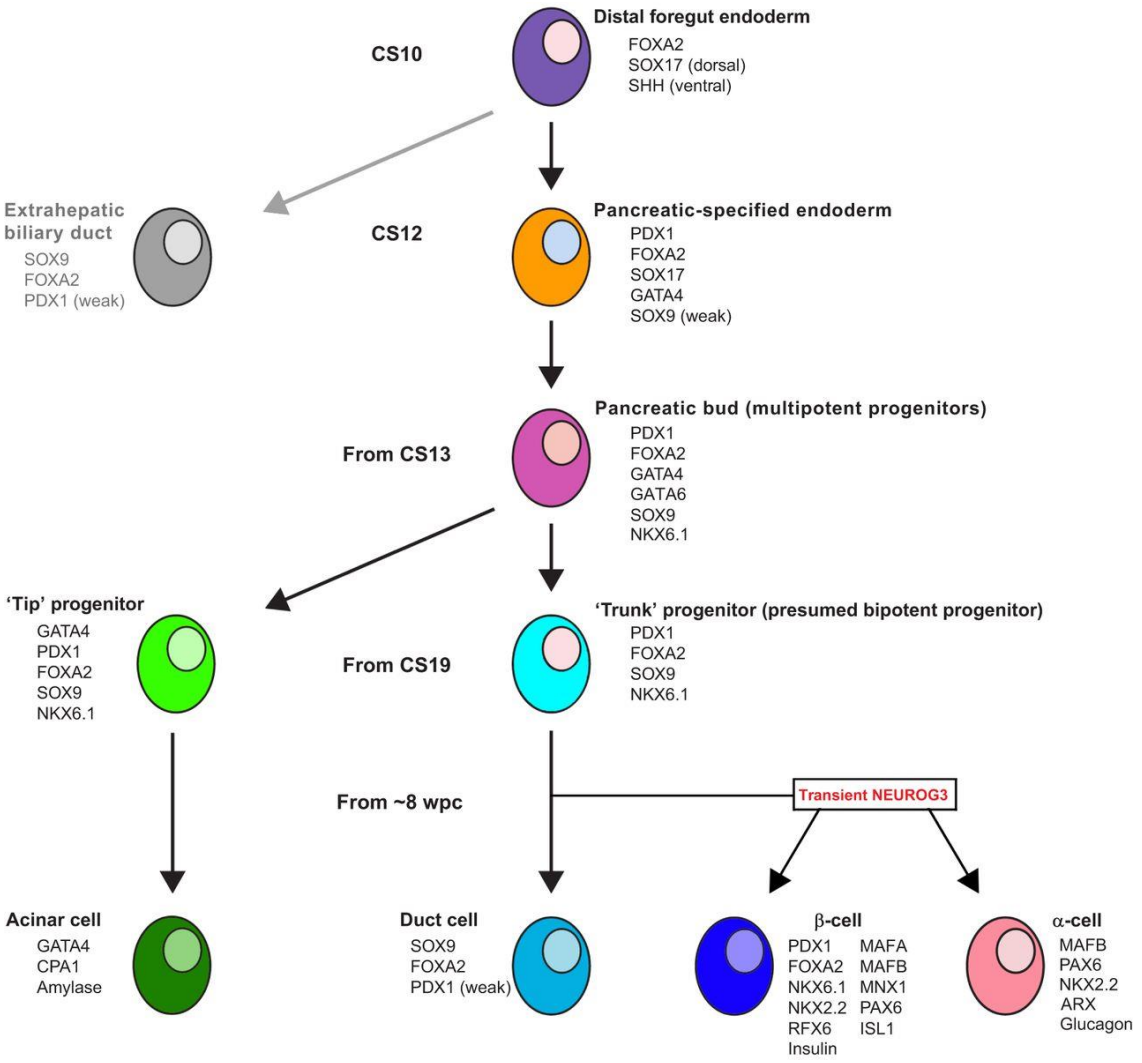

Figure 1-2 | Developmental map of the differentiation of the cells of the pancreas showing the critical fate-determining steps. Transcription factors at each step are based on immunohistochemical data. Development is broken down into Carnegie Stages (CS) (Jennings *et al.*, 2015).

1.1.2 Islets of Langerhans

The islets of Langerhans reside within the pancreas and contain the five main endocrine cell types: alpha, beta, delta, epsilon and gamma cells (also known as pancreatic polypeptide [PP] cells). The relative contribution of each of these cell types and their architecture is highly variable between different species (Steiner *et al.*, 2010). In mouse islets, alpha, beta and delta cells make up 19%, 75% and 6% of the islet, respectively (Brissova *et al.*, 2005). The mouse islet core is made up of beta cells with a corona of alpha cells (Steiner *et al.*, 2010). Whereas in human islets, alpha cells account for approximately 35% of the total cell number, beta cells about 55% and delta cells 10%, with the rest made up of gamma and epsilon cells and non-endocrine cells such as epithelial cells (Brissova *et al.*, 2005). Also, the cells within the human islet are more randomly arranged than in the mouse islet. Although there are obvious differences between human and mouse islets, it has been demonstrated that there is much greater variation between different human samples than there is between the average mouse and human (Bonner-Weir, Sullivan and Weir, 2015). Examples of a mouse islet and a human islet, along with their relative compositions of cell is shown in (Figure 1-3).

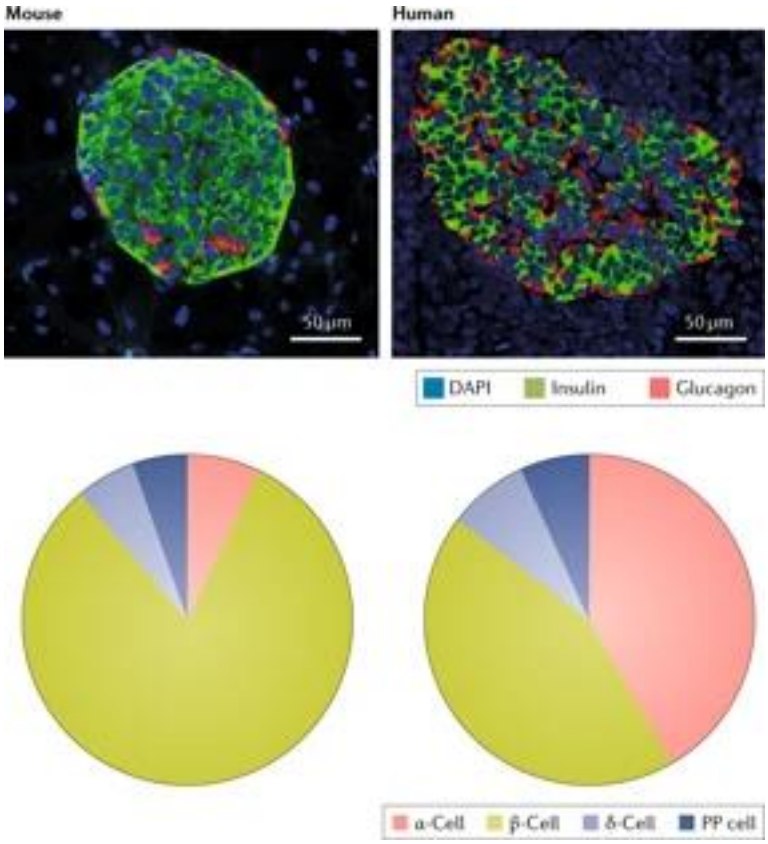

Figure 1-3 | A comparison of cell distribution in mouse and human pancreatic islets. Top panel: Example of mouse (left) and human (right) pancreatic islets stained with antibodies for insulin (green) and glucagon (red) and with DAPI (blue), showing beta cells, alpha cells, and nuclei respectively. Bottom panel: Pie charts showing the proportion of the four main cell types of the islet (alpha, beta, delta and PP) in mouse (left) and human (right) (Gromada, Chabosseau and Rutter, 2018).

As aforementioned, the most populous cell type in the pancreatic islet is the beta cell. These cells are responsible for sensing increases in blood glucose (>11 mM) and releasing the polypeptide hormone insulin which increases glucose uptake and utilisation throughout the body (Gromada, Chabosseau and Rutter, 2018).

The alpha cell is the second most common cell type in the islet. Alpha cells are active at low blood glucose concentrations (<3 mM) during fasting and respond by secreting glucagon. Glucagon signals through cyclic adenosine monophosphate (cAMP) and protein kinase A (PKA) to inhibit glycolysis and

glycogenesis and promote glycogenolysis and gluconeogenesis. This process prevents hypoglycaemia and acts in opposition to the beta cell (Gromada, Chabosseau and Rutter, 2018).

Thirdly, delta cells modulate alpha and beta cell activity via the secretion of somatostatin in response to a nutrient stimulus. Somatostatin acts locally through binding to members of the G-protein coupled somatostatin receptor family, of which there are five subtypes (SSTR1-5). Somatostatin inhibits secretion from multiple endocrine and exocrine cells, including the alpha and beta cell. Binding of the SSTR by its ligand signals through activation of $G\alpha_i$-protein which, in turn, inhibits adenylate cyclase activity to reduce cAMP production (Patel, 1999). Delta cells can contact more neighbouring cells due to long protrusions which extend from the cell body to signal in a paracrine fashion (Larsson *et al.*, 1979; Arrojo e Drigo *et al.*, 2019).

Epsilon cells secrete ghrelin, a growth hormone secretagogue originally extracted from human and rat stomachs. Circulating ghrelin can act on the pituitary to regulate the release of growth-hormone (Kojima *et al.*, 1999). In the islet, ghrelin inhibits glucose-stimulated insulin secretion (Yada *et al.*, 2014). More recently, transcriptomics has revealed that the action of ghrelin on the beta cell is through activation of the delta cell (Adriaenssens *et al.*, 2016; DiGruccio *et al.*, 2016).

Finally, gamma cells secrete pancreatic polypeptide (PPY) for four to six hours after intake of food via stimulation by the Vagus nerve, and influences GI mobility, food intake and metabolism. PPY can inhibit glucagon secretion and

evidence from people with Prada-Willi syndrome, who lack PPY, suggests it acts on satiety as they suffer from insatiable hunger (Tomita *et al.*, 1989).

All these cell types act in concert to maintain normal blood glucose and avoid both hypo- and hyper-glycaemia. This system is so important to higher organisms that these cells are highly conserved across species, from humans, through rodents all the way to zebrafish who possess a single islet.

As previously stated, the overall function of the islet is to maintain normoglycemia, defined as a normal blood glucose concentration of between 4.0 to 5.4 mmol/L when fasting and up to 7.8 mmol/L two hours post-prandially, primarily through secretion of insulin and glucagon. Insulin is especially important in the context of diabetes mellitus where blood sugar levels become dangerously high without treatment, as will be discussed later in this chapter. The following section details the mechanisms through which raised blood glucose levels are sensed and restored to normal via insulin secretion from the beta cell.

1.2 Glucose metabolism

Glucose is the main source of energy for the cells of the body. Regulation of blood glucose is vital for life, as both high and low levels can be detrimental to our health. The osmotic pressure of high glucose can cause damage to the peripheral tissue, especially blood vessels and nerves within the eyes and extremities, potentially leading to blindness or limb amputation if left untreated. Conversely, if blood glucose is too low, it can lead to hypoglycaemic coma as

the brain utilises 20% of the body's glucose-derived energy (Mergenthaler *et al.*, 2013).

Glucose is transported into most cells by the constitutively expressed glucose transporter (GLUT)1. However, in cardiac and skeletal muscle and adipocytes, insulin and exercise (in muscle) can upregulate glucose uptake by translocating GLUT4 to the cell membrane as shown in Figure 1-4 (James *et al.*, 1988).

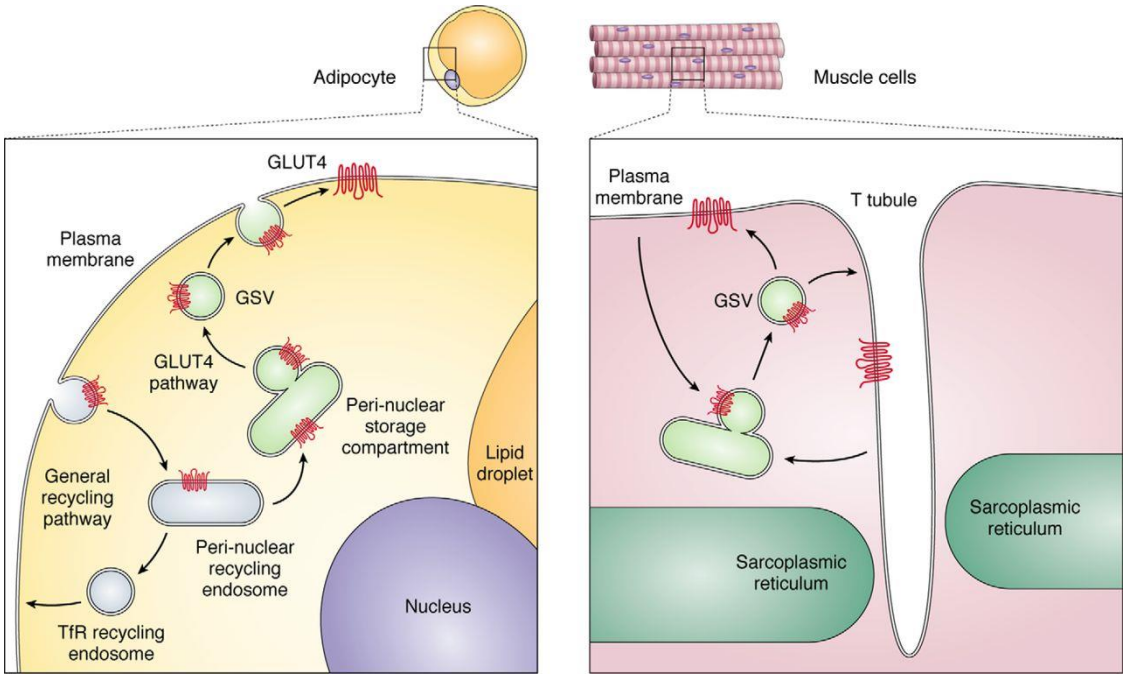

Figure 1-4 | Schematic representation of the GLUT4 transportation pathways. GLUT4 is transported to the plasma membrane in response to insulin in adipocytes (left) and muscle (right). Contraction also transports GLUT4 to the plasma membrane in muscle (right) (Klip, McGraw and James, 2019).

However, glucose cannot be used by cells directly. Instead, it must first be metabolised, generating energy to phosphorylate adenosine diphosphate (ADP) into adenosine triphosphate (ATP). ATP can then release this energy to power various cellular processes. The major steps of glucose metabolism are

glycolysis, the link reaction, the citric acid cycle, and oxidative phosphorylation (Lindquist *et al.*, 2019). This is summarised in Figure 1-5.

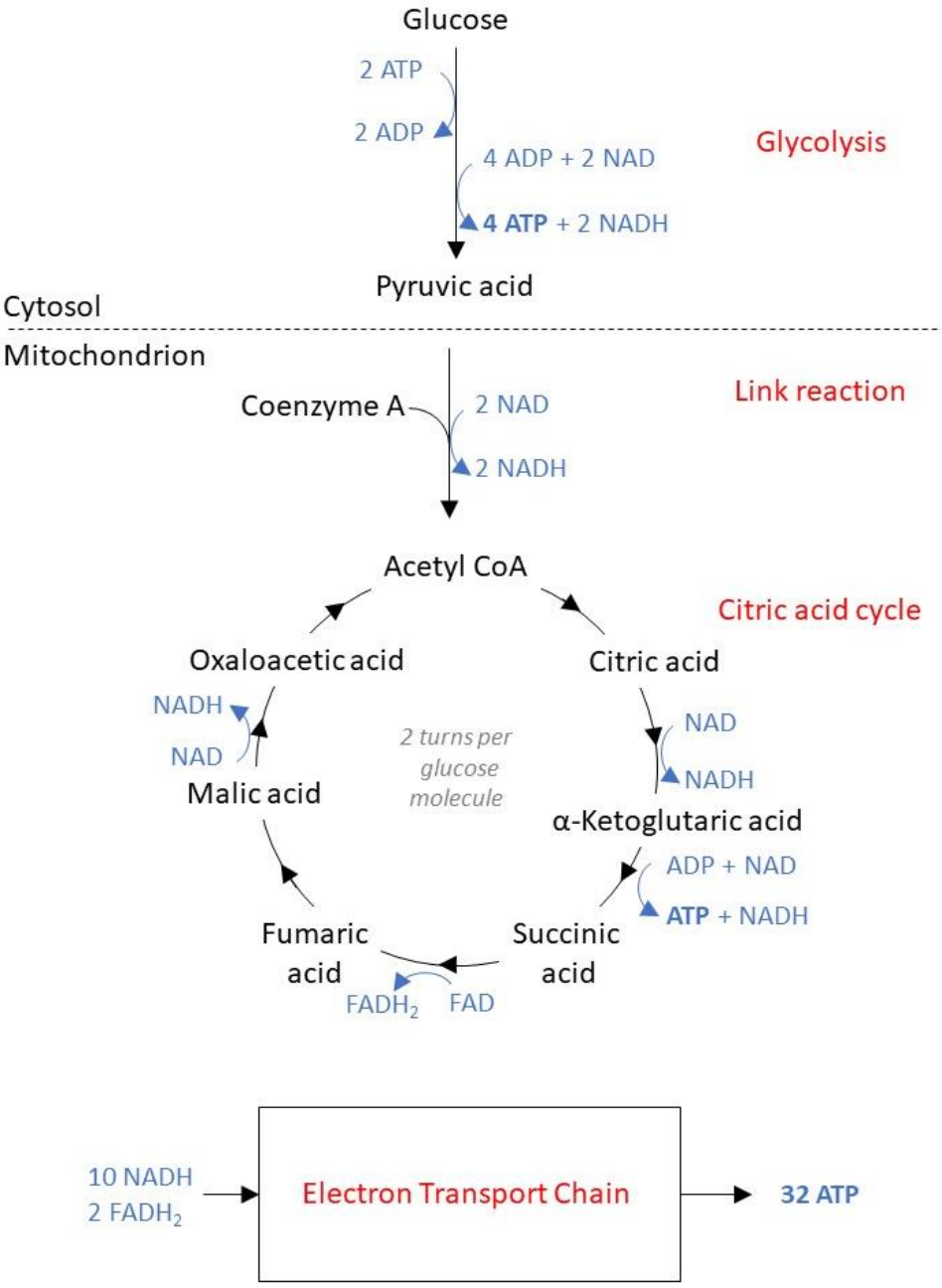

Figure 1-5 | Summary of the main steps in glucose metabolism. Glucose goes through a series of enzymatic reactions as it is metabolised into ATP. Black text and arrows represent metabolism of substrates as they move through the pathway. Blue summarises the reduction or oxidation of molecules for the storage and utilisation of energy. The main steps are described as glycolysis, the link reaction, the citric acid cycle, and the oxidative phosphorylation via the electron transport chain.

1.2.1 Glycolysis and the link reaction

Glycolysis is a series of ten enzymatic reactions which occur in the cytoplasm, starting with the phosphorylation of glucose by glucokinase (GCK) producing glucose-6-phosphate (G6P) (Figure 1-5). It takes place in the absence of oxygen and is evolutionarily conserved, serving as the only source of energy generation for many species. Glycolysis requires two molecules of ATP for every molecule of glucose metabolised, but produces a net yield of two pyruvic acids, two ATP and two reduced nicotinamide adenine dinucleotide (NADH) molecules (MacDonald, Joseph and Rorsman, 2005).

The link reaction takes place in the matrix of the mitochondria (Figure 1-5). Here, this pyruvic acid is decarboxylated, oxidised and combined with coenzyme A (CoA) to produce acetyl-coenzyme A (acetyl-CoA). This reaction also produces one carbon dioxide (CO_2) and one NADH molecule (Alberts *et al.*, 2008; Lindquist *et al.*, 2019).

1.2.2 The citric acid cycle

In the citric acid cycle, each acetyl-CoA molecule from the link reaction is combined with oxaloacetic acid, which releases coenzyme A and forms citric acid. Citric acid is then decarboxylated to α-ketoglutaric acid, reducing one molecule of NAD in the process. This is then further decarboxylated back into oxaloacetic acid via the intermediaries, succinic acid, fumaric acid, and malic acid, which also reduces another two NAD and one flavin adenine dinucleotide (FAD) molecule, as well as converting one ADP into ATP. This oxaloacetic acid

can then combine with another acetyl-CoA molecule, which continues the titular cycle (Alberts *et al.*, 2008; Lindquist *et al.*, 2019).

1.2.3 Oxidative phosphorylation

All the NADH and $FADH_2$ molecules produce during glycolysis, the link reaction and the citric acid cycle are used in a process called oxidative phosphorylation, which generates most of the ATP derived from glucose. In the matrix of the mitochondria, NADH and $FADH_2$ are oxidised to NAD and FAD respectively, and the hydrogen molecules released are split into electrons and protons. The energy from these electrons is used by complex I, II, III and IV of the respiratory complex to pump the protons into the periplasmic space between the inner and outer mitochondrial membranes, creating an electrochemical gradient. This gradient is utilised by complex V of the respiratory complex, also known as ATP synthase, to phosphorylate ADP into ATP. In theory, each NADH produces enough energy for three ATP and $FADH_2$ two molecules. In practice, however, some of this energy is expended moving ADP and ATP across the mitochondrial membrane (Alberts *et al.*, 2008; Sharma, Lu and Bai, 2009).

1.2.4 Beta cell glucose metabolism

Beta cells are specially adapted, allowing them to act as the main blood glucose sensor. Murine beta cells constitutively express *Slc2a2*, encoding the low-affinity glucose transporter-2 (GLUT2) channel, which allows rapid transport of glucose across the membrane into the cell (Thorens *et al.*, 1988). Homozygous deletion of *Slc2a2* leads to chronic hyper-glycaemia and relative hypo-

insulinemia, and these mice have a life expectancy of just three weeks, therefore highlighting the important role of GLUT2 in glucose homeostasis (Guillam *et al.*, 1997).

The primary glucose transporter in human beta cells is GLUT1 (*SLC2A1*), which has a higher affinity than GLUT2, and possibly explains their activation at lower blood glucose concentrations compared with mice (McCulloch *et al.*, 2011). Other forms of GLUT are expressed, including GLUT2 but at lower levels; however, mutations in GLUT2 do not phenocopy the mouse knockout model. There are some associations between mutations in GLUT2 and diabetic parameters, but this may be due to expression in other tissues, such as the liver.

Once glucose is transported into the beta cell, it is processed by GCK into pyruvic acid. This step is the principal component of glucose sensing in the beta cell, and beta cells without GCK do not release insulin in response to glucose, whereas pyruvic acid and pyruvic acid analogues can elicit a response (Rorsman and Ashcroft, 2018). GCK is the rate-limiting enzyme for glucose metabolism, and therefore glucose-stimulated insulin secretion (GSIS). Mutations in the *GCK* gene cause hypoglycaemia and maturity-onset diabetes in the young (MODY), which will be discussed further in 1.6.4 (Froguel *et al.*, 1992). The role of GCK as the primary glucose sensor was demonstrated in Basco *et al.,* in which alpha cell specific knockout of *GCK* led to an inability of alpha cells to suppress glucagon secretion in response to increasing glucose concentrations (Basco *et al.*, 2018).

Glucose is metabolised in the beta cell as previously described, but glucose metabolism also leads to a phenomenon within the beta cell known as stimulus-secretion coupling, which synchronises insulin secretion with increases in blood glucose.

1.3 Stimulus-secretion coupling

Metabolism of glucose within the beta cell leads to an increase in ATP. This increases the ratio of ATP to ADP, which causes ATP-sensitive potassium (K_{ATP}) channels to close. The resulting depolarisation of the cell opens the voltage-dependent Ca^{2+} channels (VDCC) which, in turn, initiates a cascade of Ca^{2+} signalling events and the subsequent exocytosis of insulin from the readily releasable vesicle pool. ATP generated by glycolysis is the main driver of stimulus-secretion coupling, despite more ATP being generated by the citric acid cycle than by glycolysis (Mertz *et al.*, 1996).

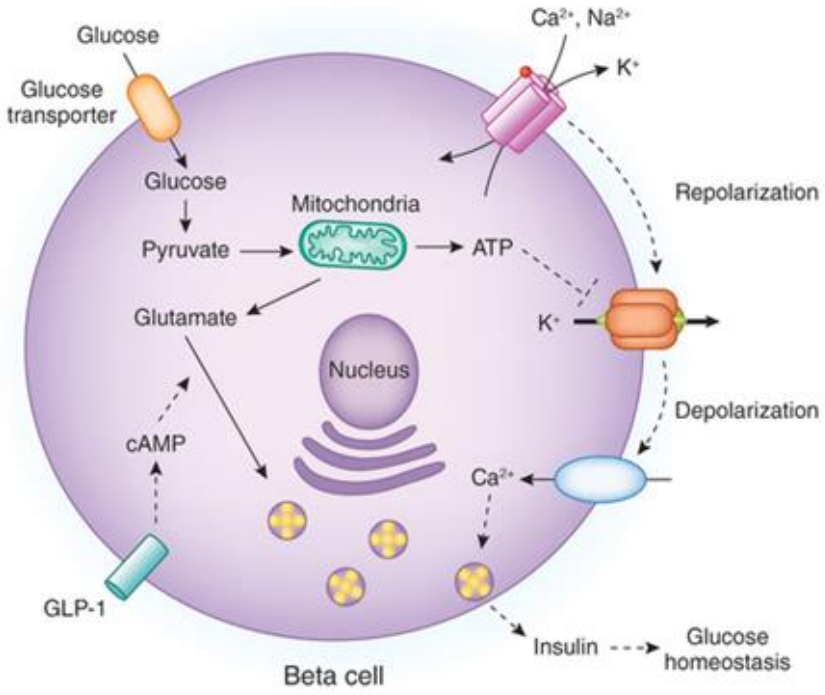

Figure 1-6 | Schematic representation of stimulus-secretion coupling in beta cells. Glucose enters via the GLUT and is metabolised into ATP. This increases the ATP/ADP ratio causes closure of the K_{ATP} channels, depolarizing the cell which opens Ca^{2+} channels. This Increased intracellular Ca^{2+} leads to insulin exocytosis. Figure adapted with permission from (Wollheim and Maechler, 2015).

1.3.1 ATP-sensitive potassium channels

In beta cells, K_{ATP} channels are made up of peptides encoded by two neighbouring genes on chromosome 11. The first is the ATP binding sulphonylurea receptor (*SUR*); mutations in which lead to a rare condition known as persistent hyperinsulinemia hyperglycaemia of infancy. However, SUR is non-functional in the absence of a second subunit, Kir6.2. Kir6.2 in combination with SUR acts as an inward-rectifier potassium channel, allowing potassium ions to flow out of the beta cell under basal conditions, maintaining the membrane potential at around -70 mV (Figure 1-6). However, when the ATP/ADP ratio increases within the beta cell in response to rising blood

glucose, binding of ATP to the SUR causes closure of the K_{ATP} channels and prevents potassium ions leaving the cell (Inagaki *et al.*, 1995; MacDonald, Joseph and Rorsman, 2005). This build-up of positively charged potassium ions within the beta cell increases the membrane potential, and this depolarisation causes opening of the VDCCs (Figure 1-6).

1.3.2 Voltage-dependent Ca^{2+} channels

Beta cells possess VDCCs which open in response to depolarisation (Figure 1-6), allowing Ca^{2+} to flow into the cell down a concentration gradient (Keahey *et al.*, 1989). VDCCs are considered to be the main effectors of insulin secretion as their inhibition by Ca^{2+} blockers, such as nifedipine, is sufficient to impair secretion (Ohneda, Kobayashi and Nihei, 1983).

VDCCs are made up of a combination of subunits designated α_1, β, γ and $\alpha_2\delta$ (Table 1). However, the pore-forming, voltage sensing α_1 subunit is the primary determinant of electrical properties of the VDCC. There are several classifications of VDCC, whose nomenclature originates from early patch-clamp experiments which grouped them according to their sensitivity to inhibitors (Ertel *et al.*, 2000). They all fall into these groups: L, P/Q, N, R and T; and their type is determined by the α_1 subunit (Table 1).

Channel Type	L	P/Q	N	R	T
α_1 subunit	$Ca_v1.1$ $Ca_v1.2$ $Ca_v1.3$ $Ca_v1.4$	$Ca_v2.1$	$Ca_v2.2$	$Ca_v2.3$	$Ca_v3.1$ $Ca_v3.2$ $Ca_v3.3$
Activation voltage	>-30 mV	>-20 mV			>-70 mV
Inactivation time	>500 ms	50-80 ms			20-50 ms
Inhibitors	DHP	ω-Aga IVA	ω-CTX GVIA	SNX 482	Mibefradil

Table 1 | Table of VDCC types and their biophysical properties. VDCC are defined by their α1 subunits, activation voltage, inactivation time and susceptibility to various inhibitors (Yang and Berggren, 2006).

The L-type VDCC are characterised by rapid firing, slower inactivation, and inhibition by dihydropyridines (DHP). L-type channels are predominantly responsible for Ca^{2+} fluxes in beta cells. There are four possible L-type VDCC α_1 subunits: $Ca_v1.1$, $Ca_v1.2$, $Ca_v1.3$, and $Ca_v1.4$; with cells often expressing more than one type of VDCC. In murine beta cells, for example, the $Ca_v1.3$ L-type channel is required for insulin secretion, but in mice lacking R-type $Ca_v2.3$, the second phase of insulin secretion is impaired (Jing *et al.*, 2005). The compound effect of expression of multiple VDCCs gives excitable cells their unique biophysical properties (Yang and Berggren, 2006).

Furthermore, there are species differences in VDCC composition. While beta cells within rodent islets show consistent Ca^{2+} channel opening characteristics, human beta cells display a degree of heterogeneity. Despite initial reports which suggested that human beta cells only express Ca_v3 and rodent beta cells Ca_v1, in fact all beta cells express multiple Ca_v subunits regardless of species. Those beta cells fall into three categories: 1) those that display L-type current, 2) those that possess currents resembling non-L-type currents, and 3) those that appear to have a combination of channel types (Yang and Berggren, 2006).

1.3.3 Ca^{2+}-induced Ca^{2+} release

Cytosolic Ca^{2+} concentrations are further increased by Ca^{2+}-induced Ca^{2+} release from intracellular stores (Wollheim and Sharp, 1981; Graves and Hinkle, 2003). Following an initial rise, intracellular Ca^{2+} levels oscillate, and the speed of oscillations correlate positively to the concentration of glucose (Barbosa *et al.*, 1998). Ca^{2+} is a potent signalling molecule, at Ca^{2+} in the beta cell leads to exocytosis of insulin granules (Figure 1-6).

1.3.4 Insulin granule exocytosis

Exocytosis is the final step in stimulation-secretion coupling, resulting in insulin being released into the blood to have systemic effects to normalise glycaemia after a meal. A basic overview of the process can be seen in Figure 1-7.

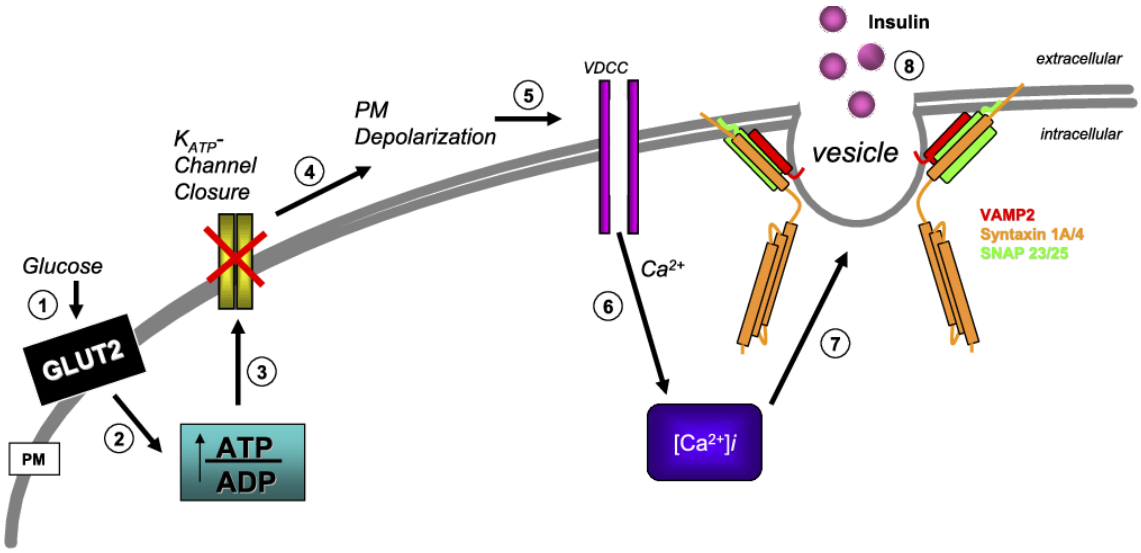

Figure 1-7 | Overview of regulated exocytosis of insulin. The steps that occur in glucose stimulated insulin secretion have been previously described. The stop following increased Ca^{2+} leads to largely uncharacterized series of events, the SNARE proteins mediate vesicle fusion to facilitate insulin release. (Jewell, Oh and Thurmond, 2010).

Insulin granules are distributed between three locations throughout the cell: the readily releasable pool (RRP), the morphologically docked pool and the intracellular pool. The RRP is primed for release in response to Ca^{2+} fluxes and, while only comprising about 1% of the total insulin, is responsible for the first phase of insulin secretion (Bratanova-Tochkova *et al.*, 2002; Olofsson *et al.*, 2002). This RRP is replenished by docked pools, which require mobilisation and priming which, in turn, is replaced by granules from the intracellular pools. The docked and intracellular pools comprise approximately 10% and 90% of the total insulin, respectively. Insulin granule mobilisation accounts for the second phase of glucose-stimulated insulin secretion and can be upregulated by increased glucose, ATP and cAMP (Gembal, Gilon and Henquin, 1992).

Upon normalisation of blood glucose concentration, beta cell ATP/ADP ratios return to normal, which closes K_{ATP} channels and limits Ca^{2+} fluxes, which ends insulin secretion (MacDonald, Joseph and Rorsman, 2005).

1.3.5 Incretin action

In addition to the main Ca^{2+}-dependent signalling pathway, there is an additional amplifying pathway through which beta cells are primed for insulin release by the binding of incretins to their receptors. Incretins are peptides released by the intestine in response to a meal, and the most important incretins involved in insulin secretion are glucagon-like peptide 1 (GLP-1) and glucose-dependent insulinotropic polypeptide (GIP) (Kreymann *et al.*, 1987; Mojsov, Weir and Habener, 1987; Wang *et al.*, 1995).

GLP-1 is secreted by the endocrine L-cells of the gut and binds to the GLP-1 receptor (GLP-1R) on the beta cell. GLP-1R is a member of the G-protein coupled receptor (GPCR) family of proteins and acts through inositol 1,4,5-trisphosphate (IP3) and cAMP to improve the beta cells' secretory response to glucose. This pathway will be important in the first results chapter, in which cAMP plays a major role.

GIP is produced in the K-cells of the gut in response to nutrient intake. GIP was initially named gastric inhibitory protein when it was demonstrated that treatment of dog gastric tissue with GIP caused decreased secretions (Brown *et al.*, 1975; Dworken, 1982). However, upon the discovery of its ability to stimulate insulin secretion from the pancreas, it was more appropriately named glucose-dependent insulinotropic peptide.

1.4 Insulin synthesis and signalling

1.4.1 Insulin synthesis and maturation

Insulin is a 6 kDa, 51 amino acid protein made up of two peptides, an A chain and a B chain, connected by two disulphide bonds (Sanger, 1959). It is initially translated as preproinsulin before being cleaved into proinsulin, at which point it folds and the disulphide bonds form (Steiner and Oyer, 1967; Steiner *et al.*, 1967). The sequence that links the A and B chain is cleaved by two endonucleases, prohormone convertases 1/3 and 2. This cleavage releases C-peptide, a protein with minor hormone actions that can be used as a proxy for the measure of insulin release, as they are secreted in equimolar quantities (Weiss *et al.*, 1990). Carboxypeptidase E subsequently cleaves the remaining basic residues creating a bioactive hormone (Davidson and Hutton, 1987). This maturation occurs in the trans-Golgi network within highly acidic, clathrin-coated vesicles in the presence of zinc (Orci *et al.*, 1987). The finished insulin molecule is packaged into hexamers with a dense zinc core, forming the mature insulin granule, which makes up the pool of insulin primed for release (

Figure 1-8).

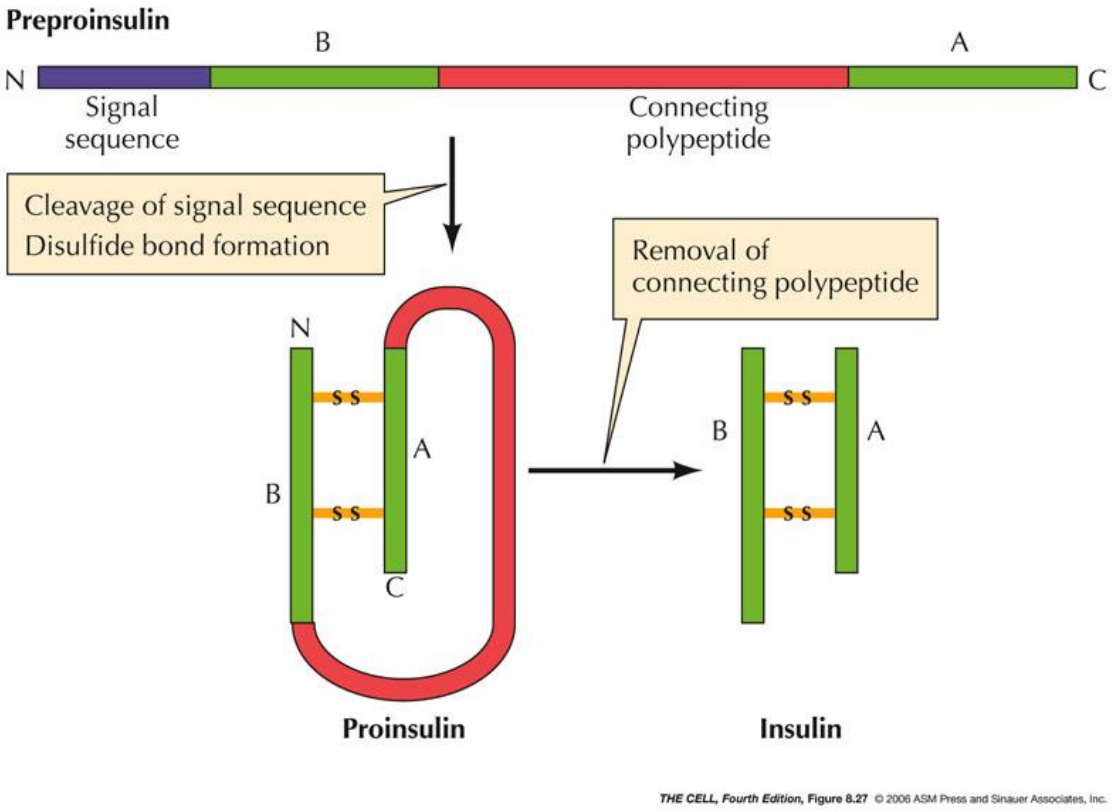

Figure 1-8 | Diagram showing the process of insulin maturation. Preproinsulin is converted into proinsulin by cleavage of the signal sequence and disulphide bond formation. Finally, removal of the connecting polypeptide results in the mature insulin protein (Cooper and Hausman, 2006).

1.4.2 Insulin signalling

The effects of insulin are mediated through its binding to the insulin receptor (IR) on the plasma membrane of its target cells. The IR is comprised of an alpha and a beta subunit. The alpha subunit protrudes out of the cell membrane and possesses ligand-binding capabilities (Ebina *et al.*, 1985; Ullrich *et al.*, 1985). Upon binding of insulin to the alpha subunit, the tyrosine kinase activity of the IR is activated, leading to phosphorylation of the beta subunit and members of the IR substrate family, which translate this signal into downstream effects via protein kinase B (AKT) and phosphoinositide 3-kinase (Kohn,

Kovacina and Roth, 1995). AKT translates this tyrosine phosphorylation signal into a serine/threonine phosphorylation signal, which is required for most of the effects of insulin signalling, such as GLUT4 translocation and synthesis of glycogen, lipids, and proteins (Figure 1-9).

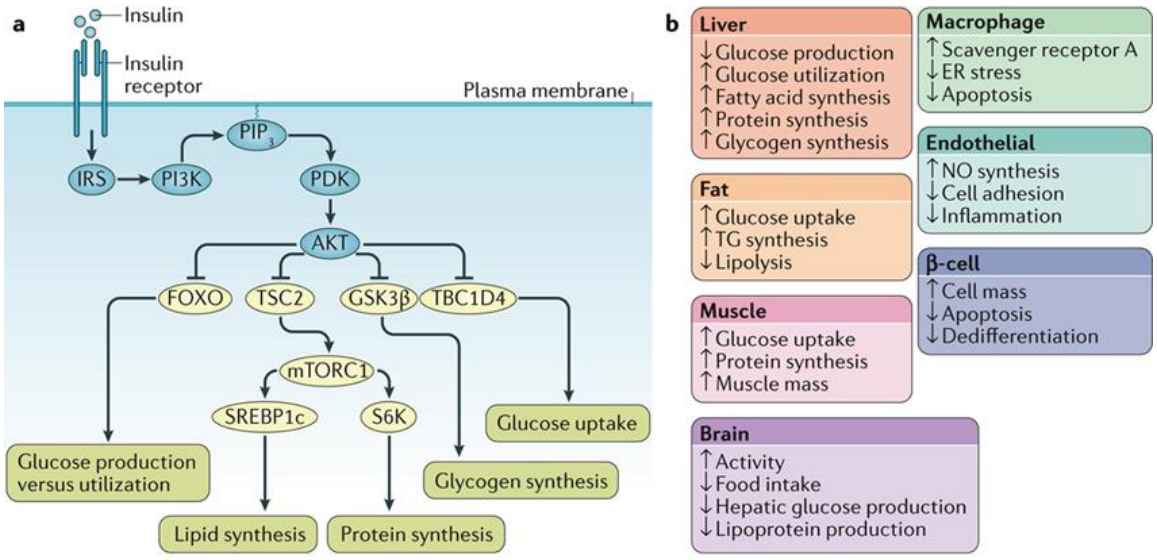

Figure 1-9 | An overview of the effects of insulin signalling. AKT translates the signal from the insulin receptor into changes in gene expression via inhibition of key transcription factors (Haeusler, McGraw and Accili, 2018).

1.5 Beta cells regulation

1.5.1 Beta cell connectivity

An additional layer of insulin regulation appears to come from communication between beta cells by way of electrical and Ca^{2+} signals. When beta cells are dissociated and cultured, they attempt to reaggregate. Those that successfully form bonds with one or more beta cells have improved GSIS per beta cell over those that remain separate (Bosco, Orci and Meda, 1989). This improvement is not seen in beta cells which only contact other islet cell types. In addition to

impaired GSIS, dissociated rat islets have increased basal insulin secretion showing failed regulation (Halban *et al.*, 1982).

This beta cell communication appears to be facilitated by gap junctions, as this phenomenon is impaired in islets from mice in which *Connexin36* has been knocked out. This connectivity determines how signals evoked by external stimuli that occur across the beta cell population are integrated to result in appropriate insulin release. For example, some beta cells act as pacemakers, synchronising Ca^{2+} signals across the islet in order to amplify insulin secretion at stimulatory levels of glucose and to suppress secretion at fasting levels (Valdeolmillos *et al.*, 1989; Speier *et al.*, 2007). These pacemaker cells have been termed ‘hubs’ and are characterised by increased glucose metabolism but lower expression levels of beta cell maturity markers (Johnston *et al.*, 2016). This implies a further role for immature beta cells within the islet.

1.5.2 Islet regulation

Insulin secretion is also regulated by paracrine signals from alpha and delta cells within the islet. Despite their opposing systemic actions, glucagon secreted from the alpha cell stimulates the beta cell through activation of adenylate cyclase, raising cAMP levels (Samols, Marri and Marks, 1965). Indeed, in xenotransplantation experiments investigating the homeostatic set point of islets from different species, glucagon was shown to be required for normal GSIS (Rodriguez-Diaz *et al.*, 2018). Excessive stimulation by glucagon is kept in check through inhibition of the alpha cell by both the beta cell and the delta cell via insulin and somatostatin, respectively. Delta cells are stimulated by

Urocortin-3 (UCN3) produced by beta cells, which provides negative feedback through inhibition of beta cells by somatostatin (Salehi *et al.*, 2007). This complex web of stimulation and inhibition of cells within the islet allows precise regulation of insulin and glucagon secretion to maintain normal blood glucose (Figure 1-10).

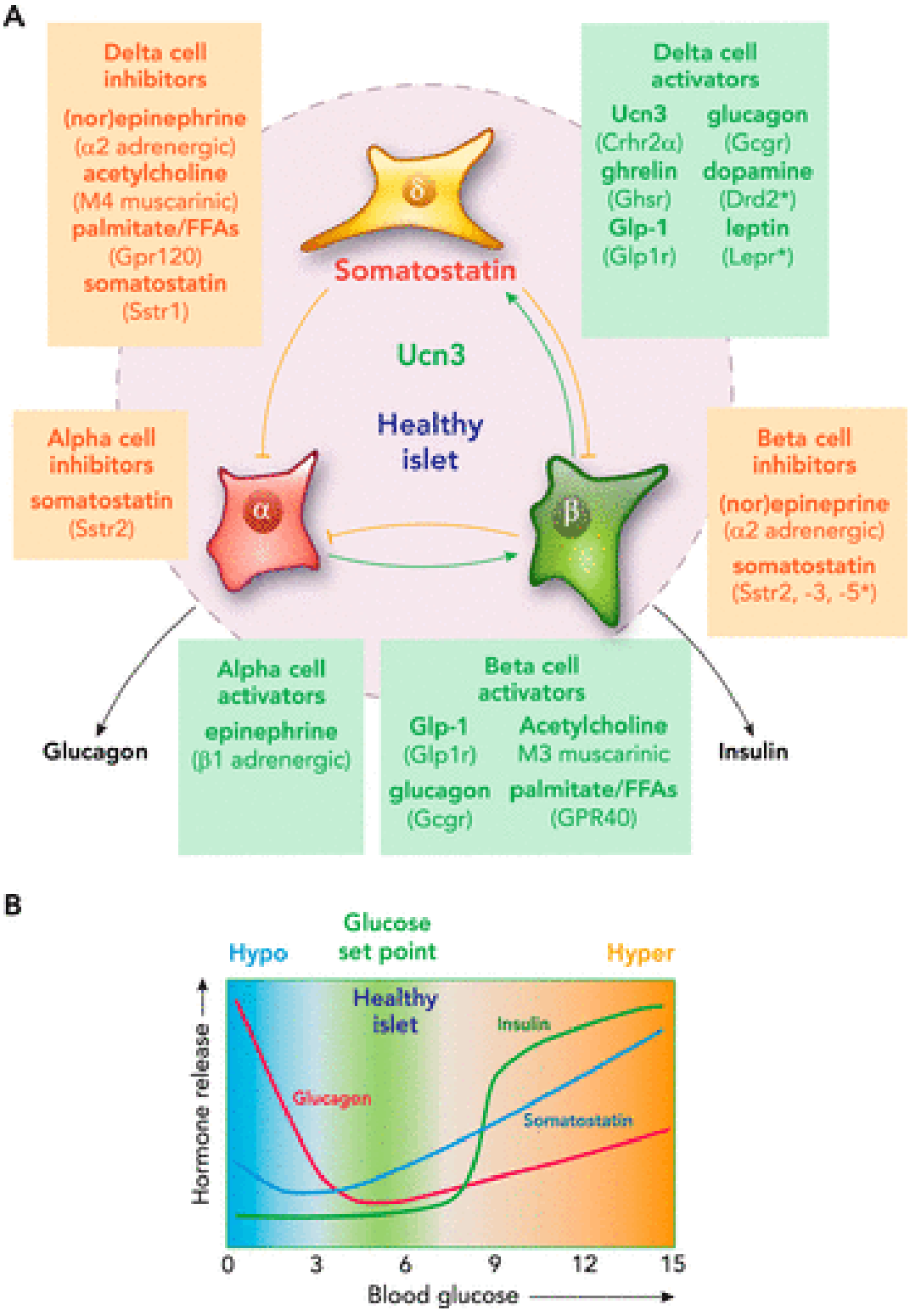

Figure 1-10 | Schematic of intra-islet paracrine signalling. (A) Paracrine factors released from the alpha (red), beta (green) and delta (yellow) cells have both stimulatory and inhibitory actions on the other islet cells. Paracrine factors are in bold type, with the corresponding receptors given in parentheses underneath each factor. (B) Graph showing hormone secretion from the alpha (red), beta (green) and delta (blue) cells in response to blood glucose concentration (Huising et al., 2018).

1.5.3 Disallowed genes

The concept of disallowed genes in the beta cell field has existed for several years and states that not only do beta cells express genes required to function as glucose sensors but they also do not express genes normally expressed ubiquitously, known as housekeeping genes (Thorrez *et al.*, 2011). Two examples of genes that are disallowed in the beta cell are hexokinase and monocarboxylate transporter 1 (*MCT1*).

Hexokinase is a low affinity enzyme that converts glucose into G6P, initialising glucose metabolism. However, hexokinase is absent in beta cells and, as a result, this first step is controlled by GCK, which acts as a rate limiting step in glucose metabolism, rather than glucose transport as in other cell types. This prevents inappropriate insulin secretion from beta cells at low blood glucose concentrations (Quintens *et al.*, 2008). Indeed, there was an increase in glycolytic flux at low glucose in min6 cells overexpressing Hexokinase I compared with control (Ishihara *et al.*, 1994).

Secondly, MCT1, which is normally responsible for the transport of pyruvic acid across the plasma membrane, is absent from pancreatic beta cells. This prevents insulin secretion in response to pyruvic acid outside of the beta cell. However, in experiments using cells overexpressing *MCT1*, pyruvic acid was able to stimulate insulin secretion (Ishihara *et al.*, 1999).

1.6 Overview of diabetes

1.6.1 History of diabetes

The symptoms of diabetes have been observed for thousands of years, mainly excessive urination and muscle wasting, and eventually mortality. The word diabetes comes from the ancient Greek word for “to pass through”. It was later noted that the urine of some sufferers attracted ants and had a sweet taste, leading to the addition of the term, *Mellitus*, from *mel* for honey (Lakhtakia, 2013).

In recent times, the term diabetes can be applied to two conditions: diabetes insipidus and diabetes mellitus. They both share the symptoms of increased thirst and urination; however, diabetes insipidus is caused by hypothalamic issues which prevent the kidneys from producing sufficiently concentrated urine, rather than a dysregulation of the control of blood glucose seen in diabetes mellitus. Diabetes insipidus is much rarer, affecting only 1 in 25000 (Andrea, Natascia and Iorgi, 2012), compared with 1 in 11 for diabetes mellitus (Saeedi *et al.*, 2019). As a result of this high prevalence, diabetes mellitus will be the focus of this thesis and any further mention of diabetes will refer specifically to diabetes mellitus.

Diabetes mellitus affected approximately 463 million people worldwide in 2019 and this number is expected to rise to 700 million by the year 2045 (Saeedi *et al.*, 2019). It directly accounts for more than 10% of global healthcare spending,

amounting to more than 760 billion US dollars (Williams *et al.*, 2020), and the cost will continue to increase with the rise in prevalence.

Complications from diabetes put a huge burden on health services around the world. The cost of treating a single case of ketoacidosis in adolescents with diabetes in the UK is estimated to be £1387 (Dhatariya *et al.*, 2019). Other complications can result from poorly managed diabetes, including retinopathy, peripheral neuropathy and kidney disease, while co-morbidities can be exacerbated by diabetes, such as cardiac disease and hypertension (Henning, 2018).

There are two main types of diabetes mellitus: type 1 (T1D) and type 2 (T2D). In both diseases, there is a deficiency in the hormone responsible for lowering blood glucose: insulin. However, there are several other rarer forms of diabetes, as described in 1.6.4, which provide insight into glucose homeostasis due to their single gene mutation causes, however, they will not be looked at in any detail in this work. Throughout this thesis, the focus will be on T2D due to its rising increase in prevalence and the insights into normal beta cell physiology we can gain through its study.

1.6.2 Type 1 diabetes

T1D is caused by an autoimmune response against antigens produced by the beta cells. This leads to the near destruction of the population and therefore the ability of the body to respond to changes in blood glucose. T1D is a severe disease if untreated and requires constant blood glucose monitoring and multiple daily injections of insulin. Although both main forms of diabetes are

caused by a combination of environmental and genetic factors, T1D has a higher genetic component based on concordance in twin studies (Kaprio *et al.*, 1992).

1.6.3 Type 2 diabetes

While T1D traditionally occurs in childhood, T2D normally occurs later in life, although its prevalence in the young is rising. Excessive consumption of high-fat and sugar diets in overweight individuals causes peripheral tissue to become resistant to the action of insulin. This ‘insulin resistance’ requires beta cells to produce ever-increasing amounts of insulin, which creates a burden on the secretory capacity of the beta cells. Eventually, the combination of worsening insulin resistance and beta cell stress leads to their failure and death. This is detailed further in 1.7 below.

Some recent studies have shown that, in people with T2D, ultra-low-calorie diet (600 kcal a day) comprising of specially formulated milkshakes and starchy vegetables can cause remission of the disease (Lim *et al.*, 2011; Rehackova *et al.*, 2017). The mechanisms for remission are however not well characterized at the beta cell level, follow-up is still ongoing with regards to length of remission, and a large proportion of patients do not tolerate well an ultra-low-calorie diet. Moreover, current drugs such as tirzepatide are leading to outcomes that match or better those obtained with a ultra-low-calorie diet (Thomas *et al.*, 2021).

1.6.4 Rare forms of diabetes

Firstly, impaired glucose tolerance is a condition which affects the pregnancies of 16.9% live births, and has recently been subdivided into two subcategories: “mild impaired glucose intolerance”, referred to historically as gestational diabetes, and the more severe “diabetes in pregnancy” (Guariguata *et al.*, 2014). A link has been shown between gestational diabetes and T2D, as those that suffer from gestational diabetes have increased risk of developing T2D (Zhu and Zhang, 2016).

Another rare form of diabetes is MODY, a highly heritable condition caused by mutations in single genes such as *GCK* or *HNF1/4-alpha/beta*. MODY normally affects people under the age of 25 who have a parent with diabetes and a family history of diabetes, but it is regularly misdiagnosed due to its rarity (Anik *et al.*, 2015).

1.7 Pathophysiology of type 2 diabetes

Humans evolved to be hunter-gatherers, living from one meal to the next. As a result, we developed a thrifty phenotype, surviving by storing biochemical energy in times of feast and using those stored resources during periods of famine. In recent times, food has become more readily available through improvements in agricultural technology, and lifestyles have become more sedentary. This has resulted in an environment where the calorific balance has skewed massively towards an increase in calorie intake (Taylor, 2013).

1.7.1 Insulin resistance

Beta cells are under pressure to battle the constant flow of excessive carbohydrates into the body by producing more insulin, while peripheral tissues, especially muscle and adipose tissue, are being constantly primed to respond to that insulin. Over time, these peripheral tissues become desensitised to the constant barrage of insulin, leading to a condition known as insulin resistance (IR), where greater levels of insulin are required to have the same effects as previously needed. While the exact mechanisms underlying IR are unknown, it is agreed that multiple factors converge to increase IR risk, for example genetics, age, physical activity, body fat distribution, obesity and diet (Kahn, 2003).

Indeed, there are just a handful of rare monogenic disorders characterised by IR. Defects in insulin receptor signalling have been identified, including primary defects in signalling (INSR mutations), antibodies against the receptor itself, or downstream signalling issues (IRS, PI3K)(Koprulu *et al.*, 2022). Defects in insulin receptor signalling result in extreme hyperinsulinemia and insulin resistance, requiring very high insulin doses (10-fold higher) to treat. Severe insulin resistance can also be secondary to lipodystrophies, for example those due to mutations in AGPAT2 (Agarwal *et al.*, 2002) or dominant negative mutations in the ligand binding domain of PPARG (Barroso *et al.*, 1999). Lastly, severe insulin resistance can be a feature of complex syndromes such as Alstrom's disease, which is associated with an increase in adipose tissue mass and lipodystrophy (Geberhiwot *et al.*, 2021).

The link between age and IR is less clear. In a comparison of groups of 18-35 year-old and 57-82 year-old men, there was a higher incidence of glucose intolerance in the aged group, resulting from both IR and a beta cell defect. The insulin sensitivity index in the older group was reduced 63%. Importantly, this reduction was not related to differences in body fat (Chen *et al.*, 1985). However, a slightly larger study including both men and women concluded that age only accounts for 10% of IR, and there is a larger association with waist circumference and adiposity (Kohrt *et al.*, 1993). This was corroborated by a much larger study (approximately 1150) of European participants, which stated that “We conclude that in healthy Europeans, age per se is not a significant cause of insulin resistance of glucose metabolism or lipolysis” (Ferrannini *et al.*, 1996).

As skeletal muscle is one of the main targets for insulin, accounting for between 60% and 80% of insulin metabolism (Ng *et al.*, 2012), it clearly has a role to play in insulin resistance. It has been postulated that short term IR is in fact a compensatory mechanism to prevent the harmful effect of intracellular glucose on muscle tissue (Goodpaster and Sparks, 2017). This compensation, or “metabolic flexibility”, may not always be pathophysiological. For instance, in long-distance trained individuals, challenged with lipid oversupply, they responded with decreased glucose oxidation, increased fatty acid utilisation and reduced consumption of glycogen when compared with untrained individuals (Dubé *et al.*, 2014).

It has been shown that higher levels of intra-abdominal fat deposition correlate with IR, whereas there is a correlation between subcutaneous fat and circulating

leptin levels (Cnop *et al.*, 2002). While the mechanisms through which these phenomena occur are unclear, increased lipolysis from visceral adipose tissue may increase circulating fatty acid which may deposit in skeletal muscle and result in insulin resistance (Phillips *et al.*, 1996). NMR data from Gerald Shulman leads to him hypothesising that “increasing intracellular fatty acid metabolites, such as diacylglycerol, fatty acyl CoA’s, or ceramides activates a serine/threonine kinase cascade leading to phosphorylation of serine/threonine sites on insulin receptor substrates. Serine-phosphorylated forms of these proteins fail to associate with or to activate PI3-kinase, resulting in decreased activation of glucose transport and other downstream events” (Shulman, 2000).

In summary, IR results from a complex interplay between genetic, physical and lifestyle factors. Nonetheless, IR is widely accepted as one of the main triggers of beta cell failure during T2D (itself a complex disease), although the timings and exact mechanisms underlying changes in IR and beta cell function remain difficult to define.

1.7.2 Beta cell dysfunction and failure

Insulin resistance sets up a vicious cycle whereby beta cells need to expand their protein synthesis capacity to produce more insulin (Malhotra *et al.*, 2008). Once ER stress is triggered, in part due to REDOX changes, beta cells undergo the unfolded protein response leading to their eventual apoptosis (Murphy, 2013; Hotamisligil and Davis, 2016). There are reports that beta cells are able to rebound from short periods of ER stress, even increasing protein production after returning to normal conditions. However, when exposed to repeated bouts

of ER stress, those same beta cell lose that plasticity, which may be mirrored in T2D pathophysiology (Chen *et al.*, 2022). Due to the low proliferation rates, particularly in the aged pancreas, these cells are not replenished, or replaced with less mature cells, and functional beta cell mass declines (Salinno *et al.*, 2019). Along this pathway, beta cells also de-differentiate and begin to take on features of alpha cells, such as expression of *glucagon* and *MafB*, with a concomitant decrease in their responsiveness to high glucose (Kahn, 2003; Talchai *et al.*, 2012). This results in a decreased ability for the pancreatic islet to appropriately secrete insulin.

1.7.3 Peripheral neuropathy

Peripheral neuropathy (PN) is a common complication with T2D. It normally starts at the extremities, characterised by numbness and reduced motor function, which spreads proximally. It is a major risk factor for diabetic foot ulceration and is the most common cause of non-traumatic amputation (Smith *et al.*, 2022).

The primary cause of PN is thought to be damage to unmyelinated C fibres because they are not as well protected to metabolism insults as myelinated cells. However, as damage occurs, this protection retreats, leading to the characteristic creep of symptoms from the periphery in a proximal direction. Increased uptake of glucose from the blood supply to these cells increases glycolysis and conversion and production of sorbitol by aldose reductase, as well as raised inflammation and oxidative stress (Feldman *et al.*, 2017).

Increase in glycolysis leads to intermediaries such as diacylglycerol which in turn activates Protein Kinase C (PKC). Activated neuronal PKC leads to a range of impairments in metabolism such as insulin resistance, disrupted Na/K ATPase activity and gene alterations, which eventually lead to vasoconstriction, hypoxia and neuronal damage (Geraldes and King, 2010).

Sorbitol is slowly metabolised and a build-up in C fibres upsets the osmotic balance of the cells, leading to a compensatory efflux of other metabolites vital for the normal activity of neuronal function. This is further compounded by a build-up of reactive oxygen species which mediates cellular dysfunction and intracellular injury (Oates, 2008).

Under conditions of glucose and lipid excess, neurons increase ATP generation through oxidative phosphorylation and as a result increased NADH and $FADH_2$ electron donors. This is associated with altered firing potentials and eventually the inability to maintain distal nerve endings (Fernyhough, 2015).

1.8 Glucocorticoids

The interplay between glucose metabolism and glucocorticoids (GC) has long been established. For example, increased insulin resistance is a common symptom of Cushing's disease, which is characterised by excess GC. Indeed, in approximately 80% of Cushing's cases, patients also suffer from type-2 diabetes or increased insulin resistance (Boscaro *et al.*, 2001).

Glucocorticoids are a family of corticosteroid hormones that have many physiological effects, including carbohydrate and amino acid metabolism, stress

responses, blood pressure and hepatic gluconeogenesis (Munck and Náray-Fejes-Tóth, 1992; de Kloet *et al.*, 2019). The effects of glucocorticoid on glucose metabolism are shown in Figure 1-11. While the effects of glucocorticoid directly on the beta cell are unclear due to the compounding effects of peripheral insulin resistance and beta cell mass, we can postulate that as GCs inhibit the insulin signalling pathway, this would cause an impairment in first phase glucose stimulated insulin secretion. This postulation is based upon the fact that beta cell specific knockout of the insulin receptor leads to increased circulating insulin and impaired glucose- (but not arginine) stimulated insulin secretion (Kulkarni *et al.*, 1999). It is also important to note that most studies looking at the impact of GCs on beta cell function employ dexamethasone which has a relative potency of 25-100 times that of endogenous GCs. We use GCs at physiological levels to gain a greater understanding of normal beta cell responses.

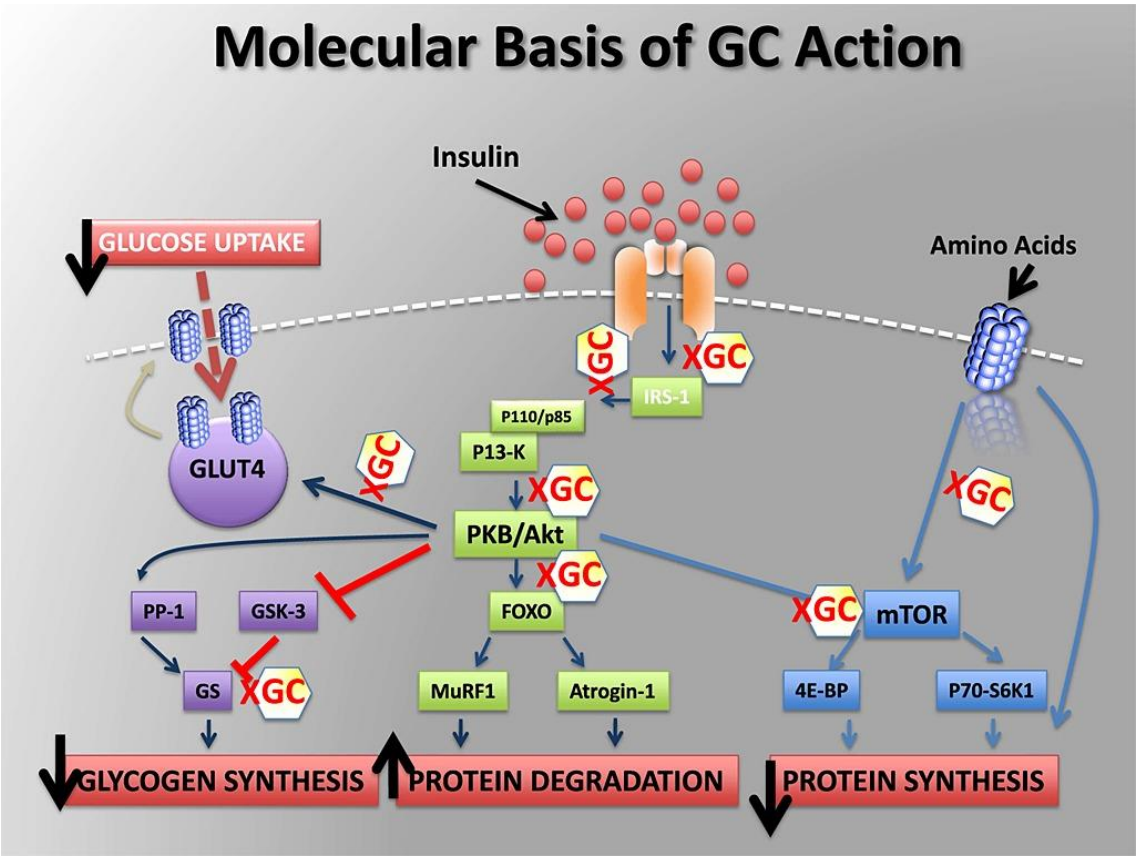

Figure 1-11 | Molecular basis of glucocorticoid action. In targets for insulin action such as the liver and adipose tissue, insulin binds the insulin receptor which, signals through protein kinase B (PKB) to translocate GLUT4 to the membrane to increase glucose uptake. Glucocorticoids inhibit multiple steps of this pathway, leading to reduced glucose uptake and synthesis, increased protein degradation, and decreased protein synthesis (Hwang and Weiss, 2014).

GCs are synthesised in, and secreted by, the adrenal cortex in response to adrenocorticotrophic hormone (ACTH) as the final step of the hypothalamic-pituitary-adrenal (HPA) axis (Figure 1-12). GCs exert negative feedback on every step of their production to prevent inappropriate excess circulating GCs. Pertinently, these feedback mechanisms contribute to ultradian pulsatility in which cortisol is released in short bursts, with GC receptive genes responding to these bursts in a biologically meaningful way (Walker *et al.*, 2012).

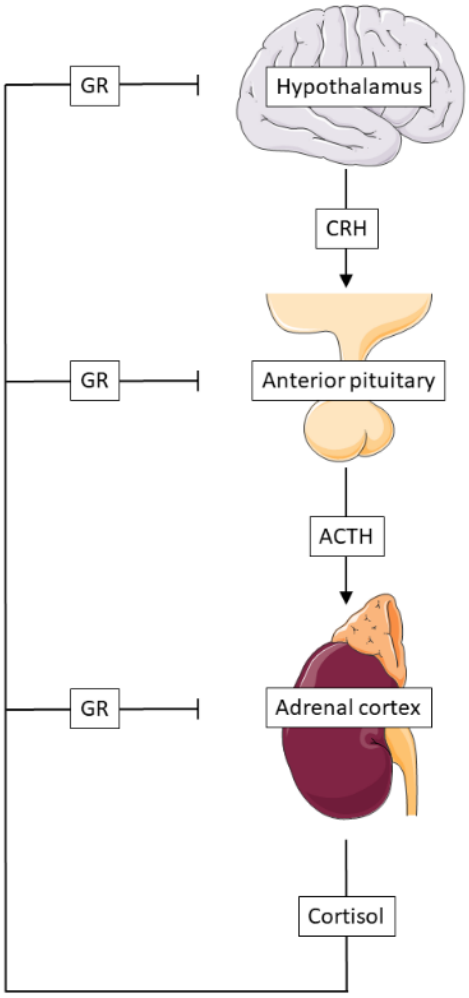

Figure 1-12 | Schematic representation of the hypothalamic-pituitary-adrenal axis responsible for the regulation of glucocorticoid synthesis and secretion in response to stress. Stress signals received by the hypothalamus prompt the release of corticotrophin releasing hormone (CRH), which promotes the anterior pituitary to release adrenocorticotrophic hormone (ACTH). ACTH stimulates the adrenal glands, leading to the secretion of cortisol into the blood stream. Cortisol has a negative feedback effect on both the anterior pituitary and the hypothalamus to prevent harmful levels of circulating cortisol. Image is a modified version of that found in (Dickens and Pawluski, 2018).

There are less and more active forms of GCs: 11-dihydrocorticosterone (11-DHC) and corticosterone (Cort) in mouse; and cortisone and cortisol in humans, respectively. Interconversion between these two forms is mediated by the enzyme 11β-hydroxysteroid dehydrogenase type 1 (HSD11B1), which activates/reactivates GCs to determine local tissue level concentration (Tomlinson, Walker, *et al.*, 2004). HSD11B1 possesses both 11-beta-

dehydrogenase (cortisol to cortisone in man, 11-DHC to corticosterone in mouse) and 11-oxoreductase (cortisone to cortisol in man, corticosterone to 11-DHC in mouse) activity, and the direction in which it converts GC is dependent on the ratio of nicotinamide adenine dinucleotide phosphate (NADP) to reduced NADP (NADPH) in the cell. The canonical mode of HSB11B1, 11-oxoreductase, can only be maintained in the presence of an abundant NADPH supplied by the activity of hexose-6-phosphate dehydrogenase (H6PD). It has been shown that inheritance of three or more mutant alleles in HSD11B1 and H6PD can cause a deficiency in cortisol concentrations by impairing conversion of cortisone into cortisol. This condition is termed cortisone reductase deficiency (Draper *et al.*, 2003). The mouse homologue of HSD11B1 is *Hsd11b1* which converts corticosterone into cortisol (11-oxoreductase) and vice versa (11-beta-dehydrogenase).

In addition to *HSD11B1*, there is another isoform of this enzyme: 11β-hydroxysteroid dehydrogenase type 2 (*HSD11B2*), which converts cortisol and corticosterone into their less active counterparts (cortisone and 11-DHC, respectively). This helps protect mineralocorticoid sensitive tissues, such as the kidneys, parotid and colon, from inappropriate GC excess as cortisol and corticosterone can bind to the mineralocorticoid receptor and prevent it from activating inappropriately (Funder *et al.*, 1988).

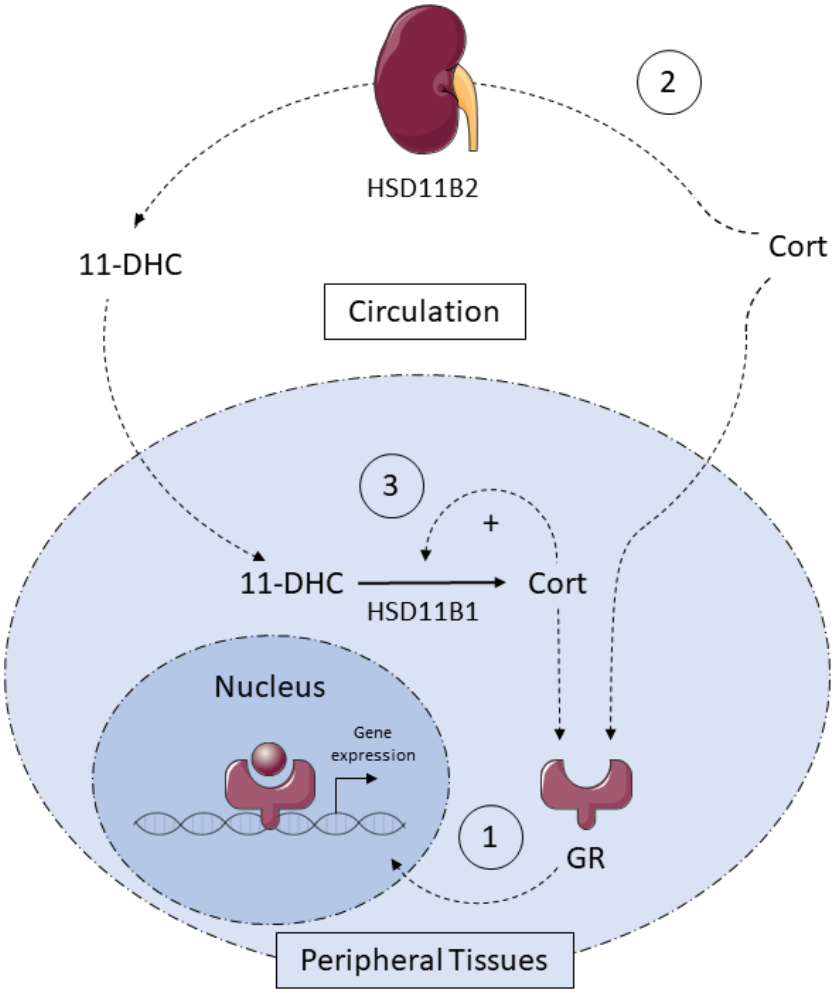

Figure 1-13 | Schematic of interconversion of 11-DHC and corticosterone in the peripheral tissue by HSD11B1 and HSD11B2. (1) Corticosterone (cort) in circulation directly affects gene expression in peripheral tissues via the GR. (2) Cort is inactivated in the kidney by HSD11B2 and reactivated by HSD11B1 in the periphery. (3) Glucocorticoid receptor (GR) activity provides positive feedback on HSD11B1 activity, therefore increasing cort availability. Adapted from (Morgan *et al.*, 2014).

GCs act by binding to the glucocorticoid receptor (GR), which is expressed ubiquitously throughout the body. However, there are splice variants of the GR, with GRα and GRβ being the most commonly studied isoforms (Oakley and Cidlowski, 2011). GRα is responsible for the action of GCs, and there are at least eight isoforms of GRα, with GRα-C being the dominant isoform in the pancreas (Lu and Cidlowski, 2005). GCs are highly lipophilic and cross the cell membrane from the circulation, before directly binding GR in the cytoplasm. The

GC-GR complex then migrates into the nucleus to bind specific GC response elements and subsequently modify the transcription of thousands of genes relating to metabolism, immunity and proliferation, depending on the cell type (Schiller *et al.*, 2014; Ramamoorthy and Cidlowski, 2016).

1.8.1 Cushing's disease

Cushing's disease is caused by a chronic elevation of cortisol leading to various co-morbidities, including truncal obesity, diabetes or glucose intolerance, gonadal dysfunction, hirsutism, hypertension, muscle weakness, mood disorders and osteoporosis (Boscaro *et al.*, 2001). Some of these symptoms when taken together have come to be termed 'metabolic syndrome', specifically the interplay between hypertension, hyperglycaemia, and dyslipidaemia, all of which have strong associations. Indeed, it has been suggested that metabolic syndrome is caused by increased HSD11B1 activity (Bujalska, Kumar and M Stewart, 1997; Cooper and Stewart, 2009).

1.8.2 Glucocorticoids in inflammation and diabetes

Diabetes mellitus is considered an inflammatory disease, especially in the setting of metabolic syndrome in which adiposity is increased. This might explain the interplay between beta cell function and GCs. Human islets from donors with T2D show signs of inflammation and macrophage infiltration (Butcher *et al.*, 2014).

One of the primary roles of GCs is the suppression of the immune response. Most circulating cortisol is inactivated by cortisol binding globulin (CBG). When

it diffuses through areas of inflammation, factors secreted by neutrophils cause the cleavage of CBG, releasing cortisol into the immediate area where it can exert anti-inflammatory effects by repression of genes such as cytokines (Pemberton *et al.*, 1988).

One such cytokine is Interleukin 6 (IL-6), which is elevated in response to acute exercise as well as chronic obesity. In addition, IL-6 has been shown to be raised in patients with T2D (Pradhan *et al.*, 2001). It has also been shown that IL-6 can upregulate the number of glucocorticoid receptors, and potentially increase sensitivity to GCs which, in turn, acts to suppress the production of IL-6 (Dovio *et al.*, 2001). Whether this feedback occurs in the pancreatic islets, or in conditions of chronic elevated IL-6 remains unclear.

Another cytokine of interest with therapeutic potential is Interleukin-1 beta (IL1-β). However, in clinical trials using IL1-β inhibitors, there was no reduction in diabetes prevalence in the cohort after a median period of treatment of 3.7 years (Everett *et al.*, 2018). This has led to some debate in the field with regards to the importance of IL1-β.

1.8.3 Glucocorticoids and diabetes

Surplus GCs have been shown to cause insulin resistance and increased hepatic gluconeogenesis, as well as dyslipidaemia, therefore implicating them in type-2 diabetes (Dallman *et al.*, 1993). Additionally, overexpression of the GR in mice has been shown to impair insulin release (Delaunay *et al.*, 1997). Conditions such as Cushing's disease in which GC is chronically elevated requires an insulin tolerance test for definitive diagnosis (Crapo, 1979).

However, this GC excess is frequently paired with dyslipidaemia which makes it difficult to identify the contribution of each factor and may be relevant in light of the work presented in this thesis (Arnaldi *et al.*, 2010).

While systemic administration of potent synthetic GCs, such as dexamethasone, induces a compensatory increase in beta cell mass and eventually insulin secretory failure (Ogawa *et al.*, 1992), the effects directly on beta cell function are less well understood. Beta cell-specific GR overexpression reduces glucose tolerance, suggesting an important link between GCs and insulin release (Delaunay *et al.*, 1997). However, *in vitro* studies using isolated islets have shown inhibitory or no effect of GCs on glucose-stimulated insulin secretion, depending on the steroid potency, concentration and treatment duration (Gremlich, Roduit and Thorens, 1997; Lambillotte, Gilon and Henquin, 1997; Davani *et al.*, 2000; Koizumi and Yada, 2008; Swali *et al.*, 2008). By contrast, pre-receptor regulation via HSD11B1 impairs beta cell function in islets both *in vitro* and *in vivo* by increasing the GC bioavailability (Davani *et al.*, 2000; Ortsäter *et al.*, 2005; Turban *et al.*, 2012). Whereas 11-DHC has consistently been shown to impair beta cell function in islets from obese animals, conflicting reports exist regarding its effects on normal islets (Ortsäter *et al.*, 2005; Swali *et al.*, 2008).

More generally, the signalling components targeted by GCs are not well defined. While the exogenous application of GC subtly decreases NADP, cAMP and inositol phosphate production (Lambillotte, Gilon and Henquin, 1997) as well as insulin release, these studies were performed using high doses of dexamethasone, a synthetic GC with a 25-100 fold increased potency

compared with cortisol. Conversely, administration of dexamethasone in drinking water augments insulin release by increasing the number of docked exocytotic vesicles as well as beta cell mitochondrial potential/metabolism (Rafacho *et al.*, 2010). However, indirect effects of insulin resistance cannot be excluded, as studies in high fat diet-fed mice have shown that compensatory beta cell responses, including proliferation, occur within a few days (Stamateris *et al.*, 2013). Lastly, GC administration or GR knockdown in the early neonatal period alters the beta cell developmental programme, leading to reductions in the expression of key maturity markers including *Pdx1*, *Nkx6.1* and *Pax6* (Shen *et al.*, 2003; Gesina *et al.*, 2004). Whether this is also seen in adult islets, as is thought to occur during diabetes, is unknown (Guo *et al.*, 2013).

1.9 Aims and hypothesis

This work aims to further investigate the regulation of the pancreatic islet by glucocorticoids, as well as, if decreased heterogeneity of the pancreatic islet by overexpression of markers of beta cell identity causes impaired function. The overall objective of the work is to add to the body of knowledge regarding beta cell plasticity in order to open avenues for novel treatments for diabetes.

The first two results chapters focus on the effects of increased glucocorticoids on glucose responses in mouse and human islets respectively. The literature suggests that glucocorticoid excess will have a detrimental impact of beta cell function, a phenomenon seen in Cushing’s disease.

The final results chapter investigates how forced upregulation in genes for beta cell identity alter glucose homeostasis both *in vivo* and in isolated mouse islets. Previous work from (Johnston *et al.*, 2016) discovered a subset of immature beta cells which contribute to the synchronous nature of the islet. We hypothesised that ablation of this less mature subpopulation would lead to reduced coordination and, as a result, impaired function.

2 CHAPTER TWO – MATERIALS AND METHODS

2.1 Cell and tissue culture

2.1.1 Animal maintenance and breeding schemes

Mice were housed in the Biomedical Services Unit at the University of Birmingham and maintained under a 12-hour light/dark cycle and fed standard chow *ad libitum* unless stated otherwise. Tissue for *ex-vitro* work was normally harvested from mice between the ages of 8 and 12 weeks old unless they had previously been on a diet intervention which would have been a maximum of 4 weeks, starting at 8 weeks. Studies were regulated by the Animals (Scientific Procedures) Act 1986 of the UK, and the University of Birmingham's Animal Welfare and Ethical Review Body.

Male CD1 mice between the age of 8 and 12 weeks old from Charles River were used as wild type tissue donors for initial experiments using glucocorticoids. Subsequently, *Hsd11b1* null mice lacking exons 3 and 4 were on a C57BL background as previously described in (Kotelevtsev et al., 1997). Both sexes were used in knockout experiments, using littermate controls. Data from both genders were collected but pooled at analysis so any gender differences will be obscured.

Mice selectively overexpressing *Pdx1*, *Mafa* and *Ngn3* in response to doxycycline (dox) were generated by crossing mice harbouring two copies of the tetracycline trans-activator under the control of the *Ins2* promoter (RIP7rtTA)(Milo-Landesman *et al.*, 2001; Pullen *et al.*, 2012) with heterozygous animals engineered to possess M3C upstream of a tetracycline response

element (M3C-TetON) (Zhou *et al.*, 2008; Ariyachet *et al.*, 2016). Both genders were used as mentioned in the *Hsd11b1* methods above. Further information on the RIP7rtTA and M3C-TetOn mice can be found in 5.2.1.

2.1.2 Mouse islet isolation and culture

For each mouse, 5 mL of 1 mg/mL solution of collagenase NB 8 broad range (Nordmark Biochemicals, Uetersen, Germany; SERVA GmbH, Heidelberg, Germany) dissolved in Roswell Park Memorial Institute 1640 Medium (RPMI; Sigma, Poole, UK) was prepared, syringe filtered and placed on ice. Animals were culled by cervical dislocation and death was confirmed by the absence of heartbeat before the thoracic cavity was opened. Under a binocular dissecting microscope, the ampulla of Vater was clamped and the collagenase solution was injected into the bile duct using a 5 mL syringe and a 30-gauge needle. After inflation, the pancreas was removed and placed in a 50 mL Falcon tube with any remaining collagenase from the syringe and placed on ice.

Once all the pancreata had been removed, they were transported to the lab where they were warmed to 37°C in a water bath for 12 minutes for digestion. RPMI was added to the collagenase to make it up to 15 mL and centrifuged at 1500 rpm for 1 minute. The supernatant was discarded and 15 mL fresh RPMI was added. The Falcon tubes were shaken vigorously for 30 seconds to fully dissociate the pancreata and then centrifuged at 1500 rpm for 1 minute. This wash was repeated twice but with less vigorous shaking. After the final wash, the pellets were each resuspended thoroughly in 4 mL Histopaque 1.119 g/mL (Sigma, Poole, UK) using a plastic Pasteur pipette before being transferred to a

15 mL Falcon tube, and a further 4 mL Histopaque 1.083 g/mL (Sigma, Poole, UK) was added drop by drop. The tubes were topped up gently to 12 mL with RPMI and then centrifuged at 2500 rpm for 20 minutes with no deceleration at room temperature. The islets were removed from the interface between the Histopaque 1.083 g/mL and the RPMI using a plastic Pasteur pipette and transferred to a fresh 15 mL Falcon tube and topped up to 15 mL with RPMI to dilute the residual Histopaque. After centrifugation for 3 minutes at 1500 rpm, the supernatant was removed and the pellet resuspended in 10 mL “complete” RPMI supplemented with 10% foetal bovine serum (FBS), 100 units/ml penicillin and 100 µg/mL streptomycin (Thermo Fisher, Loughborough, UK). This was then transferred to a 10 cm petri dish and the islets picked manually into another petri dish containing complete medium and allowed to recover overnight.

Alternatively, if Histopaque 1.119 g/mL was unavailable, the digested pellets were resuspended in 10 mL Ficoll-Paque Plus 1.078 g/mL (GE Healthcare, Chalfont St Giles, UK) with 5 mL of RPMI layered on top before continuing with the 20-minute centrifugation step.

In all cases, figure legends refer to number of mice or number of islets or both. Number of mice represent biological replicates, to control for variation between inbred mice caused by differences in feeding or health state, combined with differences in islet prep (*e.g.,* complete or partial inflation of the pancreas). In all experiments islets from each mouse were divided evenly between all control and experimental conditions to mitigate for these biological effects. Subtle differences might be caused by different sizes of islet but again, islets were size

matched by eye using light microscopy to ensure this was minimal, as well as secretion measures corrected for total insulin content. Technical replicates, *i.e.* how many times each assay or condition was replicated to account for variation in read out from assays, are averaged before presentation as datapoints.

2.2 Live cell confocal imaging

All islet imaging experiments were conducted in ATP buffer, comprising HEPES-bicarbonate buffer saturated with CO_2, containing 120 mM NaCl, 4.8 mM KCl, 24 mM $NaHCO_3$, 0.5 mM Na_2HPO_4, 5 mM HEPES, 2.5 mM $CaCl_2$, and 1.2 mM $MgCl_2$.

2.2.1 Free Ca^{2+} measurements

Live cell intracellular Ca^{2+} imaging was performed using fluorescent dyes, either Fluo-8 (Stratech, Newmarket, UK) or Fura-2 AM (Hello Bio, Bristol, UK), which were initially resuspended in 9 µL DMSO and 2 µL pluronic acid to a stock concentration of 10 mM. Isolated islets (n=10-12) were loaded with one of these dyes diluted in HEPES-bicarbonate buffer to a final concentration of 10 µM for 45-50 minutes at 37°C, 5% CO_2. Ca^{2+} imaging was performed at 37°C using a temperature-controlled atmospheric chamber and heated chamber and insert. Assessment of Ca^{2+} responses to increasing stimulation was performed in ATP buffer containing 3 mM glucose for 3 minutes after which glucose concentration was increased to 11, 15 or 17 mM. Subsequently, after 20 minutes, KCl (10 or 30 mM) was added to induce a maximum response before ending the

experiment at 25 minutes. Images were taken every 3 seconds for standard Ca^{2+} imaging or every 150 ms for hub cell imaging.

Fluo-8 imaging was performed using either a Crest X Light spinning disk head coupled to a Nikon Ti-E automated base and 10 x/0.4 NA objective, or a Zeiss LSM780 meta-confocal and 10 x/0.45 NA objective. For the Crest system, excitation was delivered at λ = 458–482 nm (400 ms exposure; 0.33 Hz) using a Lumencor Spectra X Light Engine, and emitted signals detected at λ = 500–550 nm using a Photometrics Evolve Delta 512 EMCCD. For the Zeiss system, excitation was delivered at λ = 488 nm with an Argon laser, and emitted signals detected at λ = 499–578 nm using a GaAsP PMT spectral detector.

Fura-2 imaging was conducted using the spinning disk microscope detailed above using excitation at λ = 340 nm and λ = 385 nm delivered by a FuraLED system, with emitted signals detected at λ = 470–550 nm.

Fluo-8 fluorescence (F) was normalised to the minimum fluorescence (F_{min}) displayed as F/F_{min}. Fura-2 imaging was analysed using the “Ratio Plus” ImageJ plugin to generate 340/380 nm.

2.2.2 cAMP measurements

Changes in cAMP were measured using a modified Epac2-camps, a genetically encoded cAMP probe. Epac2-camps is a combination of the cAMP binding domain of exchange protein directly activated by cAMP 2 (Epac2) and two fluorophores able to undergo Förster energy resonance transfer (FRET) when <10 nm apart: a cyan fluorescent protein (CFP) and a yellow fluorescent protein

(YFP). Upon binding of cAMP to the nucleotide-binding domain, a conformation change occurs, increasing the distance between the two fluorophores, causing a decrease in FRET which can be measured using fluorescent microscopy (Nikolaev *et al.*, 2004). In this study, Cerulean/Citrine (Ce/Ci) Epac2-camps was used, which was generated by Cooper *et al*. and replaces the CFP and YFP with cerulean and citrine fluorophores, respectively (Everett and Cooper, 2013). This modification results in a less pH-sensitive probe to reduce imaging artefacts.

Pancreatic islets were transduced with 1µL of an adenoviral vector containing (Ce/Ci) Epac2-camps in 2 ml RPMI for 48 hours. Images of cyan and yellow were taken every 5 seconds to measure changes in cAMP concentration in response to increasing glucose concentrations (3 to 17 mM) using the Crest spinning disk microscope at an excitation of λ = 430-450 nm. Results were expressed as the ratio of cerulean (emission λ = 460-500 nm) to citrine (emission λ = 520-550 nm). Forskolin (FSK) 100 µM was used as a positive control to exert a maximal cAMP response.

2.2.3 ATP: ADP measurements

Changes in intracellular ATP: ADP ratios were measured using the modified GFP probe Perceval. Perceval contains a circularised Venus fluorophore inserted between the tyrosine 51 and isoleucine 52 residues of the bacterial protein GlnK1, normally responsible for sensing healthy metabolism. Binding of ATP to Perceval causes structural changes leading to an increase in the fluorescence at the 530 nm peak (Berg, Hung and Yellen, 2009).

Islets were treated with 1μL adenovirus encoding Perceval in 2 mL RPMI for 48 hours. Islets were imaged on the Crest spinning disk microscope (excitation λ = 458–482 nm; emission λ = 500–550 nm). Glucose concentrations were increased from 3 mM to 17 mM after 5 minutes and images were taken every 5 seconds.

2.3 Islet cell biology

2.3.1 Immunohistochemistry of islets

Isolated islets were washed once in phosphate-buffered saline (PBS) before being fixed in a solution of 4% formaldehyde in PBS at room temperature for between 15 minutes and 2 hours. Fixed islets were then washed with PBS and stored in PBS + 0.1% sodium azide at 4°C.

Primary antibodies (see Table 2) were diluted in blocking buffer (PBS containing 0.1% Triton X-100, 2% BSA) and added to islets before incubating overnight at 4°C. After two washes with PBS, secondary antibodies (see Table 2) were added (diluted 1:1000 in blocking buffer) and the samples were incubated for 1-2 hours at room temperature. Islets were then mounted on Superfrost glass slides (Thermo Fisher, Loughborough, UK) using VECTASHIELD Hardset Antifade Mounting Medium with DAPI (Vector Labs, Peterborough, UK) and allowed to set overnight at 4°C before imaging.

An additional antigen retrieval step was conducted for MAFA staining prior to blocking, in which the fixed islets were incubated in 500 μL citrate buffer (10 mM citric acid, 0.05% Tween 20, pH 6.0) for 20 minutes at 95°C. Citrate buffer was

removed after centrifugation at 1000 rpm for 1 minute and islets were resuspended in blocking buffer and incubated for 1 hour at room temperature.

2.3.2 Immunohistochemistry of pancreatic sections

Animals were culled and the pancreata were removed and placed on filter paper before being submerged in 10% formalin overnight at room temperature in bijous. The formalin was replaced with ethanol and stored long term at 4˚C.

Pacreata were washed with hot wax and then embedded in wax and allowed to set overnight before removal from the mould. They were sliced using a microtome and placed on Superfrost Plus glass slides (Thermo Fisher, Loughborough, UK).

The slides were washed three times in Histoclear for 2 minutes then for 5 minutes in ethanol (100%, 95% and 70%). Slides were then washed twice in deionised water for 2 minutes.

The pancreata on the slides were then circled with a hydrophobic barrier pen (Vector Labs, Peterborough, UK), and incubated with blocking buffer for 60 minutes at room temperature. The blocking buffer was then removed and blocking buffer containing diluted primary antibodies (see Table 2) was added and incubated overnight at 4˚C in a humidified chamber.

The pancreata were then washed three times for 10 minutes with blocking buffer and were incubated with secondary antibody (see Table 2) for 2 hours at room temperature in the dark. They were then washed a further three times for 10 minutes in blocking buffer and then incubated in 1µg/mL of Hoechst 33342

diluted in blocking solution (1:1000 dilution from stock). Excess liquid was removed and a drop of VECTASHIELD Hardset Antifade Mounting Medium with DAPI (Vector Labs, Peterborough, UK) was added and sealed under a coverslip. Slides were dried overnight before imaging and stored at 4˚C.

2.3.3 Table of antibodies

Target	Clone	Dilution	Company (Cat no.)
Primary Antibodies			
Anti-INSULIN	Rabbit monoclonal (C27C9)	1:500	Cell Signalling (3014S)
Anti-GLUCAGON	Mouse monoclonal (K79bB10)	1:2000	Sigma-Aldrich (G2654)
Anti-PDX1	Mouse monoclonal n/a	1:500	DSHB (F6A11)
Anti-MAFA	Rabbit polyclonal n/a	1:500	Bethyl Laboratories (IHC-00352)
Anti-SST	Mouse monoclonal (ICDCLS)	1:1000	Invitrogen (14-9751-80)
Anti-HA tag	Rabbit polyclonal (Poly9023)	1:500	BioLegend (902303)
Secondary Antibodies			
Anti-rabbit (DyLight 488)	Donkey polyclonal IgG	1:1000	Thermo Fisher Scientific (SA5-10038)
Anti-rabbit (Alexa Fluo 488)	Donkey polyclonal IgG	1:1000	Thermo Fisher Scientific (A-21206)
Anti-mouse (Alexa Fluo 568)	Goat polyclonal IgG	1:1000	Thermo Fisher Scientific (A-11004)
Anti-mouse (DyLight 633)	Goat polyclonal IgG	1:1000	Thermo Fisher Scientific (35513)
Anti-rabbit (Alexa Fluo 633)	Goat polyclonal IgG	1:1000	Thermo Fisher Scientific (A-21071)

Table 2 | Compilation of primary and secondary used in immunohistochemistry and immunocytochemistry experiments within this thesis. HA= hemagglutinin.

2.3.4 Glucose-stimulated insulin secretion

Islets were sorted by size and condition before 10-12 size-matched islets were transferred to 1.5 mL Protein LoBind Eppendorf tubes (Eppendorf, Stevenage,

UK) containing 500 mL ATP buffer containing 0.1% BSA and D-Glucose 3 mM. Tubes were transferred to a 37°C water bath and allowed to equilibrate for 30 minutes. The buffer was then discarded and carefully replaced with fresh ATP buffer containing 3 mM glucose and incubated for 30 minutes at 37°C. The supernatant was transferred to another 1.5 mL Protein LoBind Eppendorf tube and the islets were incubated with ATP buffer containing high glucose (11, 15 or 17 mM) for another 30 minutes in the water bath. The supernatants were transferred to fresh LoBind tubes, and the islets were resuspended in high glucose ATP buffer containing either KCl (10 mM) or exendin-4 (10-20 nM). After a 30-minute incubation at 37°C, the supernatant was transferred to a 1.5 mL LoBind Eppendorf and replaced with 500-1000 mL acid ethanol (75% ethanol, 1.5% 1 M HCl, 0.1% Triton X-100). Samples were then placed in a sonicating water bath for 5 minutes to lyse the cells, allowing measurement of total insulin.

Secreted and total insulin were measured after appropriate dilution using homogenous time-resolved fluorescence (HTRF). HTRF is a technique based on the Nobel prize-winning work on cryptands by Jean-Marie Lehn which used two antibodies linked to either Europium cryptate or XL665 which undergo FRET when bound to the protein of interest, in this case, insulin. This FRET can be measured using an appropriate plate reader and is relative to the amount of insulin in each well (Farino *et al.*, 2016). The kit used was the Insulin Ultra-Sensitive HTRF assay (Cisbio, Codolet, France) and the protocol was modified to allow smaller reactions (5 µL sample and 5 µL of combined antibody) in a 384 well plate. All other parameters were as per manufacturer's instructions.

Fluorescence was measured on a PHERAstar FS microplate reader (BMG labtech, Aylesbury, UK).

2.4 Molecular biology

2.4.1 DNA extraction and PCR for genotyping mice

Ear clips were digested overnight at 55°C in 200 µL lysis buffer containing 0.5 mg/mL proteinase K (Promega, Southampton, UK), 100mM Tris HCl (pH 8.5; Sigma, Poole, UK), 5 mM EDTA, 200 mM NaCl. Proteinase K was inactivated at 95°C for 1 hour. Genotyping was performed using 2x PCRBIO Taq Mix Red (PCRbio, London, UK) according to the manufacturer's protocol.

2.4.2 RNA extraction

RNA was isolated using phenol-chloroform extraction using a fume hood for all steps involving phenol. 50-100 islets were added to 1 mL TRIzol (Invitrogen, Paisley, UK), vortexed for 15 seconds and then incubated for 5 minutes at room temperature. 200 µL chloroform (Sigma, Poole, UK) was then added before vortexing thoroughly and incubating for 2 minutes at room temperature. After centrifuging at 12000 G for 15 minutes at 4°C, the aqueous phase was carefully transferred to a new RNAse-free tube. Following this, 0.5 mL 2-propanol (Sigma, Poole, UK) containing 2 µL RNA-grade glycogen (Fisher Scientific, Loughborough, UK) was added to the samples and the tube was gently inverted prior to incubation for 10 minutes at room temperature. Subsequently, the samples were centrifuged at 12000 G for 10 minutes at 4°C and the

supernatant removed. The pellets were washed with 1 mL molecular-grade ethanol (Sigma, Poole, UK) and centrifuged at 7500 G for 5 minutes at 4°C. The supernatant was carefully but thoroughly removed before the tubes were air-dried using a cover to avoid contamination from the air. The pellets were finally resuspended in 16 µL nuclease-free water (QIAGEN, Manchester, UK) and RNA concentration was measured using a NanoDrop ND-1000 Spectrophotometer (NanoDrop, DE, USA).

2.4.3 Reverse transcription

RNA samples were diluted to match the sample with the lowest concentration with nuclease-free water before using a High-Capacity cDNA Reverse Transcription Kit (Thermo Fisher, Loughborough, UK) according to the manufacturer's protocol.

2.4.4 Quantitative real-time PCR

Quantitative real-time PCR (RT-qPCR) was performed on either an Applied Biosystems 7500 or QuantStudio 5 instrument using PowerUp SYBR Green Master Mix (Thermo Fisher, Loughborough, UK). SYBR Green is a dye that combines with doubled stranded DNA, giving a signal relative to the quantity. The cDNA was diluted so that each well originally contained approximately 5 ng RNA and the RT-qPCR was run using a total volume of 10 µL. Samples were run in triplicate. All other parameters were as per the manufacturer's specifications. Fold-change in mRNA expression versus the housekeeping gene *β-actin* was calculated using the $2^{-\Delta\Delta Ct}$ method. *β-actin* was chosen as the

housekeeping gene, since it is the least influenced by GCs, which exert global transcriptomic actions on basic cell function. Nonetheless, going forward, it will be prudent to repeat studies using a panel of housekeeping genes, which can be internally calibrated e.g., via NanoString assays or similar. In experiments in which *Hsd11b1 mRNA* expression was measured in chapters 3 and 4, pre-validated TaqMan probes were used.

For a full list of oligonucleotides used for RT-qPCR, consult Table 3. Melt curves were always run to ensure a single peak and therefore product was being amplified. All primers were designed in such a way to avoid primer dimer and their efficiency was tested by generating a standard curve using known quantities of RNA to ensure we were detecting changes in the linear region of amplification.

2.4.5 Table of oligonucleotide primers

Oligos were synthesised by Sigma-Aldrich at 10 nmol scale and purified by desalting (Table 3).

Gene	Forward sequence	Reverse sequence
B-actin	CGAGTCGCGTCCACCC	CATCCATGGCGAACTGGTG
Ins1	GCTGGTGGGCATCCAGTAA	AATGACCTGCTTGCTGATGGT
Pdx1	CCAAAGCTCACGCGTGGA	TGTTTTCCTCGGGTTCCG
Nkx6.1	GCCTGTACCCCCCATCAAG	GTGGGTCTGGTGTGTTTTCTCTT
Mafa	CGGGAACGGTGATTGCTTAG	GGAGGTTGGGACGCAGAA
Ngn3	GGAGGTTGGGACGCAGAA	ACCGTCCCTGCAACTCACACTTTA
Cacna1d	GAAGCTGCTTGACCAAGTTGT	AACTTCCCCACGGTTACCTC
Cacna1c	CCAACCTCATCCTCTTCTTCA	ACATAGTCTGCATTGCCTAGGAT
Cacnb2	GCAGGAGAGCCAGATGGA	TCCTGGCTCCTTTTCCATAG
Adcy1	CGGAATTGCATGCCTTGAA	TCCATTCTTTTGTGCATGCTACAT
Adcy5	CTTCACCAGCCCCAAGAAAC	GAAGCGGCAGAGCACAGAAC
Adcy6	AGCCTTGGATAGGAAGGGACTACT	CTCCCTGCTTTGGCTTATATACCT
Adcy8	TTGGGCTTCCTACACCTTGACT	CGGTAGCTGTATCCTCCATTGAG
Adcy9	CATACAGAAGGCACCGATAG	CCGAACAGGTCATTGAGTAG
Cox6a2	GCCCAGCAAGATTCTGTGATG	TCTGGATGTCGGGTAAGGCAT
G6pc2	ACTCCACAGAAAGGACCAGG	GTCATGGTAACAGCTGCCCT
Pkib	CTGCTCCCTTAACTGCTGGAT	GATTGTGGAAAAGCGTGTGGT
Rgs4	GAGTGCAAAGGACATGAAACATC	TTTTCCAACGATTCAGCCCAT
Ucn3	AAGCCTCTCCCACAAGTTCTA	GAGGTGCGTTTGGTTGTCATC

Table 3 | Forward and reverse RT-qPCR primer sequences used in these studies.

2.5 Statistical analyses

All data were analysed using either GraphPad Prism 7, 8 or 9 (San Diego, CA, USA). Data were checked for normality using column statistic with the Shapiro-Wilk's test. If normal, pairwise comparisons were made by student’s t-test and multiple comparisons were made using one or two-way ANOVA as appropriate (with Bonferroni or Tukey post hoc test). Differences were considered significant if the P-value was less than 0.05. * $P < 0.05$, ** $P < 0.01$.

3 CHAPTER THREE – GLUCOCORTICOIDS REPROGRAM MURINE BETA CELLS TO PRESERVE INSULIN SECRETION

3.1 Introduction

Exposure to excessive glucocorticoid has been shown have a negative impact on pancreatic beta cell function and insulin release (Ogawa *et al.*, 1992). However, GCs at physiological levels are essential for many homeostatic processes, including glycaemic control (Andrews and Walker, 1999). Moreover, most studies look at islets taken from animals treated systemically with GC (e.g., in drinking water), making it impossible to untangle their effects from compounding variables such as dyslipidaemia and insulin resistance. GC levels at the tissue level are controlled by the enzyme HSD11B1 and diseases characterised by elevated circulating GC (Cushing's) show insulin resistance and glucose intolerance (Tomlinson, Walker, *et al.*, 2004). Other studies have used supraphysiological concentrations of GC, or highly active synthetic GCs, resulting in unrealistic outcomes (Ogawa *et al.*, 1992; Gremlich, Roduit and Thorens, 1997; Lambillotte, Gilon and Henquin, 1997).

While the connection between glucocorticoids and diabetes has long been established, the mechanisms through with they interact, and the implications for health and disease are unknown (Dallman *et al.*, 1993). Corticosterone is elevated under fasting conditions and in streptozotocin-induced diabetes. Blood insulin levels can be partially protected from the effects of streptozotocin by adrenalectomy. 48 hour treatment with high levels of corticosterone leads to reduced insulin and leptin levels (Makimura *et al.*, 2003). Adrenalectomy leads to a significant reduction in proinsulin mRNA in both fasting and fed states (Fiedorek and Permutt, 1989).

To provide clarity to the field, mouse islets treated for 48 hours with GC were subjected to a variety of functional analyses. Live cell imaging, using fluorescent dyes, was used to measure glucose and KCl induced calcium changes, the primary step proximal to insulin secretion (as described in 1.3), as well as the secondary amplifying pathway mediated by cAMP generation. Glucose stimulated insulin secretion was also assayed using HTRF as the primary readout of islet function. In addition, mRNA was quantified using RT-qPCR. However, how the pancreatic beta cells react to the increase in circulating GC is unknown. This chapter seeks to establish the adaptations that might occur at the level of the islet in response to physiologically relevant levels of GC excess.

3.1.1 Aims and hypothesis

The aim of this chapter was to elucidate the effects of elevated, but physiological, levels of GCs directly on beta cell function. Given the available literature, and the profound glucose intolerance seen in people suffering from Cushing's, we hypothesised that glucocorticoids would have a negative impact on beta cell function, specifically glucose stimulated insulin secretion.

3.2 Methods

3.2.1 Animals

Wild-type mice (C57BL6 or CD1) were ordered from Charles River and used for breeding or as tissue donors between the age of 8 and 12 weeks. Whole body *Hsd11b1* null mice (*Hsd11b1*$^{-/-}$) lacking exons 3 and 4, previously described in (Kotelevtsev *et al.*, 1997), were donated by Professor Gareth Lavery. These mice were reported to have no detectable levels of *Hsd11b1* mRNA in liver tissue assessed by northern blot, and hepatic HSD11B1 activity was less than 5% of wild type. HSD11B2 activity in these mice was normal (Kotelevtsev *et al.*, 1997).

3.2.2 Glucocorticoid treatment

Islets were cultured as previously described. Mouse islets were treated for 48 hrs with either 11-DHC or corticosterone. 48 hours was chosen to elicit a short term response, while avoiding long term changes. GCs were diluted in 100% molecular grade ethanol (Sigma, Poole, UK) at a stock concentration of 1 mM in glass vials before being diluted in complete RPMI for a final concentration either 20nM or 200 nM 11-DHC, or 20 nM corticosterone. These concentrations and times were based upon previous work, allowing us to replicate data and make direct cross-comparisons (Swali *et al.*, 2008). Control samples were treated with 100% ethanol only (0.2% final concentration in media).

In experiments using the GR antagonist, RU486 (aka mifepristone) was used at a concentration of 1 µM and was applied in parallel with the GC, therefore treatment time was 48 hours. This concentration was used as recommended by work previously carried out in the department (Swali *et al.*, 2008).

3.2.3 ATP quantification

ATP was measured in batches of 25 islets incubated with either 3 mM or 17 mM glucose using an ATP Determination Kit, 200-1,000 assays (Thermo Fisher Scientific, Loughborough, UK) according to the manufacturer's recommendations. Luminescence was measured using a PHERAstar FS microplate reader (BMG Labtech, Aylesbury, UK). Total ATP was then normalised to protein, which was measured using a nanodrop.

3.2.4 Super-resolution imaging

Islets were fixed using 4% paraformaldehyde overnight at 4ºC before immunostaining using rabbit monoclonal anti-insulin (Cell Signalling Technology; 1:400) and goat anti-rabbit Alexa568 (1:1000). Super-resolution imaging was performed in three-dimensions using a VisiTech iSIM module coupled to a Nikon Ti-E microscope and a 100x/1 1.49 NA objective (125 nm resolution; 350 nm axial resolution). Excitation was delivered using a λ = 561 nm laser and emitted signals captured at λ = 633-647 nm using a Hamamatsu ORCA-Flash4.0 sCMOS.

3.2.5 Electrophysiology

All electrophysiology and analysis of said electrophysiology was kindly performed by Dr Nicholas Vierra and Dr David Jacobson from the University of California, Davis. VDCC currents were recorded from dispersed mouse β-cells as previously described (Zhu *et al.*, 2017). Patch electrodes were pulled to a resistance of 3–4 MΩ then filled with an intracellular solution containing (in mmol/L) 125 CsCl, 10 tetraethylammonium Cl, 1 $MgCl_2$, 5 EGTA, 10 HEPES, 3 MgATP, pH 7.22 with CsOH. Cells were patched in HEPES-buffered solution + 17 mmol/L glucose. Upon obtaining the whole-cell configuration with a seal resistance >1 GΩ, the bath solution was exchanged for a modified HEPES-buffered solution containing (in mmol/L) 62 NaCl, 20 tetraethylammonium Cl, 30 $CaCl_2$, 1 $MgCl_2$, 5 CsCl, 10 HEPES, 17 glucose, 0.1 tolbutamide, pH 7.35 with NaOH. β-Cells were perfused for 3 min with this solution before initiating the VDCC recording protocol. Voltage steps of 10 mV were applied from a holding potential of −80 mV; linear leak currents were subtracted online by using a P/4 protocol. Data were analysed by using Clampfit software (Molecular Devices).

3.3 Results

3.3.1 Glucocorticoids impair beta cell Ca^{2+} fluxes

Pancreatic islets from wild-type mice were treated with either 20 nM or 200 nM 11-DHC or 20 nM corticosterone before Ca^{2+} imaging. Using this approach, it was seen that, while low dose 11-DHC (20 nM) has no effect of Ca^{2+} fluxes, both 200 nM 11-DHC and 20 nM corticosterone treatment led to impaired Ca^{2+} signalling (Figure 3-1 A-E). Changes in fluorescence in fluo-8 treated islets in response to glucose (ΔF), as well as the area under the curve (AUC), were both significantly reduced in islets treated with either 200 nM 11-DHC or 20 nM corticosterone, compared with control (Figure 3-1 A-D). When challenged with 10 mM KCl to exert a maximal depolarising response, significant impairment of Ca^{2+} fluxes were only observed in islets treated with 20 nM corticosterone (Figure 3-1 E).

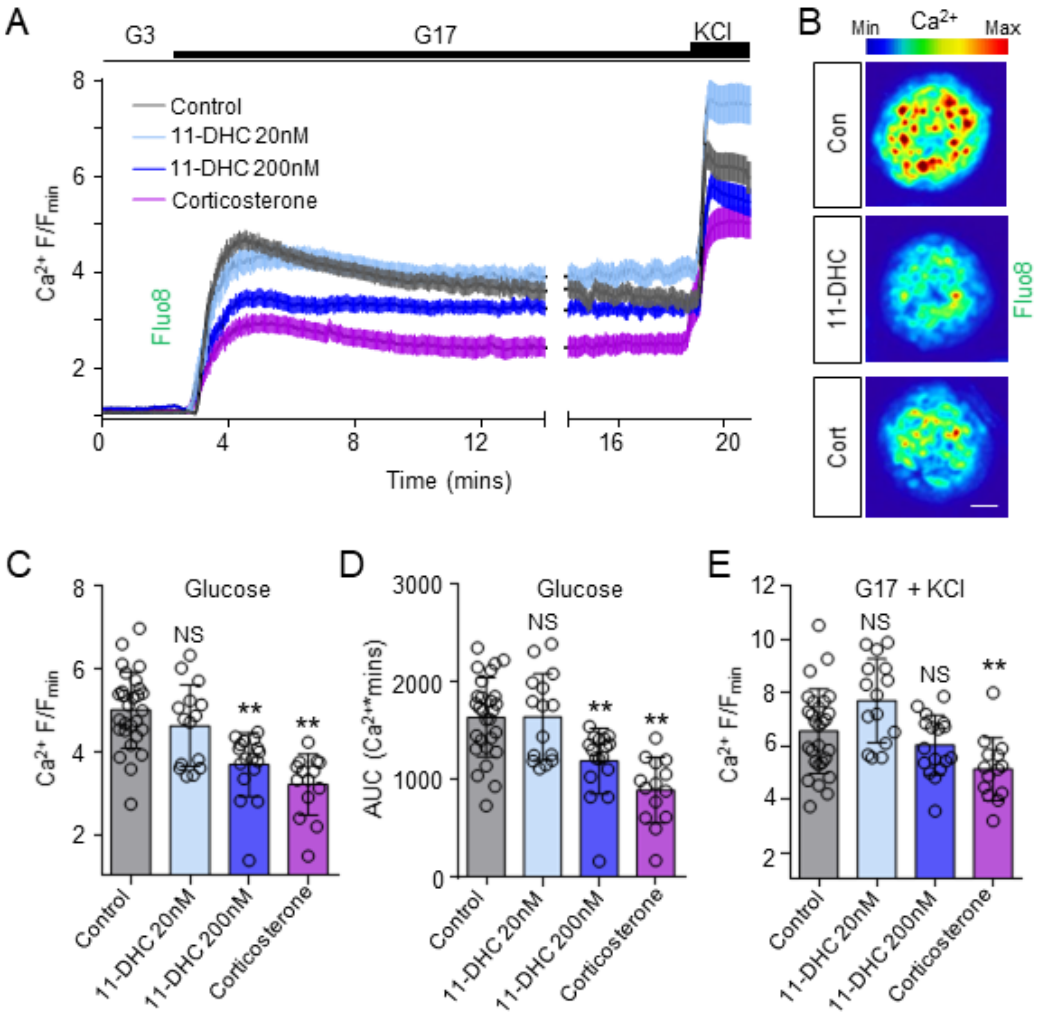

Figure 3-1 | GCs impair Ca^{2+} fluxes in mouse islets. (n = 14–28 islets from six animals). (A) Mean traces of Ca^{2+} imaging of mouse islets treated with either vehicle, 20 nM 11-DHC, 200 nM 11-DHC or 20 nM corticosterone. Glucose concentration increased from 3 mM to 17 mM after 3 minutes and 10 mM KCl added at 20 minutes. F/F_{min} plotted every 3s. Error bars are SEM. (B) Maximum fluorescence projection of islets treated with either vehicle or GC. (Scale bar = 20 µm) (images cropped to show a single islet). (C) Max F/F_{min} response to 17 mM glucose. Error bars are SD. (D) The area under the curve of traces from A for the first 20 minutes representing glucose response. Error bars are SD. (E) Bar graph showing max F/F_{min} response to 10 mM KCl in islets from A. Error bars are SD.

To further investigate Ca^{2+} dynamics in these islets, the change in frequency of Ca^{2+} oscillations at 11 mM glucose was measured and found to be significantly decreased in 200 nM 11-DHC and 20 nM corticosterone treated islets when compared with vehicle only (Figure 3-2 A&B).

Subsequently, we wondered if the incretin induced Ca^{2+} dynamics of these islets were changed after GC treatment. To interrogate this, islets treated with GC were incubated at 11 mM glucose and Ca^{2+} oscillations were observed using Fluo-8. 20 nM exendin-4 was added and oscillation frequency before and after was compared. Despite robust increases in oscillation frequency after addition of exendin-4, there were no differences in islets treated with 200 nM 11-DHC or 20 nM corticosterone (Figure 3-2 C-E), suggesting that neither 11-DHC or corticosterone impact GLP1R signalling.

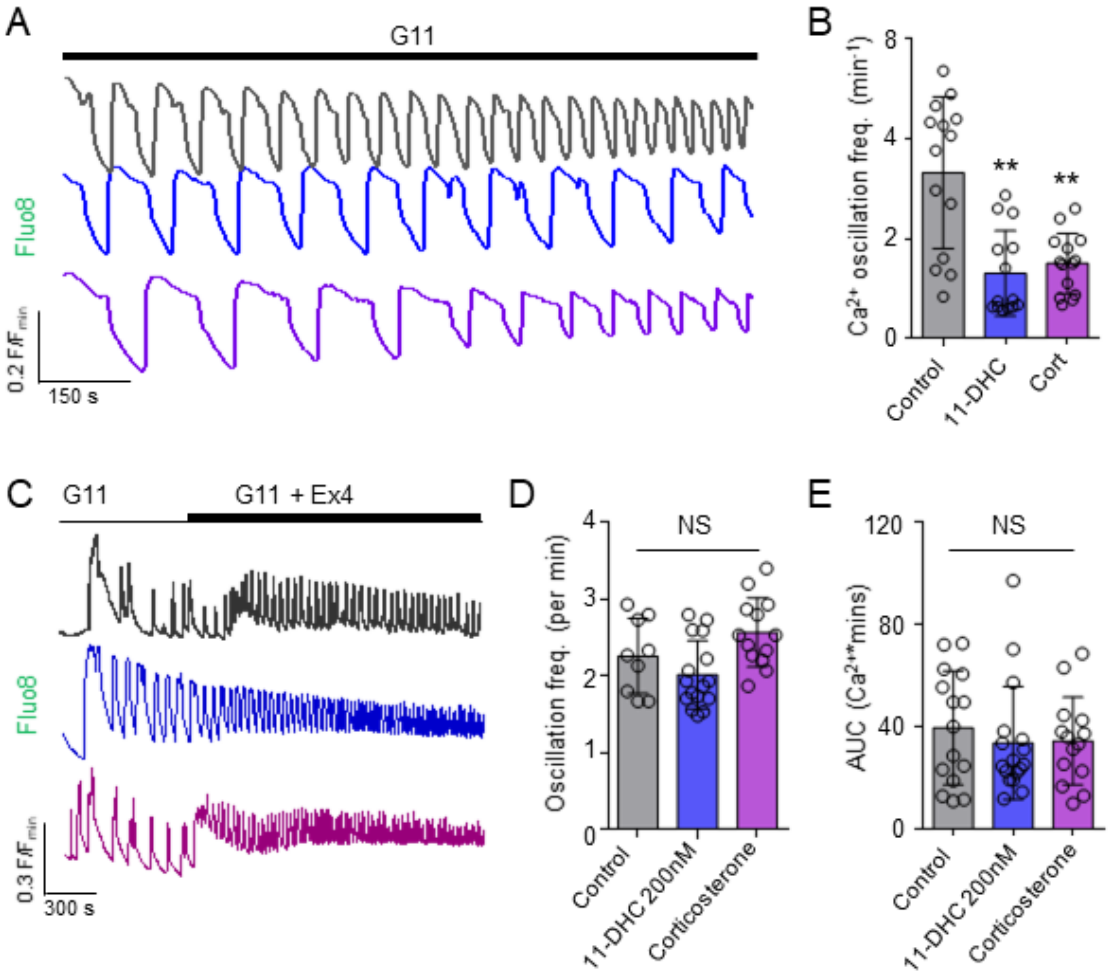

Figure 3-2 | GCs impair Ca^{2+} spiking activity in mouse islets. (A) Representative traces showing Ca^{2+} oscillations at 11 mM glucose in mouse islets treated with either vehicle (top), 200 nM 11-DHC (middle) or 20 nM corticosterone (bottom) reported using Fluo-8. (n = 14 islets from three animals). (B) Bar graph of mean Ca^{2+} oscillation frequencies demonstrated in A. Error bars are SD. (C) Response to 10 nM exendin-4 (Ex4) of mouse islets treated with either vehicle (top), 200 nM 11-DHC (middle) or 20 nM corticosterone (bottom). (n = 14–17 islets from three animals). (D) Bar graph of mean oscillation frequency from traces in C shows no effect of GC treatment. Error bars are SD. (E) Bar graph of mean area under the curve (AUC) of traces from C demonstrate no change in response to GC treatment. Error bars are SD.

3.3.2 Glucocorticoids do not alter beta cell identity, metabolism or VDCC subunit gene expression, but do impair VDCC function.

To determine if changes in beta cell identity could be responsible for altered Ca^{2+} fluxes, we measured gene expression of the primary beta cell differentiation markers, *Pdx1* and *Nkx6.1* (Figure 3-3). However, there were no significant differences in these genes when compared with the housekeeping control gene, *β-actin*, for 11-DHC and corticosterone. This suggests that GCs do not elicit detectable effects on beta cell maturation/differentiation.

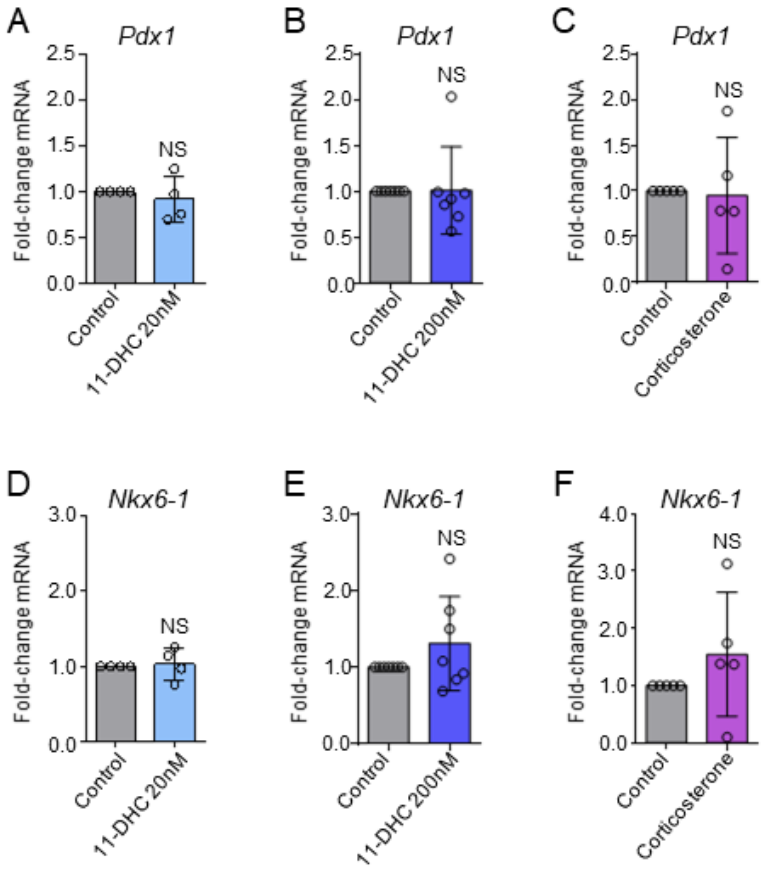

Figure 3-3 | Gene expression quantification of key beta cell maturity markers in mouse islets. *Pdx1* (A-C) and *Nkx6.1* (D-F) showed no change in islets treated with either 20 nM 11-DHC (A&D), 200 nM 11-DHC (B&E) or 20 nM corticosterone (C&F). Data is displayed as $2^{\Delta\Delta Ct}$ against *β-actin*. Error bars are SD. (n = 4–7 animals).

With this is mind, RT-qPCR was used to determine if expression of genes responsible for the expression of the major VDCC subunits, *Cacna1c*, *Cacna1d and Cacnb2,* might instead underlie altered Ca^{2+} fluxes. Upon investigation of these genes, there also appeared to be no statistical differences in mRNA expression in islets after treatment with GCs (Figure 3-4).

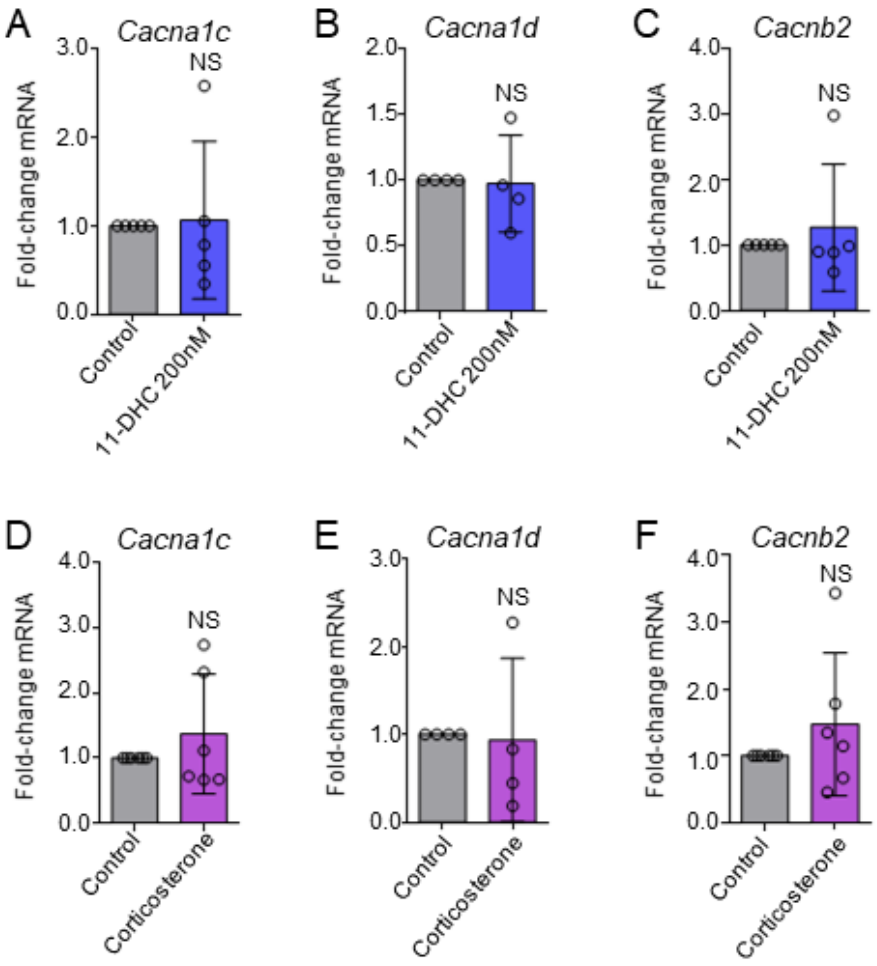

Figure 3-4 | Despite impaired calcium fluxes, mouse islets treated with GCs show normal mRNA expression of key VDCC subunits. (A-C) mRNA expression of the VDCC subunits, *Cacna1c*, *Cacna1d and Cacnb2* in islets treated with 200 nM 11-DHC. (D-F) *Cacna1c*, *Cacnb2* and *Cacna1d* expression in islets treated with 20 nM corticosterone. Data is displayed as $2^{\Delta\Delta Ct}$ vs *β-actin*. Error bars are SD. (n = 4–6 animals).

Despite the unchanged gene expression of the VDCCs in islets treated with GCs, we went on to check if the function of these channels is affected to explain the reduced calcium fluxes. Using patch clamp electrophysiology to interrogate the electrical properties of these islets, a marked reduction in Ca^{2+} conductance was detected, suggesting that Ca^{2+} is unable to properly enter the cell following GC treatment (Figure 3-5).

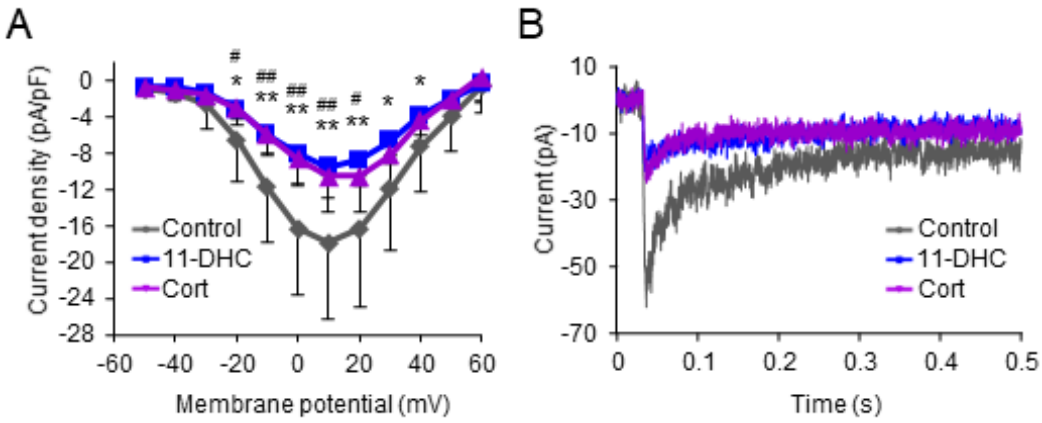

Figure 3-5 | GC-treated mouse islets show impaired Ca^{2+} conductance. (A) 11-DHC and corticosterone reduce VDCC conductance, as shown by the voltage-current relationship. Error bars are SD. (B) Representative Ca^{2+} current traces of VDCC conductance shown in A. (n = 4 animals).

Since altered Ca^{2+} fluxes could plausibly stem from defective K_{ATP} channel conductance (as implied by KCl stimulation), as well as changes in cell metabolism, ATP/ADP ratios were imaged. There was no difference in glucose-induced changes in ATP/ADP ratios in mouse islets treated with 11-DHC or corticosterone, determined using Perceval (Figure 3-6 A&B). Additionally, the duration of the lag period between addition of glucose and the ramp up of ATP generation was unaffected. This excludes the possibility that cytosolic Ca^{2+} deficits in GC-treated islets were caused by metabolic defects. This finding is supported by static biochemical ATP luciferase assays in which no changes

were seen in total ATP in mouse islets treated with GC (Figure 3-6 C). Such confirmation was necessary since GC treatment might influence Perceval expression or pH (which would impact GFP intensity). By contrast, luciferase is largely pH stable and does not require cell transduction.

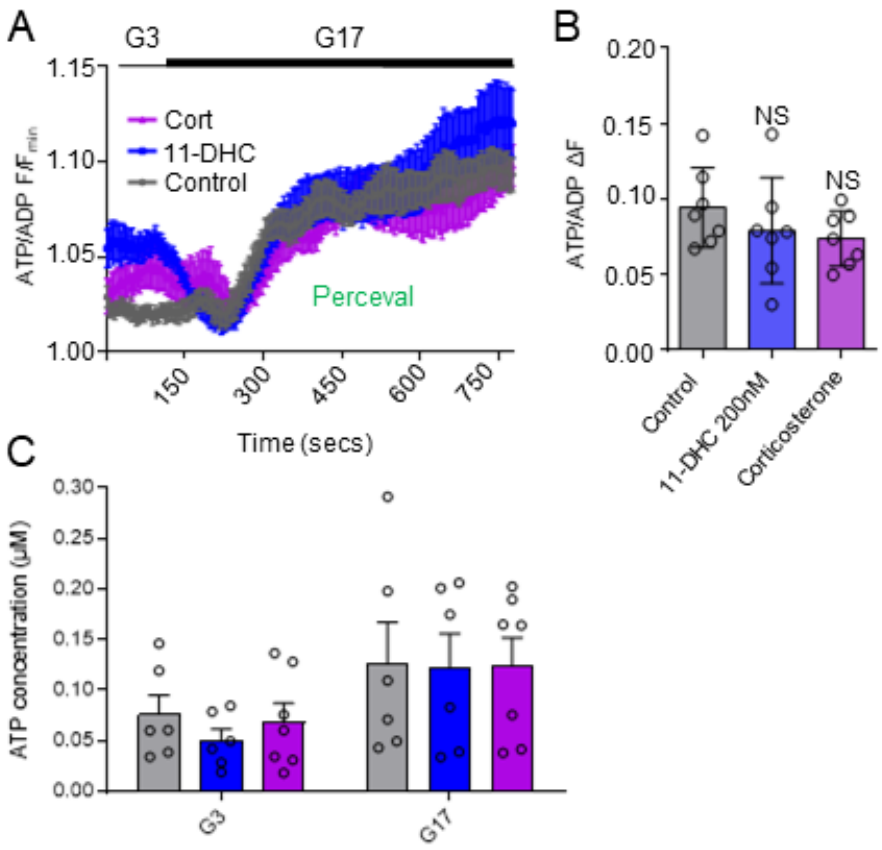

Figure 3-6 | Changes in ATP/ADP ratios and absolute ATP levels in response to glucose remain unchanged in mouse islets treated with GCs, compared with control islets. (A) Mean ATP/ADP traces from Perceval imaging experiments. Error bars are SEM. (n = 7 islets from 4 animals) (B) Scatter plot with bars showing delta fluorescence for A. Error bars are SD. (C) ATP concentrations in islets in either 3- or 17-mM glucose treated with either vehicle (grey), 200 nM 11-DHC (blue) or 20 nM corticosterone (purple). Quantified by luciferase assay. Error bars are SD. (n= 6-7 animals)

3.3.3 Insulin secretion and gene expression are unchanged in mouse islets treated with glucocorticoids

Despite defects in Ca^{2+} signalling, GC-treated mouse islets were found to possess normal secretory capacity and total insulin content (Figure 3-7 A&B), which correlated with unchanged *Ins1* mRNA levels versus control islets (Figure 3-7 C-E).

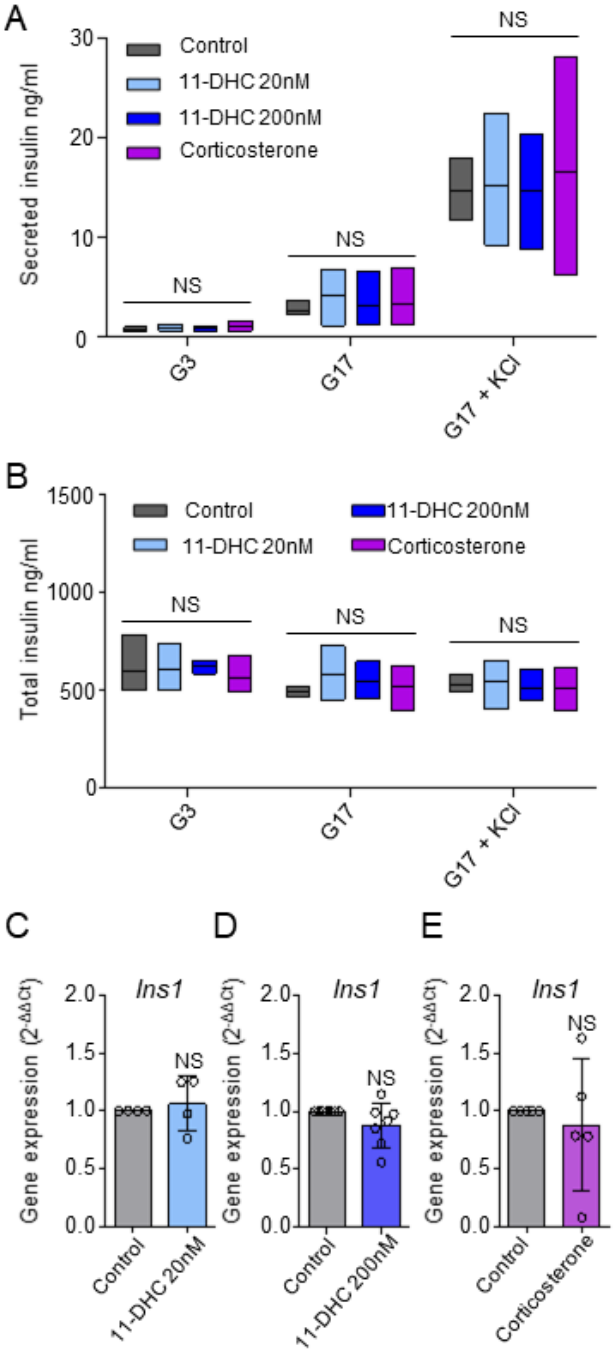

Figure 3-7 | GC treatment does not affect GSIS in mouse islets. (A) Box plot showing glucose-stimulated insulin secretion (GSIS) in mouse islets treated with either control, 20 nM 11-DHC, 200 nM 11-DHC or 20 nM corticosterone. (n = 5 animals) (B) Box plot of total insulin content of islets used for GSIS experiment in A. (n = 3 animals) (C&D) Bar graph of relative *Ins1* mRNA quantity in GC-treated islets vs control ($2^{-\Delta\Delta Ct}$). Error bars are SD. (n = 4–7 animals).

3.3.4 Glucocorticoids upregulate cAMP generation via increased *Adyc1* gene expression

To identify the pathway responsible for normal insulin secretion in spite of impaired Ca^{2+} fluxes, we utilised an adenovirus harbouring the genetically encoded sensor EPAC2-camps to measure glucose induced rises in cAMP in islets after treatment with GC. Treatment of mouse islets with either 200 nM 11-DHC or 20 nM corticosterone caused a significant augmentation in glucose-stimulated cAMP rises (Figure 3-8 A-C).

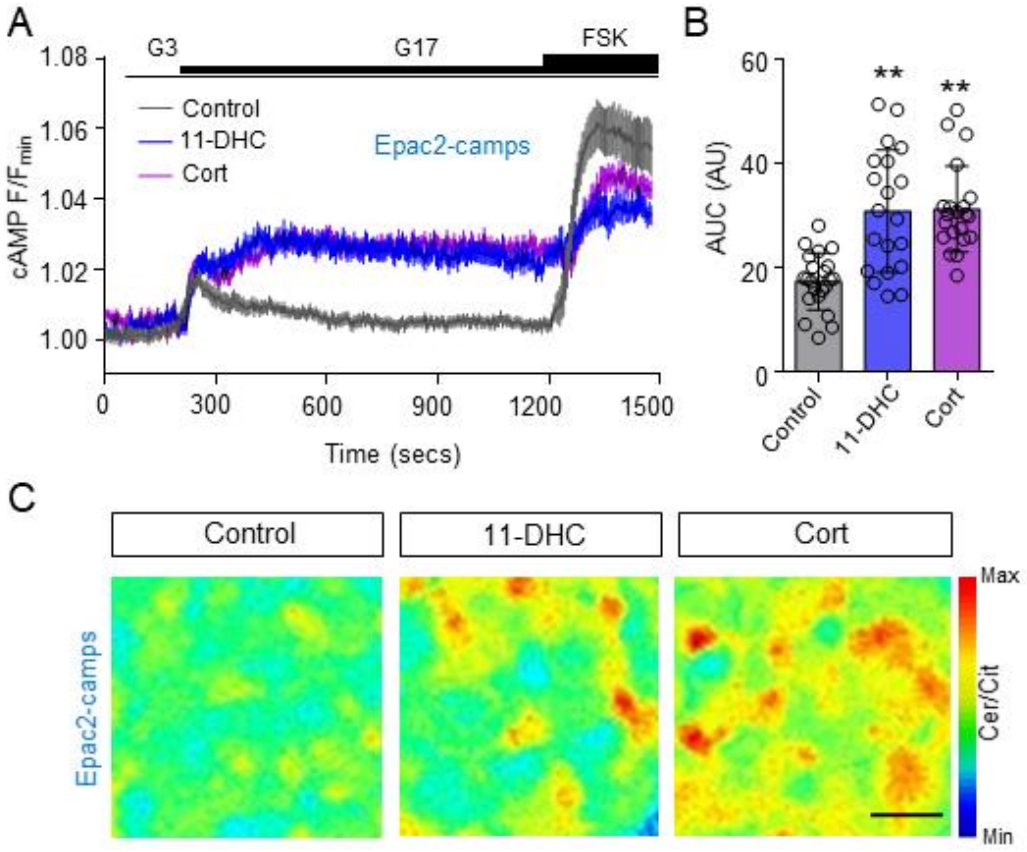

Figure 3-8 | GCs significantly increase cAMP generation in mouse islets in response to 17 mM glucose. (A) Mean traces of cAMP imaging of mouse islets treated with either control, 200 nM 11-DHC or 20 nM corticosterone. Error bars SEM. (n = 20–24 islets from 5 animals) (B) Bar chart of the area under the curve for cAMP traces in A show significant increases in those islets treated with either 11-DHC or corticosterone. Error bars are SD. (C) Pseudo-coloured representative images of cAMP imaging at 17 mM glucose. (Scale bar = 10 µm).

As the cAMP pathway is the main mechanism through which the incretin exendin-4 acts, we investigated cAMP responses after supplementation with 20 nM exendin-4. However, there was no difference in these experiments, suggesting that the improvements in cAMP generation were specific to glucose stimulation (Figure 3-9 A&B).

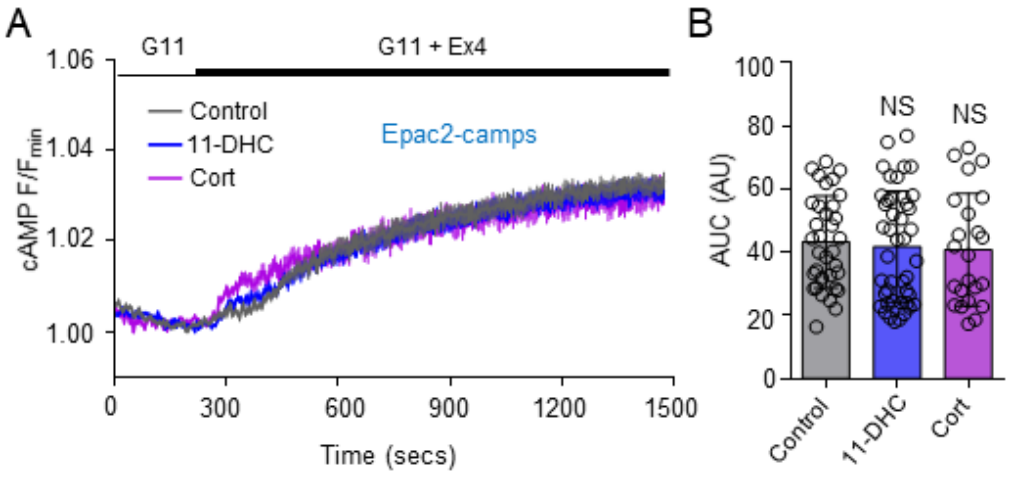

Figure 3-9 | GCs have no effect on cAMP responses to exendin-4 in mouse islets. (A) cAMP generation in response to 20 nM exendin-4 in mouse islets treated with GC for 48 hours showing no changes. Error bars are SEM. (B) Bar chart showing the AUC of traces from C. Error bars are SD. (n = 24–46 islets from 4 animals).

To further elucidate the mechanisms through which cAMP generation is improved in islets after 48-hour treatment with GCs, we measured gene expression of the adenylate cyclase family of genes, *Adcy1, Adcy5, Adcy6, Adyc8* and *Adcy9*. While most genes remained unchanged after treatment with either 11-DHC or corticosterone, *Adcy1* expression was significantly increased by both GCs (Figure 3-10). This could explain the improved cAMP responses to glucose, since *Adcy1* is stimulated by both Ca^{2+} and the intermediate calcium binding signalling molecule calmodulin (Hanoune and Defer, 2001).

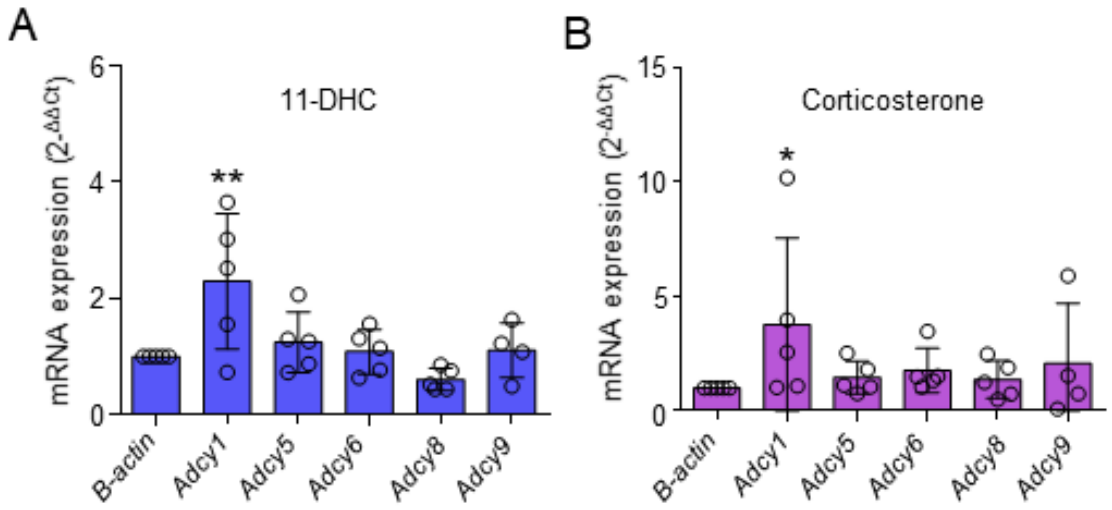

Figure 3-10 | Gene expression of *Adcy1* in mouse islets is increased after treatment with GC. Values are expressed as $2^{-\Delta\Delta Ct}$ using *β-actin* as the housekeeping gene. (A) Bar graph showing changes in mRNA levels of *Adcy* isoforms in mouse islets treated with 200 nM 11-DHC. Error bars SD. (n = 4–5 animals) (B) Bar graph showing changes in mRNA levels of *Adcy* isoforms in mouse islets treated with 20 nM corticosterone. Error bars are SD. (n = 4–5 animals).

Super resolution microscopy revealed an increase in membrane-bound secretory insulin granules in GC-treated islets, which might result from upregulated cAMP responses to glucose (Figure 3-11 A&B). To confirm this hypothesis, glucose-stimulated insulin secretion assays were repeated using 100 µM of the PKA inhibitor, H89, since PKA is downstream of cAMP in the signalling pathway. Confirming the previous result, 200 nM 11-DHC had no effect on GSIS and, while 100 µM H89 also had no effect alone, the combination of H89 and 11-DHC led to significantly reduced GSIS (Figure 3-11 C). This may be due to H89 blocking the compensatory increase in cAMP production after GC treatment while the impaired Ca^{2+} fluxes are still present, leading to reduced secretion of insulin at high glucose concentration.

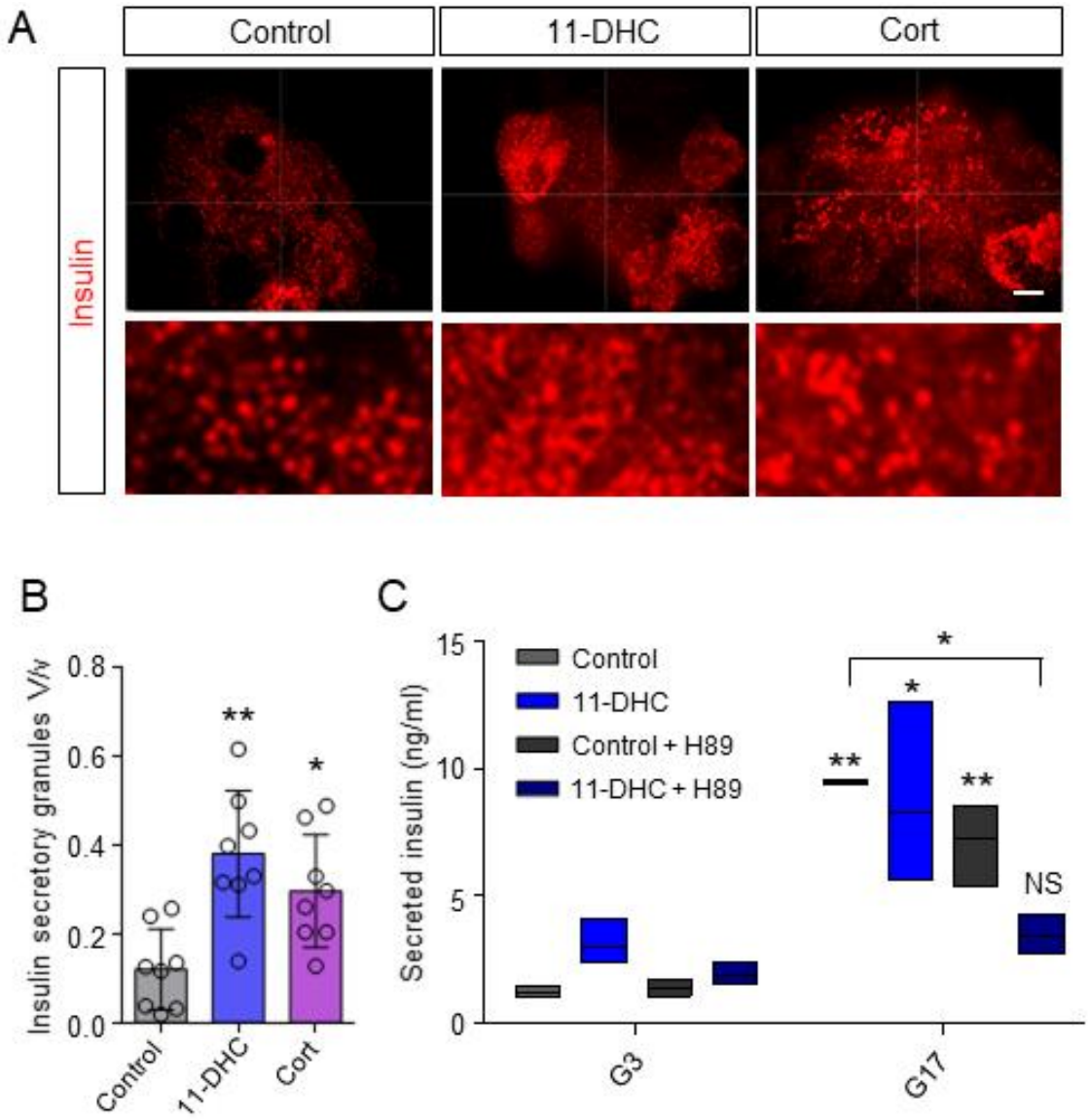

Figure 3-11 | GC-treated mouse islets have increased membrane-bound insulin secretory granules but have impaired GSIS when treated with both 11-DHC and H89. (A) Representative images of insulin granule staining in mouse islets treated with either control, 200 nM 11-DHC or 20 nM corticosterone. (Scale bar = 5 µm; bottom panel shows zoom-in) (B) Bar chart of insulin secretory granule staining quantified from A. Error bars are SD. (n = 8 cells from three animals) (C) Box plot of GSIS from islets treated with either control, 200 mM 11-DHC alone, 100 µM H89 alone, or 200 mM 11-DHC and 100 µM H89 together (n= 30 islets from 2 animals).

To confirm the contribution of adenylate cyclase in the maintenance of normal glucose secretion in islets treated with GC, mouse islets were treated with palmitate which has been shown to reduce *Adcy9* expression. Chronic exposure of 11-DHC treated islets to palmitate caused a significant decrease in

glucose-stimulated cAMP generation compared to islets treated with BSA and 11-DHC (Figure 3-12), as expected from previous studies (Tian *et al.*, 2015).

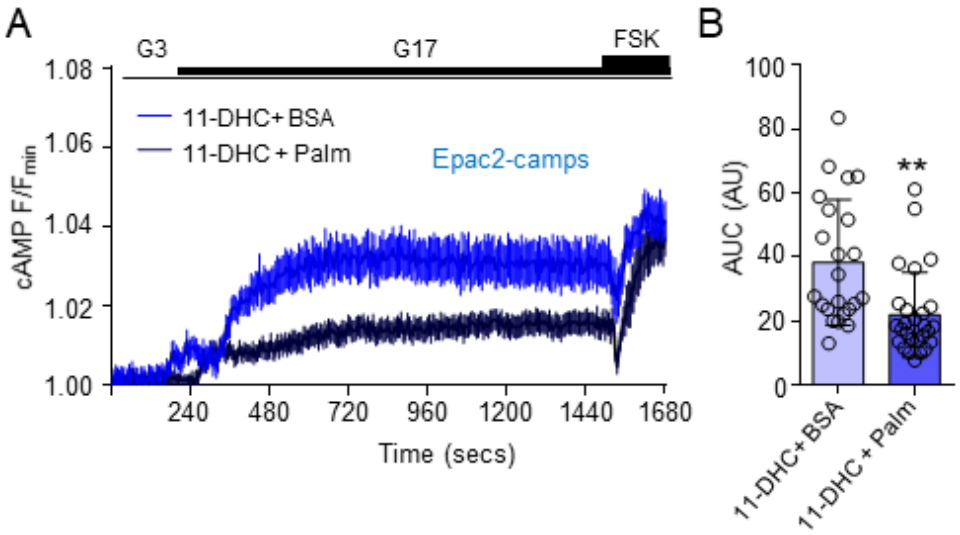

Figure 3-12 | Palmitate and 11-DHC significantly decreases cAMP production in response to glucose in mouse islets when compared with 11-DHC and BSA. (A) Mean traces of cAMP imaging experiments in islets treated with 200 nM 11-DHC and either BSA or palmitate. Error bars are SEM. (B) Bar chart showing area under the curve for cAMP traces in A. Error bars are SD. (n = 23–27 islets from 4 animals).

3.3.5 *Hsd11b1* mRNA is detectable in mouse islets and is expressed in an allele dependent manner in knock out mice

As the role of *Hsd11b1* in the pancreatic islets is a matter of debate (Pullen, Huising and Rutter, 2017), despite measurable conversion of 11-DHC to corticosterone (Davani *et al.*, 2000), we set out to confirm its presence. RNA was extracted from liver, muscle and pancreatic islet tissue taken from wild-type mice. RT-qPCR was conducted using TaqMan probes against *Hsd11b1* and *β-actin* for normalisation. *Hsd11b1* was clearly detectable in islet samples at levels similar to those in muscle; however, both islet and muscle contained much lower expression when compared with liver (Figure 3-13 A). This finding

in islets was confirmed by additional experiment using mice from a whole-body *Hsd11b1* knockout mouse, in which wildtype mice showed robust expression, with heterozygous mice showing reduced expression (approximately half) and *Hsd11b1* mRNA being undetectable in knockout mice (Figure 3-13 B).

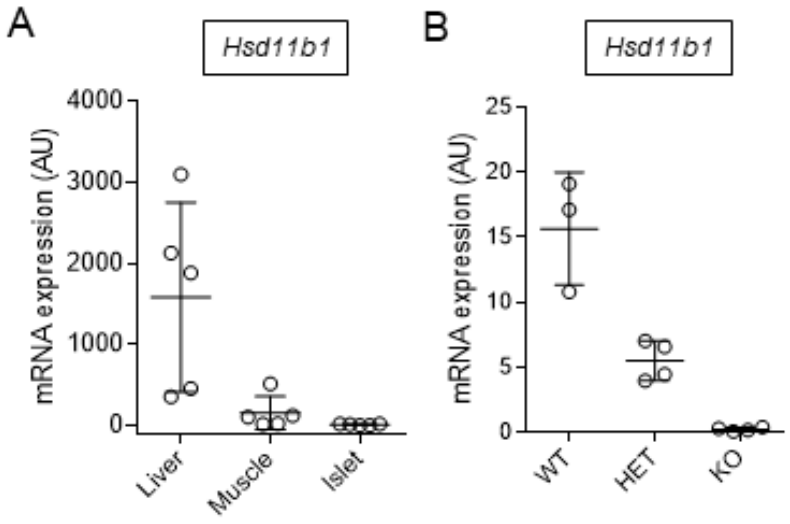

Figure 3-13 | HSD11B1 mRNA quantity in mouse tissues. Expression was measured using specific TaqMan probes controlled for using *β-actin* as a housekeeping gene. (A) While *Hsd11b1* mRNA levels are much higher in liver and muscle, expression is still detectable in islets. (n = 5 animals) (B) *Hsd11b1* expression in pancreatic islets changes in an allele dependent manner. In knockout (KO) mice lacking any copies of *Hsd11b1*, mRNA expression is absent. In mice with either one (heterozygotes, HET) or two (wild type, WT) copies of the gene there is quantifiable mRNA expression (n = 3-4 animals).

3.3.6 *Hsd11b1* knockout protects islet Ca^{2+} flux from the adverse effects of glucocorticoid exposure

To assess the role of *Hsd11b1* in the beta cell alterations seen after GC treatment, experiments were repeated in C57BL6 mice with or without a copy of the *Hsd11b1* gene. In mice with one copy of *Hsd11b1* (HET), who have been shown to be phenotypically normal, the same changes in Ca^{2+} fluxes were observed after treatment with either 200 nM 11-DHC or 20 nM corticosterone, having reduced responses to both glucose and KCl (Figure 3-14 A-E). However,

in mice completely absent of *Hsd11b1* (KO), there was no longer any significant difference between control and GC-treated islets (Figure 3-14 E-H).

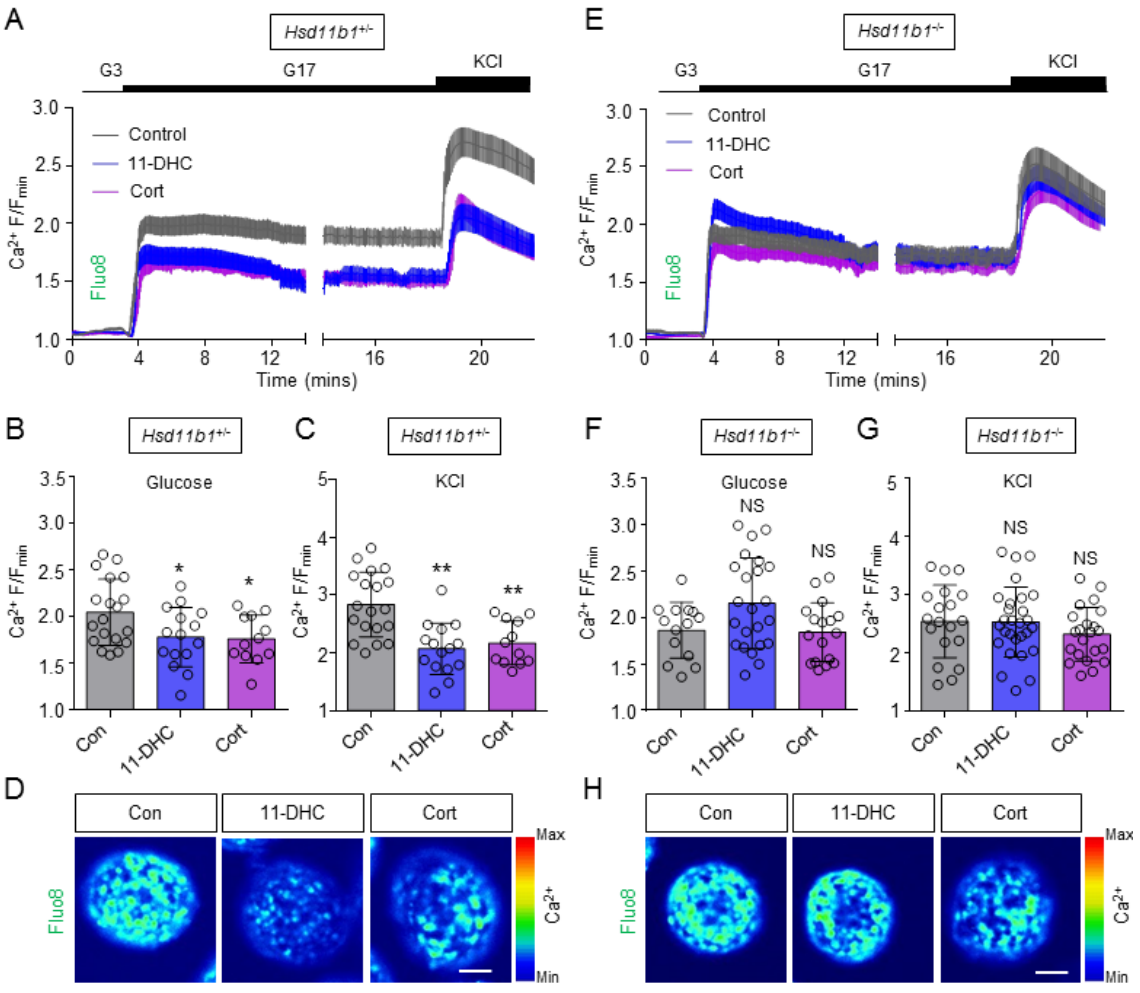

Figure 3-14 | *Hsd11b1* knockout protects mouse beta cells from the effects of GC on Ca^{2+} fluxes. (A) Mean Ca^{2+} traces of HET islets after treatment with GC. Error bars are SEM. (n = 15–19 islets from three animals) (B) Bar chart of maximum change in Ca^{2+} fluorescence in response to 17 mM glucose. Error bars are SD. (C) Bar chart of maximum change in Ca^{2+} fluorescence in response to 10 mM KCl. Error bars are SD. (D) Representative pseudo-coloured images of islets treated with Fluo-8 at 17 mM glucose under control and GC conditions. (Scale bar = 20 µm; images cropped to show a single islet) (E-H) As in A-D but using islets from mice lacking *Hsd11b1*. (n = 19–28 islets from 3 animals).

3.3.7 *Hsd11b1* knockout islets are protected against the effects of 11-DHC, but not corticosterone, on cAMP generation

When cAMP imaging experiments were repeated in *Hsd11b1* transgenic mice, mice with a single copy of the gene showed the same response to GC as in CD1 mice (Figure 3-15 A-D). However, in *Hsd11b1* null mice, while corticosterone caused the same increase in cAMP seen in HET mice, 11-DHC treated islets no longer showed any differences in glucose- or forskolin- induced changes in cAMP when compared with control treated islets (Figure 3-15 E-H).

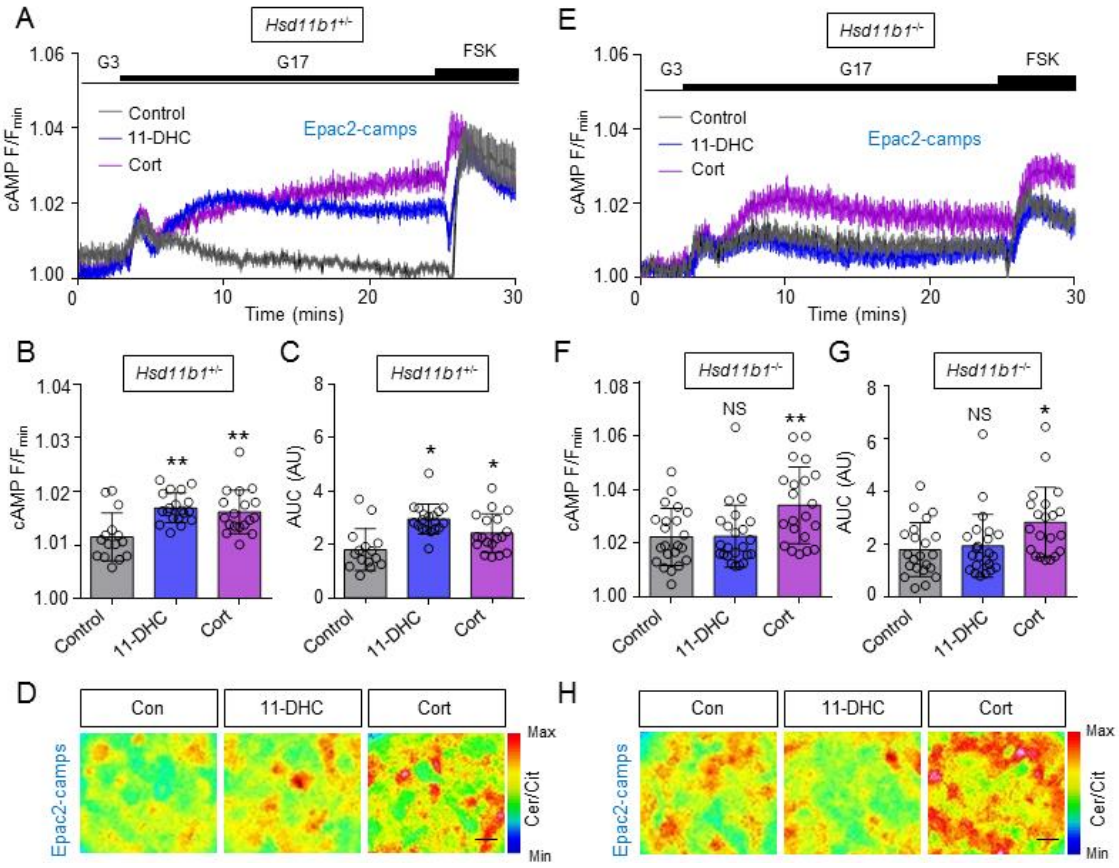

Figure 3-15 | *Hsd11b1* KO prevents upregulation of cAMP by 11-DHC, but not corticosterone. (A) Mean traces of cAMP responses to glucose (G17) and Forskolin (FSK) in mice with a single *Hsd11b1* gene treated with either control, 200 nM 11-DHC or 20 nM corticosterone. Error bars are SEM. (n = 15–19 islets from three animals). (B) Bar graph of the maximal cAMP increase in response to 17 mM glucose. (C) Bar graph of the maximal cAMP increase in response to 10 mM KCl. (D) Pseudo-coloured representative images of cAMP response to 17 mM glucose. (Scale bar = 10 µm). (E-H) As for A-D, but in *Hsd11b1* KO mice. (n = 22–23 islets from 3 animals).

To investigate the effect of *Hsd11b1* knockout on adenylate cyclase isoform gene expression, RT-qPCR was performed. In the knockout mice, 11-DHC no longer led to significantly increased expression of *Adcy1* (Figure 3-16 A), but corticosterone still produced a two-fold increase in expression (Figure 3-16 B).

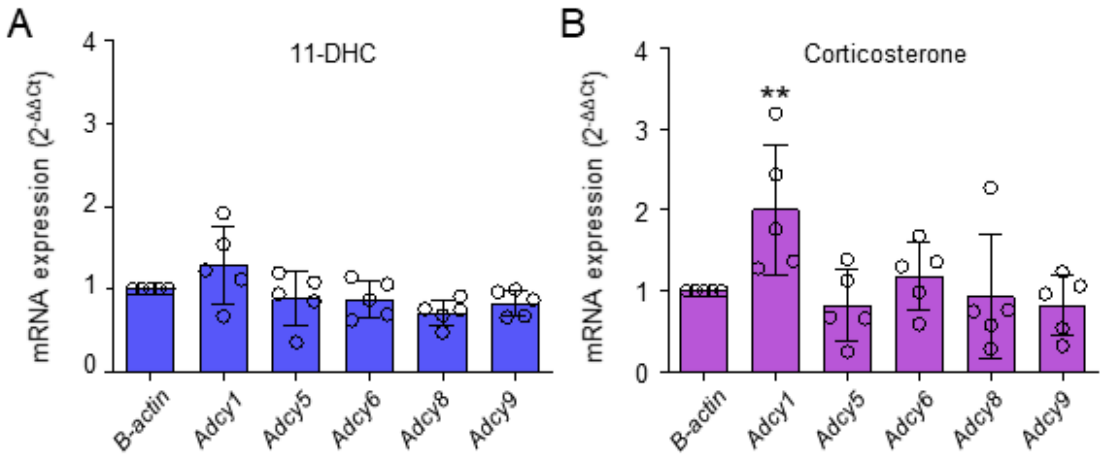

Figure 3-16 | *Adcy1* mRNA expression is significantly elevated in *Hsd11b1* null mice in response to corticosterone treatment, but not after 11-DHC treatment. (A) Scatter plot with bars showing mean *Adcy* mRNA expression relative to *β-actin* after 48-hour treatment with 200 nM 11-DHC (n = 5 animals). (B) As for A, but for corticosterone treatment. Evidently, corticosterone is still able to upregulate *Adcy1* in the absence of *Hsd11b1* (n = 5 animals). Error bars are SD.

3.3.8 Glucocorticoid receptor antagonisation protects islet Ca^{2+} fluxes from the effects of glucocorticoid treatment

To confirm whether 11-DHC and corticosterone were acting through the GR, Ca^{2+} imaging was repeated with the addition of the GR antagonist, RU486. In these experiments, as expected, treatment with 11-DHC or corticosterone alone caused decreased Ca^{2+} fluxes in response to glucose and KCl. When islets were treated with RU486 in conjunction with 11-DHC, Ca^{2+} fluxes in response to glucose and KCl returned to control levels, demonstrating that effective blockade of the GR prevents any effects of 11-DHC (Figure 3-17 A-D).

However, when using corticosterone rather than 11-DHC, RU486 normalised glucose induced Ca^{2+} fluxes in response to glucose but was unable to prevent the effects on KCl induced Ca^{2+} responses, which are independent of cAMP (Figure 3-17 E&F). Addition of RU486 to control islets caused no significant change in Ca^{2+} fluxes in response to glucose or KCl (Figure 3-17 A-D).

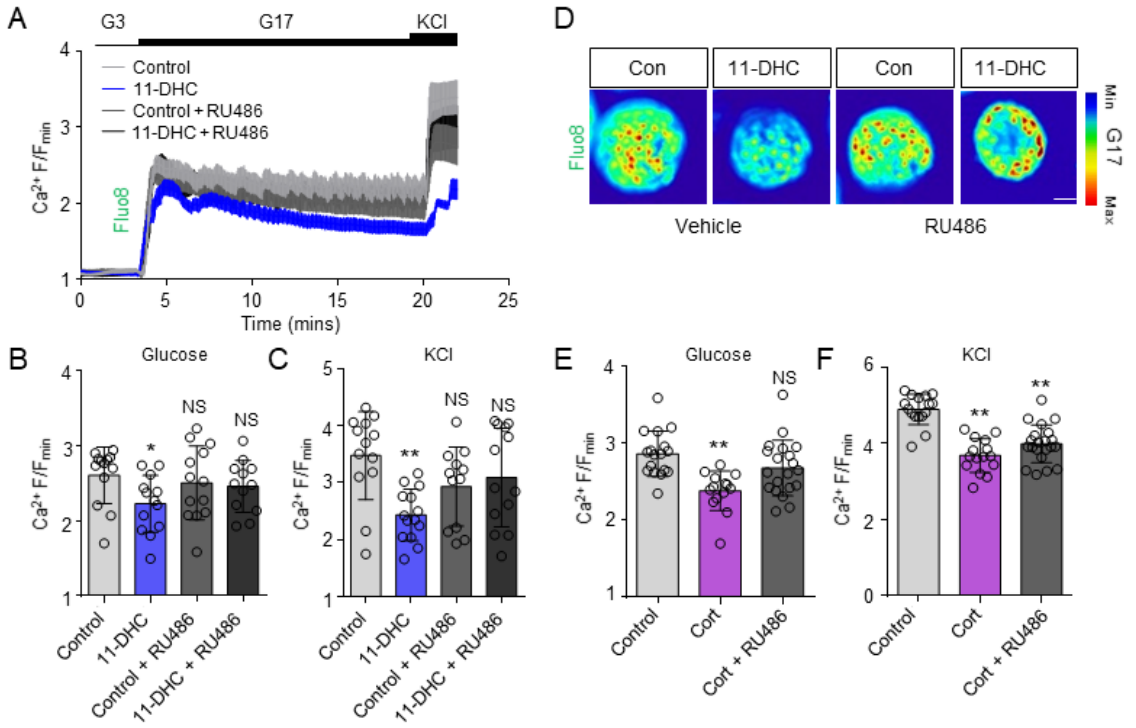

Figure 3-17 | The GR antagonist, RU486 (1 μM), inhibits the effects of 11-DHC and corticosterone (Cort) on mouse beta cell Ca^{2+} fluxes in response to glucose. However, RU486 was unable to rescue the effect of corticosterone on KCl induced Ca^{2+} fluxes. (A) Mean Ca^{2+} traces of islets treated with either control, 11-DHC, control plus RU486 or 11-DHC plus RU486. Error bars are SEM. (n = 12–13 islets from 4 animals) (B) Bar chart of maximum Ca^{2+} increase in response to 17 mM glucose in mouse islets treated with 11-DHC, RU486, or 11-DHC and RU486 combined. Error bars are SD. (C) As for B, but in response to 10 mM KCl. (D) Pseudo-coloured representative images of islets at high glucose from Ca^{2+} experiment in A. (Scale bar = 20 μm). (E) Bar graph showing maximum Ca^{2+} responses to glucose in mouse islets treated with either corticosterone, or corticosterone and RU486 (n = 14–17 islets from 6 animals) (F) As for E, but in response to 10 mM KCl.

3.4 Discussion

Corticosterone and its less active precursor, 11-DHC, impair glucose- and KCl-stimulated Ca^{2+} fluxes in murine pancreatic islets, although beta cell differentiation and metabolism were normal. However, insulin secretion is maintained by upregulating *Adcy1* expression and cAMP generation, which acts via the PKA pathway to increase the number of membrane-bound insulin granules. The effects of 11-DHC could be prevented by whole-body deletion of *Hsd11b1*, demonstrating a critical role of steroid (re)activation within the islet. In addition, the effects see in response to GCs were depended on GR activity, as demonstrated in experiments using GR antagonists. The effects were specific to glucose and no defects in incretin-mimetic-stimulated insulin secretion were detected.

3.4.1 Glucocorticoids modulate VDCC conductance leading to impaired calcium fluxes

Cytosolic Ca^{2+} levels were impaired in the presence of either 11-DHC or corticosterone (Figure 3-1). It is unlikely that this was due to defects in metabolism and K_{ATP} channel function since ATP/ADP ratios were normal (Figure 3-6). However, KCl-induced Ca^{2+} influx was drastically reduced at high glucose concentration, although RT-qPCR analyses showed no major differences in expression levels of the key VDCC subunits (Figure 3-4). Electrophysiology showed that VDCC conductance in GC-treated islets was drastically decreased (Figure 3-5). In GC-treated islets, Ca^{2+} oscillation

frequency was also affected (Figure 3-2), suggesting that GCs may also conceivably target more distal steps in Ca^{2+} flux generation. This could include depleting intracellular Ca^{2+} stores through cAMP sensitization of IP_3 receptors (Liu *et al.*, 1996), upregulating ion channels involved in voltage-inactivation (i.e. large-conductance Ca^{2+}-activated K^+ channels (Jacobson *et al.*, 2010)), or altering glucose-regulated amplifying inputs other than cAMP (Henquin, 2000). These effects are presumably specific to glucose-stimulated Ca^{2+} rises, since responses to the GLP-1 receptor agonist exendin-4 remained unchanged by GC exposure (Figure 3-2), which may be due to PKA-mediated rescue of VDCC function or Ca^{2+} release from organelles (Ämmälä, Ashcroft and Rorsman, 1993). Additionally, GC had no effect on cAMP generation in response to exendin-4, therefore confirming that their effects are independent of the GLP-1R (Figure 3-9).

3.4.2 Insulin secretion is maintained by upregulation of the cAMP pathway

Despite impaired calcium function, GC-treated mouse islets maintain normal glucose-stimulated insulin secretion (Figure 3-4). GSIS may be augmented by the parallel amplifying pathway mediated by cAMP, which is upregulated in GC-treated islets (Figure 3-8). The exact mechanisms by which 11-DHC and corticosterone boost cAMP signalling are unknown, but are likely to involve specific adenylate cyclases, since *Adcy1* gene expression was almost 2-fold higher in 11-DHC- and corticosterone-treated islets compared to controls (Figure 3-10), and to a lesser extent *Adcy9* (not significant). Support for the

concept of compensation by cAMP comes from super resolution imaging showing a three-fold increase in membrane-docked insulin secretory granules in mouse beta cells treated with GC, which is consistent with upregulated cAMP (Figure 3-11). While *Adcy9* mRNA was not significantly affected by GC, other mechanisms can account for cAMP generation, including organization of the enzyme into cell membrane microdomains (Cooper, 2003). Pertinently, *Adcy1* and *Adcy9* knockdown have been shown to reduce glucose-stimulated cAMP rises and insulin secretion in beta cells (Kitaguchi *et al.*, 2013; Tian *et al.*, 2015). Further studies are thus warranted in GC-treated *Adcy1* and *Adcy9* null islets.

cAMP has been shown to recruit non-docked insulin granules to the membrane, as well as increase the size of the available granule pool *via* Epac2 and PKA (Shibasaki *et al.*, 2007; Kaihara *et al.*, 2013). This would be expected to account for the normal secretory response to glucose and KCl. In addition, when islets were treated with 11-DHC either alone or in the presence of the PKA inhibitor H-89, islets treated with both 11-DHC and H-89 showed diminished glucose secretion at high glucose compared with control, 11-DHC only or H-89 only (Figure 3-11).

Finally, GC-treated islets were no longer able to secrete insulin at normal levels after treatment with the fatty acid palmitate, a known inhibitor of the *Adcy* family of enzymes (Tian *et al.*, 2015) (Figure 3-12). Interestingly, it has been shown that in the absence of insulin (fasting state), dexamethasone treatment leads to an increase in lipogenesis. Whereas, in the fed states in which insulin is present, dexamethasone decreases lipogenesis (Gathercole *et al.*, 2011). In the context of diabetes and hyperinsulinemia, increased glucocorticoids would lead

to chronic lipogenesis, and this lipogenesis would adversely affect the mechanisms described here (compensatory cAMP generation) in beta cell, leading to a feed-forward decline.

Upregulated cAMP signalling may thus represent a protective mechanism that is targeted by free fatty acids to induce beta cell failure in the face of excess GC. Interestingly, the endogenous elevation of GCs in humans generally leads to dyslipidaemia due to lipolysis, *de novo* fatty acid production and hepatic fat accumulation (Arnaldi *et al.*, 2010).

Both corticosterone and 11-DHC have previously been shown to exert inhibitory effects on insulin release (Davani *et al.*, 2000; Ortsäter *et al.*, 2005; Swali *et al.*, 2008; Turban *et al.*, 2012). However, these studies either used islets from chronically obese *ob/ob* mice that display highly upregulated *Hsd11b1* expression (Davani *et al.*, 2000; Ortsäter *et al.*, 2005) or incubated wild-type islets with GC for only two hours (Swali *et al.*, 2008; Turban *et al.*, 2012), which is unlikely to fully rescue the effect of disrupted Ca^{2+} fluxes by rising cAMP levels. Likewise, studies in which GCs are administered in the drinking water are complicated by insulin resistance and increased beta cell mass (Rafacho *et al.*, 2010). Thus, the effects observed in the present study more likely reflect the cellular/molecular actions of circulating GCs under normal conditions.

3.4.3 *Hsd11b1* expression is present in whole islets, and required for the effects of 11-DHC on beta cells

RNA-seq analyses have shown that *Hsd11b1* mRNA levels are unusually low in purified mouse beta cells and other islet endocrine cells (Pullen, Huising and Rutter, 2017). These findings conflict with reports that protein expression co-localizes with glucagon or insulin in rodent islets depending on the antibody used (Swali *et al.*, 2008; Chowdhury *et al.*, 2015). The reasons for these discrepancies are unclear but, in the present study, specific TaqMan assays showed consistently detectable mRNA levels in murine islets (Figure 3-13). Here, we show that both 11-DHC and corticosterone effects on Ca^{2+} fluxes could be reversed in global *Hsd11b1*$^{-/-}$ islets in which mRNA was largely absent (Figure 3-14), therefore demonstrating a vital role for *Hsd11b1* in mediating the effects of GCs through both local activation and reactivation by this enzyme. However, when the effects of GCs on cAMP responses to glucose were investigated in *Hsd11b1*-null islets, the effects of 11-DHC could be reversed by knock out, but corticosterone was still able to upregulate cAMP (Figure 3-15). This may indicate that the threshold for the effects of GC on cAMP are lower than that of Ca^{2+}, potentially leaving a sweet spot for therapeutic application, using low dose GCs in lean individuals with diabetes. In *Hsd11b1* knock out mice, *Adcy1* was no longer significantly upregulated, whereas those islets treated with corticosterone still show elevated levels of this enzyme (Figure 3-16), thus supporting the cAMP imaging data. The assumed mode of action of GCs is through the GR, and in islets treated with 11-DHC and RU486, an antagonist of the GR, Ca^{2+} responses were no longer impaired (Figure 3-17).

However, corticosterone was still able to exert its effects on Ca^{2+} responses to KCl in the presence of RU486. This may be due to only partial blockade of the GR or additional targets of corticosterone.

These findings suggest that 11-DHC is likely to affect beta cell function in a paracrine manner, possibly through actions in non-endocrine islet cell types, such as endothelial cells where expression of HSD11B1 is relatively high (Segerstolpe *et al.*, 2016) or alpha cells where HSD11B1 protein has been colocalised with glucagon (Swali *et al.*, 2008). This may form the basis of an adaptive mechanism to prevent the build-up of very high local corticosterone concentrations. Together, these data highlight the importance of the islet context for the regulation of insulin secretion and underline the requirement to consider cell-cell crosstalk when assessing the functional consequences of any gene in beta cells.

We should be wary of stating that the effects GC on Ca^{2+} signalling are causative of those cAMP responses. Since Ca^{2+} fluxes are the first step in the signalling cascade, we are assuming that aberrations in Ca^{2+} will impact the stimulus-secretion coupling mechanisms downstream. Instead, it may be that GC directly leads to increased *Adcy1* expression and activity, therefore resulting in a larger readily releasable pool of insulin granules that require a less pronounced Ca^{2+} signal to function normally.

3.4.4 Conclusion

We have identified a novel mechanism by which GCs maintain beta cell function in murine beta cells through engagement of parallel cAMP pathways. This compensatory mechanism is dependent on adenylate cyclase 1 and can be impaired by the presence of high concentrations of lipids. An overview of the mechanisms identified in this chapter are summarised in Figure 3-18

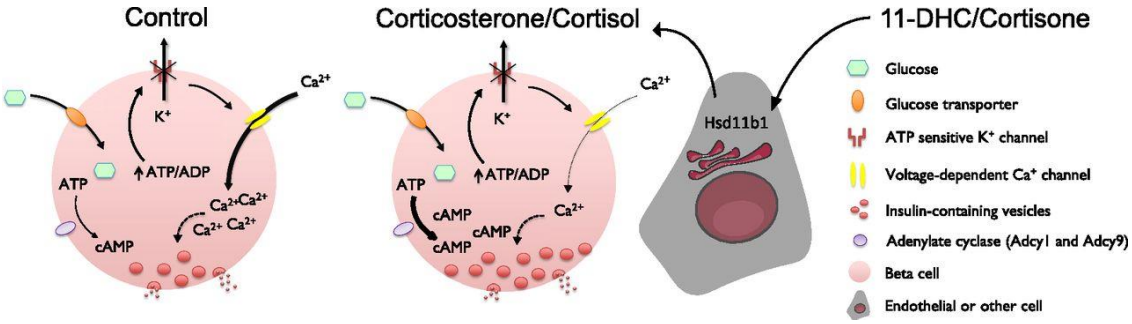

Figure 3-18 | Schematic representation of the effects of glucocorticoid treatment on mouse islets. Thick lines and thin lines represent increased and decreased action respectively. Under control conditions Ca^{2+} entry is the principal component in insulin release. When islets are treated with either corticosterone or 11-DHC (which is converted by HSD11B1), impaired VDCC channel activity reduces Ca^{2+} intake but an increase in cAMP (mediated by AC) maintains normal secretory function (Fine *et al.*, 2018).

4 CHAPTER FOUR – GLUCOCORTICOIDS REPROGRAM HUMAN BETA CELLS TO PRESERVE INSULIN SECRETION

4.1 Introduction

Since we have shown novel insights into the effect of GCs in mouse pancreatic beta cells (described in chapter 3), we turned our attention to human beta cells to assess if these results could be replicated in humans to provide translational insight. This is particularly important given the differences between human and mouse islets described in detail in chapter 1, specifically in terms of islet cell type contribution and islet architecture (Bonner-Weir, Sullivan and Weir, 2015). This would give us important information about how the human beta cell reacts to GCs in health and disease, with a view to developing potential new treatments to improve insulin secretion and beta cell heath.

There is some debate as to the activity of HSD11B1 in beta cells based upon RNA sequencing (RNA-seq) of purified fractions and whether or not this gene should be classed as a “disallowed gene” (Pullen, Huising and Rutter, 2017, see 1.5.1). Therefore, it was important to assess the effects of cortisone (the human equivalent of 11-DHC; the less-active GC) in human islets in addition to cortisol (the human equivalent of corticosterone; the more-active GC) to show active conversion by HSD11B1.

4.2 Methods

4.2.1 Human islet culture

Human islets were acquired from isolation centres in Alberta (Alberta Diabetes Institute, IsletCore), Canada, and Milan and Pisa (European consortium for islet transplantation, ECIT), Italy, with local and national ethical authorisation. Upon arrival, islets were washed once with human islet medium (RPMI supplemented with 5.5 mM glucose, 10% FBS and 100 U/mL penicillin, 100 µg/mL streptomycin, and 0.25 µg/mL Amphotericin B). Islets were then filtered using a 70 µm filter and transferred to a 10 cm petri dish containing 10 mL of the human islet medium.

Basic donor information was provided by human islet providers. This information is summarised in Table 4.

Age	Gender	BMI	Source
44	Male	34.4	Alberta IsletCore
67	Female	26.9	Alberta IsletCore
71	Female	35.5	Alberta IsletCore
73	Female	28.4	Alberta IsletCore
44	Male	33.8	Alberta IsletCore
60	Female	26.0	Alberta IsletCore
48	Male	27.7	European Consortium for Islet Transplantation
61	Female	27.7	European Consortium for Islet Transplantation
52	Female	19.0	European Consortium for Islet Transplantation
59	Female	22.2	European Consortium for Islet Transplantation
62	Female	29.3	European Consortium for Islet Transplantation
63	Female	19.5	European Consortium for Islet Transplantation

Table 4 | Human islet donor characteristics. Human islets were kindly provided by the Alberta IsletCore, Canada, and the European Consortium for Islet Transplantation in Milan and Pisa. The mean age and BMI of donors was 58.67 and 27.5 respectively.

Human islets were used in accordance with the Human Tissue Act. Donors were often used for multiple experimental methods, using control and test conditions from the same donor to avoid confounding variables within paired measurements. Given that there were differences between BMI, gender and age of the donors (see Table 4), it is possible that this may have affected results; however, unpicking these effects is not possible at this stage.

4.2.2 Glucocorticoid treatment

Human islets were cultured as above (4.2.1). Cortisol and cortisone (Sigma, Poole, UK) were diluted in 100% molecular grade ethanol (Sigma, Poole, UK) at a stock concentration of 1 mM in glass vials before being diluted in complete RPMI for a final concentration either 200 nM cortisone or 20 nM cortisol. Control samples were treated with 100% ethanol only (final concentration in media - 0.2%). Human islets were treated for 48 hours with either cortisone or cortisol. These concentrations and times were chosen due to previous work in the department (Swali *et al.*, 2008).

4.2.3 Quantitative real-time PCR

Full details of RNA extraction and cDNA synthesis can be found in the methods chapter of this thesis (2.4.4) *HSD11B1* mRNA abundance was determined by using TaqMan assays (cat. #4331182) tissue. Expression was compared to ACTB gene expression since this is one of the few housekeeping genes that has previously been shown to not be influenced by GCs. *HSD11B1* expression was calculated by using $2^{-\Delta Ct}$ x1,000, and transformed values are presented as arbitrary units.

4.3 Results

4.3.1 Human islets show impaired Ca^{2+} fluxes after glucocorticoid treatment

The effect of Ca^{2+} fluxes in mouse islets treated with GCs was replicated in human islets when treated with either 200 nM cortisone or 20 nM cortisol. GC-treated human islets showed perturbed Ca^{2+} spiking activity (Figure 4-1 A), as well as significantly reduced glucose- and KCl- induced Ca^{2+} responses, measured using Fluo-8 (Figure 4-1 B&C).

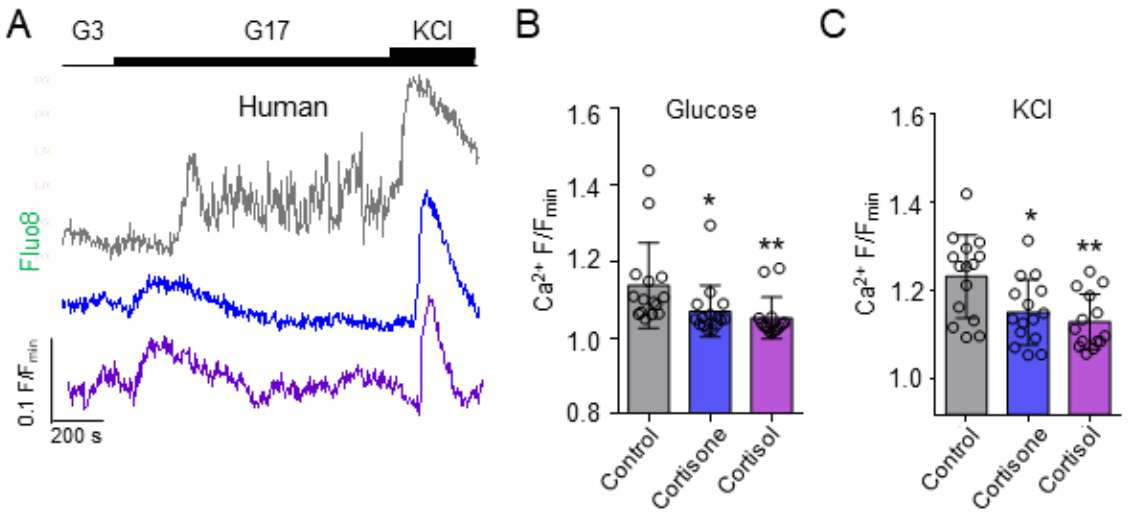

Figure 4-1 | Human islets treated with GC show impaired Ca^{2+} fluxes in response to glucose and KCl, assessed using Fluo8. (A) Representative Fluo-8 traces of human islet Ca^{2+} fluxes in response to 17 mM glucose and 17 mM glucose plus 10 mM KCl. Islets were treated with either vehicle (top), 200 nM cortisone (middle) or 20 nM cortisol (bottom). (B) Max F/F_{min} responses to 17 mM glucose in islets from A. Error bars are SD. (C) Max F/F_{min} response to 10 mM KCl. Error bars are SD. (n = 15–18 islets from three donors).

4.3.2 Human islets treated with glucocorticoids have normal insulin secretion

Impaired Ca^{2+} fluxes in beta cells would normally correlate with impaired function, mainly insulin secretion in response to glucose. Therefore, we used human islet preparations from 3 donors to assess the effects of GC on glucose- and KCl-stimulated insulin secretion. Human pancreatic islets treated for 48 hours with either 200 nM cortisone or 20 nM cortisol did not show significantly different levels of GSIS compared with control (Figure 4-2), again mirroring the results in mouse islets.

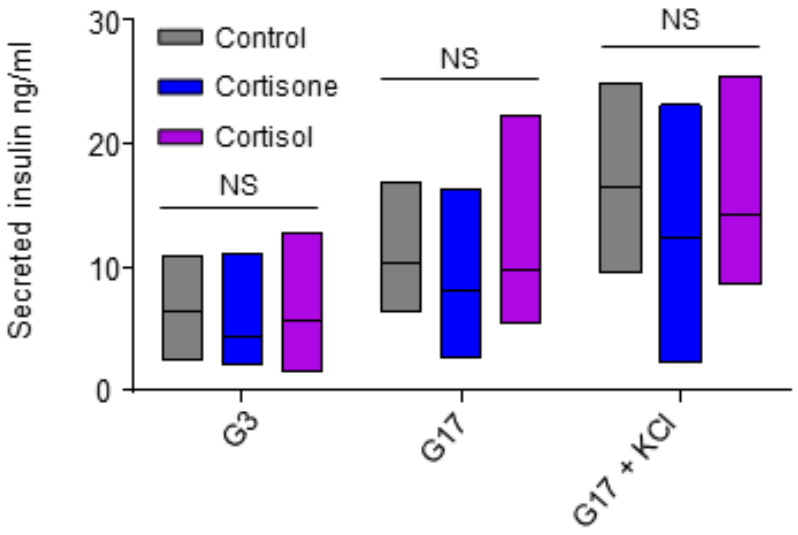

Figure 4-2 | Glucose-stimulated insulin secretion in human islets treated with GC show normal basal and secretory capacity. Box plot of human GSIS after treatment with 200 nM cortisone or 20 nM cortisol show no significant differences. (n = 3 donors).

4.3.3 Glucocorticoid treated human islets have improved cAMP generation in response to glucose

Human islets were treated with 200 nM cortisone or 20 nM cortisol for 48 hours to determine if GCs were able to increase glucose-stimulated cAMP generation. GC-treated islets produced significantly increased levels of cAMP in response to 17 mM glucose and 100 µM forskolin (Figure 4-3). This shows that the compensatory mechanism observed in mouse islets, namely an increased cAMP response to impaired Ca^{2+} fluxes in GC-treated islets, also translates into human beta cells.

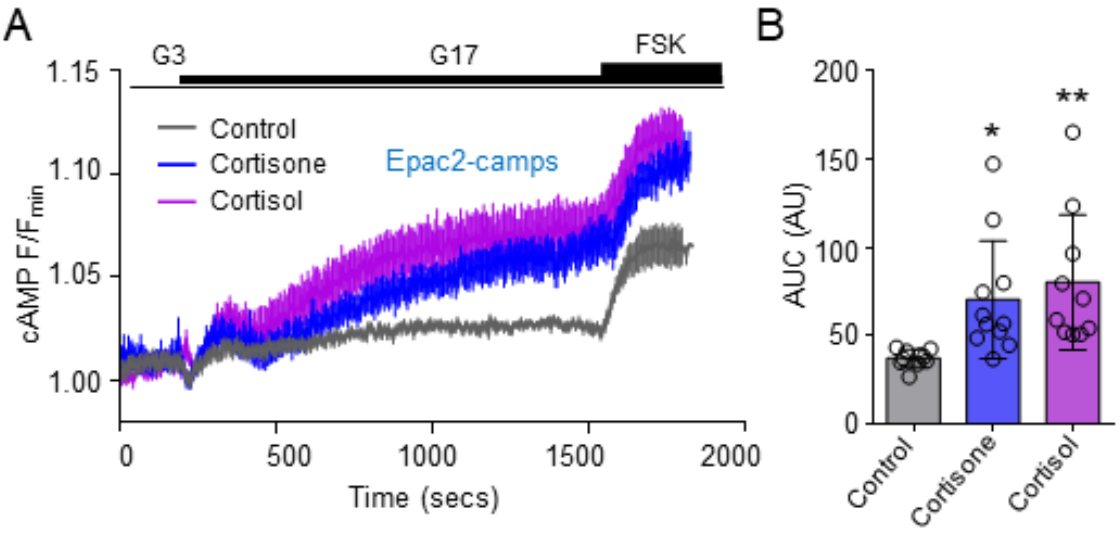

Figure 4-3 | GCs significantly increase glucose-induced cAMP responses in human islet compared with control. (A) Mean traces from cAMP imaging performed on human islets treated with control, 200 nM cortisone or 20 nM cortisol. Error bars are SEM. (B) Bar chart showing the mean AUC of traces from the cAMP imaging experiment in A. Error bars are SD. (n = 10–11 islets from three donors).

4.3.4 *HSD11B1* is detectable in human pancreatic islets

To confirm *HSD11B1* expression in human islets, RT-qPCR was conducted on islets, subcutaneous fat, and omental fat from 4-5 donors. *HSD11B1* was readily detectable in human islets, and its expression was only 10-fold lower than that of subcutaneous and omental fat, both of which are major sites for GC activation (Figure 4-4).

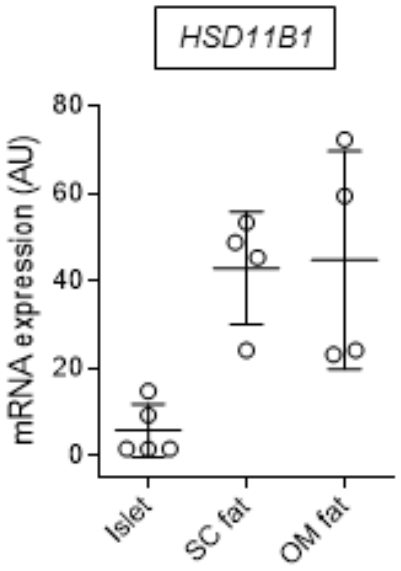

Figure 4-4 | *HSD11B1* is clearly detectable in human islet RNA preparations according to a specific TaqMan assay. However, it is expressed at a lower concentration than both subcutaneous (SC) fat or omental (OM) fat. Error bars are SD. (n = 4-5 donors).

4.4 Discussion

This chapter confirms that murine and human islets respond similarly to active and less active GCs. Indeed, human islets exposed to either cortisol or cortisone showed markedly impaired Ca^{2+} fluxes in response to glucose and glucose plus KCl (Figure 4-1), as seen in comparable mouse experiments (Figure 3-1). However, glucose-stimulated insulin secretion was unchanged in human islets treated with either cortisone or cortisol when compared with vehicle-treated islets (Figure 4-2). The compensatory increase in cAMP generation in response to glucose seen in mouse islets (Figure 3-8) were also observed in human islets (Figure 4-3).

As the effects seen in chapter 3 are dependent on the activity of HSD11B1, clinical trials involving HSD inhibitors should be mindful of these findings. Additionally, the side effects of GC therapy may be detrimental in patients with a higher adiposity due the compounding effects of these factors on beta cell function and in particular cAMP signalling.

Despite previous reports that *HSD11B1* is a disallowed gene, being “essentially undetectable” in both alpha and beta cells (Pullen, Huising and Rutter, 2017), in this study *HSD11B1* expression in human islets was only 10-fold lower than in adipose tissue (Figure 4-4), which is the major site for steroid reactivation after the liver (Tomlinson, Moore, *et al.*, 2004). This suggests that activation and reactivation of cortisone by HSD11B1 is regulated in a paracrine manner by other cells within the pancreas, possibly delta cells, endothelial cells or even

immune cells such as resident macrophages (Zinselmeyer *et al.*, 2018; Ying *et al.*, 2019).

This study has shown that less-active GCs can impact beta cell function similarly to active cortisol (Figure 4-1 & Figure 4-3). This finding suggests that activation and reactivation of cortisone occurs within the pancreatic islet, although this conversion may not take place in the beta cell itself as previously reported (Swali *et al.*, 2008). Disallowed genes may contribute to alpha and beta cell identity, but the function of the pancreatic islet is determined by multiple cell types, including stromal cells, interacting to maintain tight regulation of glucose homeostasis. Failure of this protective machinery, for example in the face of excess lipidaemia caused by obesity, may contribute to impaired insulin release during states of GC excess such as Cushing's disease (Arnaldi *et al.*, 2010).

Some weaknesses of the chapter that should be considered are the variation introduced by difference in BMI, cold ischemia, and cause of death of the donors of the human islets. This is compounded by the travel time of islets at room temperature, post isolation. Additionally, these islets are offered only after they have been rejected for the purposes of transplantation, suggesting they are not high quality. This chapter could be improved by the addition of more repeats, which would increase the reader's confidence in the reliability of some of the results, such as glucose-stimulated insulin secretion. Impaired calcium signalling and improved cAMP generation in response to glucose could lead to changes in the contribution of first and second phase secretion to insulin output, specifically a muted first phase and an augmented second phase. This could be

interrogated by conducting perifusion experiments to look at insulin secretion over time (Georgiadou *et al.*, 2020).

4.4.1 Conclusion

In summary, we have confirmed that the novel mechanism by which GCs maintain beta cell function in the face of impaired calcium fluxes, through engagement of the cAMP pathway seen in chapter 3 (Figure 3-18) is conserved in human beta cells. Additionally, we have demonstrated that *HSD11B1* is expressed in human pancreatic islets. These could be potential therapeutic targets to investigate as a result of this chapter, however further work is required to fully comprehend the mechanisms underlying the phenomenon seen here.

5 CHAPTER FIVE – THE IMPACT OF REDUCED BETA CELL HETEROGENEITY ON ISLET SIGNALLING

5.1 Introduction

5.1.1 Beta cell differentiation and maturity

As introduced in chapter 1 (1.1.1), the development and differentiation of the pancreatic beta cell is a muti-stage process, during which the cells transition through various progenitors. They start life as distal foregut endoderm cells which are positive for *FOXA2*, *SOX17* and *SHH*. These then differentiate into pancreatic endoderm cells displaying *PDX1*, *FOXA2*, *NKX6.1*, *PTF1A*, *GATA4* and *SOX9* which excludes them from a fate as biliary duct. These then continue their journey to adulthood by becoming endocrine, or 'trunk' progenitor cells, capable of further differentiation into either alpha or beta cells. These endocrine progenitor cells express transient *NGN3*, and strong *NKX6.1, PDX1*, *PAX6*, and *NEUROD1*. The subsequent step destines them to become beta cells by expression of *MAFA, PAX6, NKX6.1, PDX1* and *NGN3*. These cells are insulin positive but not capable of secreting insulin to the levels required for normal glucose maintenance. Further differentiation of these immature beta cells into mature beta cells by expression of high levels of *PDX1*, *MAFA*, *NGN3* and *UCN3*, produces cells with maximal insulin secretory capacity (Jennings *et al.*, 2015; Sun *et al.*, 2021). This information has been summarised in Figure 5-1.

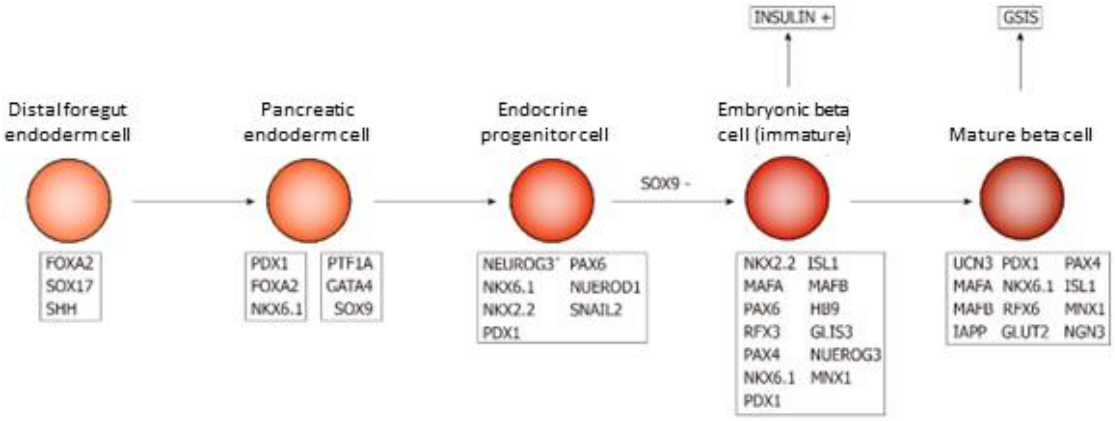

Figure 5-1 | The main steps in the maturation of the pancreatic beta cell. Development of the pancreatic beta cell starts with cells from the distal foregut endoderm cells. These transition into pancreatic endoderm cells and then endocrine progenitor cells. These then become insulin positive embryonic beta cells, aka immature beta cells, before reaching the mature beta cell status. Mature beta cells are responsible for the majority of glucose-stimulated insulin secretion (Sun *et al.*, 2021).

While early reports or simplistic models suggest that this maturation is a linear pathway of no return, more recent studies have suggested some fluctuation between maturity states. This plasticity may allow the beta cell population to either expand in response to demand (e.g., in T2D), or recover from periods of intense protein synthesis and secretion. The idea that pancreatic islets are made up of a variety of beta cells with distinct functions and gene expression profiles has been termed “beta cell heterogeneity” and is thought to be vital for normal glucose homeostasis (Pipeleers, 1992; Johnston *et al.*, 2016; Benninger and Hodson, 2018; Farack *et al.*, 2019; Nasteska *et al.*, 2021).

5.1.2 Beta cell heterogeneity

Previous chapters have focused on the effects of external stimuli, such as glucocorticoid excess on beta cell function. However, it is known that there are large differences in beta cell identity and function and that these subpopulations

dictate how signalling occurs at the level of the islet. Early observations showed that rat beta cells required different thresholds of glucose levels to initiate insulin secretion, which pointed towards heterogeneity within the beta cell population (Pipeleers, 1992). This difference in glucose sensing may be due to different degrees of maturity in beta cells. Immature beta cells are less glucose responsive and possess higher basal secretion but are better able to undergo cell division compared with their more mature counterparts (Benninger and Hodson, 2018). This immature population is relatively small (~1-20%) compared with the total number of beta cells in the islet (Nasteska *et al.*, 2021); however, gene expression analysis of dividing cells has identified upregulation of genes related to the control of the cell cycle, such as *c-Myc.* Interestingly, when *c-Myc* is overexpressed in insulin-secreting cell lines or mouse islets, it cellular proliferation increases but GSIS is reduced. Knock-down of *c-Myc* in mouse islets results in improved GSIS, but a trend towards impaired glucose tolerance *in vivo*. It has been suggested that beta cells may enter this state of lowered maturity to allow a period of recovery from ER stress or to allow proliferation to maintain or increase beta cell mass (Puri *et al.*, 2018).

‘Hubs’ are another interesting example of an immature subpopulation of beta cells which coordinate calcium fluxes throughout the islet. They have been shown to account for approximately 1-10% of the beta cell and are highly metabolic but have lower than average levels of beta cell identity markers (e.g., *Pdx1*). ‘Hubs’ rely on gap junctions to propagate electrical signals, which can be disrupted by glucolipotoxicity or cytokines, thus mimicking their dysregulation in diabetes (Johnston *et al.*, 2016).

Other subpopulations of beta cells have also been discovered, such as the ‘extreme’ beta cells identified by small-molecule fluorescent in-situ hybridisation (Farack *et al.*, 2019). These beta cells appear to be highly active in terms of protein production, with high ribosome content and proinsulin mRNA, but lower insulin protein. This indicates a high basal secretion of insulin at fasting levels of blood glucose, which is supported by an increase in extreme beta cells in diabetic mice (db/db).

Furthermore, studies investigating the role of the *Wnt*/planar cell polarity pathway in islets discovered that *Flattop* (*Fltp*) acts as a reporter to distinguish between immature and mature beta cells. *Fltp* is only present in mature secretory beta cells, and the percentage of *Fltp* positive cells is increased in 3D aggregates of beta cells. When *Fltp* is knocked-out, development occurs normally but GSIS is reduced in adult mice due to changes in the cytoskeleton, which is required for normal secretion (Bader *et al.*, 2016).

It is clear from the current literature that the beta cell possesses a range of maturity states spanning from immature to mature. Yet, we still do not understand how the presence of these different maturity states in situ impacts islet function and insulin secretion. We set out here to understand whether immature beta cells might in fact contribute to islet function, rather than take away from it, especially since they are less hindered by ER stress and have been shown to exert disproportionate influence over islet function.

5.1.3 Aims and Hypothesis

With this in mind, we aimed to further interrogate the heterogeneity seen in the beta cell population by overexpression of three proteins associated with a state of increased maturity (Pdx1, Mafa and Ngn3) in mouse pancreatic islets. This would increase the proportion of “mature” beta cells, or beta cells with a more beta cell like phenotype, relative to the total population in experimental islets vs control. We employed in vitro techniques described in previous chapters (Ca2+ and cAMP imaging, secretion assays, gene expression) in combination with *in vivo* measures of glucose tolerance to investigate whether reducing beta cell heterogeneity will have an adverse effect on the function of the pancreatic islet.

5.2 Methods

5.2.1 Mouse model of doxycycline-inducible beta cell maturity

Teto/M3C mice which express *Pdx1*, *Ngn3* and *Mafa*, as well as an mCherry reporter, were provided by Qiao Zhou at Harvard University (Zhou *et al.*, 2008).

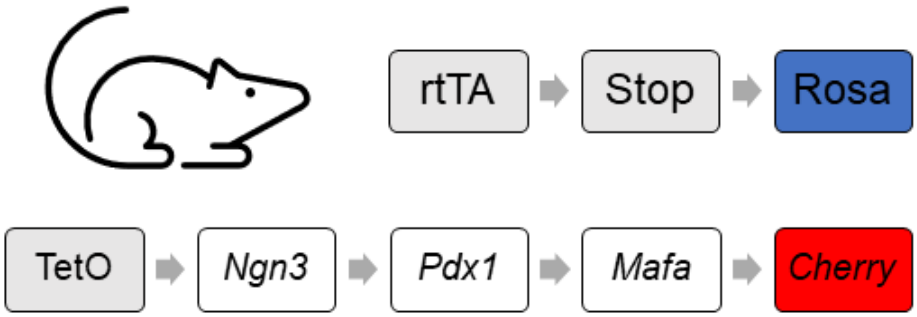

Figure 5-2 | Diagram of the Teto/M3C mouse line. It consists of a Rosa floxed rtTA and a polycistronic cassette consisting of Ngn3, Pdx1, Mafa and mCherry joined by self-cleaving 2A peptide, under the control of the tetracycline inducible TetO. More information on the TetO can be found in Figure 5-3 (Ariyachet et al., 2016).

Teto/M3C mice were genotyped using primer pairs specified in Table 5. Tetracycline-inducible RIP7rtTA mice were donated by Guy Rutter of Imperial College London (Gossen *et al.*, 1995; Milo-Landesman *et al.*, 2001; Pullen *et al.*, 2012). A schematic representation of the TetOn system can be seen in Figure 5-3

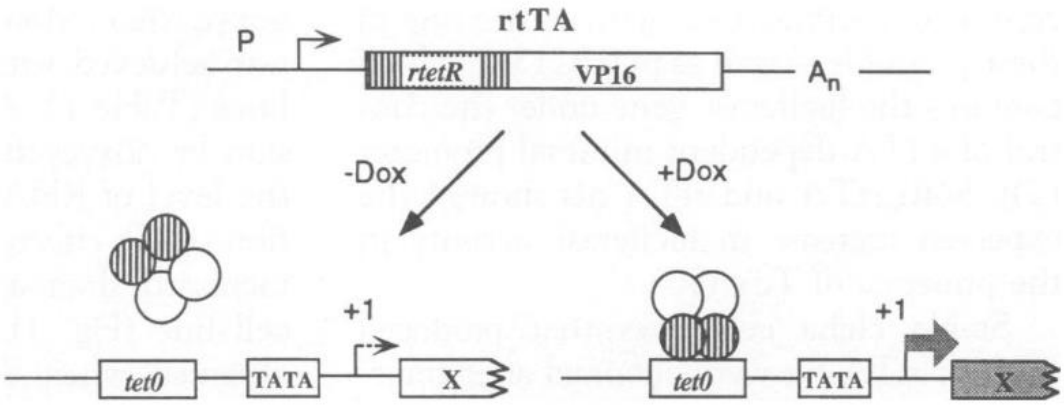

Figure 5-3 | Schematic representation of the TetOn system. In the absence of the effector dox, the transactivator does not recognize its specific DNA target sequence (TetO); therefore, transcriptional activation of gene X will not occur (broken arrow). Addition of the effector Dox results in binding of rtTA to TetO, which allows the activation of the reporter unit (shaded arrow). In this study, addition of dox leads to expression of the Teto/M3C cassette and expression of *Pdx1, Ngn3* and *Mafa* in beta cells (Gossen *et al.*, 1995).

Teto/M3C mice were crossed onto a C57BL6 background by repeated crosses and maintained as heterozygotes. Experimental breeding pairs were heterozygous Teto/M3C mice crossed with homozygous RIP7rtTA mice, producing RIP7rtTA$^{+/-}$, Teto/M3C$^{-/-}$ (Tet-NORM) and heterozygous RIP7rtTA$^{+/-}$, Teto/M3C$^{+/-}$ (Tet-MAT) mice. This breeding scheme was selected to control for any confounding effects that may be caused by either the RIP7rtTA promoter or administration of doxycycline.

Target	Forward sequence	Reverse sequence
Teto/M3C	CAGTGATGTTGAACTTGACC	CTCCTTCACCTCGAAC

Table 5 | Primer sequences used to determine genotype of Teto/M3C mice. PCR and gel electrophoresis generated an approximate 500bp band in mice positive for one or more copies of the Teto/M3C construct (Tet-MAT).

5.2.2 Doxycycline diet administration

Mice were fed a commercially available diet containing 625 mg/kg dox (Envigo, Huntingdon, UK) for up to 4 weeks. Animals were weighed weekly to ensure there were no changes in appetite or weight.

5.2.3 Intraperitoneal glucose tolerance test (IPGTT)

Mice were fasted for 5 hours, after which they were marked and baseline blood glucose (time-point “0”) was measured using a Contour XT meter (Ascensia, Newbury, UK) via an incision in the lateral tail vein after application of a local anaesthetic. A bolus of 20% w/v glucose was given by intraperitoneal (IP) injection (2 g of glucose/kg body mass) and blood glucose was sampled at time-

points 15, 30, 60 and 90 minutes. This was repeated after a minimum of 2 weeks with or without diet intervention up to a maximum of 4 times.

5.2.4 Oral glucose tolerance test (OGTT)

For oral glucose tolerance test (OGTT), mice were prepared as per IPGTT (5.2.3), however, rather than an IP injection, mice are given a bolus glucose orally (2 g/kg).

5.2.5 RNA sequencing

Islets from male Tet-NORM and Tet-MAT mice were treated with 100 ng/mL dox for 48 hours *in vitro* before RNA extraction as previously described in chapter 2 (2.4.2). The RNA was treated with DNase I, Amplification Grade (Invitrogen, Paisley, UK) according to the manufacturer's specifications before being quantified by TapeStation and Qubit. Samples with an RNA integrity number (RIN) greater than 7 were subsequently run using the Quantseq3 FWD kit (Lexogen, Wien, Austria) to generate a library. Libraries were sequenced using HiSeq2000 across a single flowcell generating 75 bp long single ended reads (Illumina Cat# 20024904). All samples were prepared and sequenced as a single pool.

Dr Ildem Akerman analysed all the data. Trimmomatic software (v0.32) and bbduk.sh script (Bbmap suite) was used to trim the ILLUMINA adapters, polyA tails and low- quality bases from reads. Trimmed reads were then uniquely aligned to the mouse genome (M30) using STAR (v2.5.2b) and the Gencode (v28, Ensembl release 92) annotation as the reference for splice junctions.

Between 4–6M mapped reads per sample were quantified using HT-seq (v0.9.1) using Gencode (v28) genes (Nasteska *et al.*, 2021). Genes of interest with a significant fold change vs control were confirmed by RT-qPCR as previously described in chapter 2 (2.4.4).

5.2.6 Differential gene expression analyses

Differential gene expression was obtained using DEseq2 with age- and sex-matched paired Tet-NORM (n = 5) and Tet-MAT samples (n = 5). Differentially expressed genes between control and Tet-MAT islets at adjusted p-value <0.05 were annotated using DAVID BP_FAT, with high stringency for clustering. Gene set enrichment analysis (GSEA) was used to interrogate specific gene sets against expression data. GSEA calculates an Enrichment Score (ES) by scanning a ranked-ordered list of genes (according to significance of differential expression (-log10 p-value)), increasing a running-sum statistic when a gene is in the gene set and decreasing it when it is not. The top of this list (red) contains genes upregulated in Tet-MAT islets while the bottom of the list (blue) represents downregulated genes. Each time a gene from the interrogated gene set is found along the list, a vertical black bar is plotted (hit). If the hits accumulate at the bottom of the list, then this gene set is enriched in downregulated genes (and vice versa). If interrogated genes are distributed homogenously across the rank-ordered list of genes, then that gene set is not enriched in any of the gene expression profiles. We converted human gene sets into homologous mouse gene sets using the homologous gene database from MGI (Nasteska *et al.*, 2021).

5.3 Results

5.3.1 Tet-MAT mouse islets express mCherry and overexpress beta cell maturity markers in response to doxycycline *in vitro.*

To confirm successful overexpression of Pdx1, Mafa and Ngn3 in Tet-MAT mice in response to dox, islets from 8-10-week-old Tet-MAT mice were treated with dox in culture for 48 hours; then mRNA and protein were quantified. Further functional characterisation was conducted to assess Ca^{2+} fluxes and insulin secretion.

5.3.1.1 Tet-MAT islets express mCherry in a dose-dependent manner when treated with doxycycline.

Upon treatment with dox, Tet-MAT islets displayed mCherry fluorescence, which confirms that RIP7rtTA is driving expression of the Teto/M3C cassette (Figure 5-4 A). We tested a range of dox concentrations (10, 100 and 1000 ng/µl), and fluorescence of mCherry was detectable via confocal microscopy at all concentrations (Figure 5-4 B). As 100 ng/µl was enough to elicit strong fluorescence at similar levels to those seen at 1000 ng/µl, and due to reports of the detrimental effects of doxycycline on mitochondrial function (Luger *et al.*, 2018), we decided to use 100 ng/µl for all future *in vitro* experiments with these mouse islets.

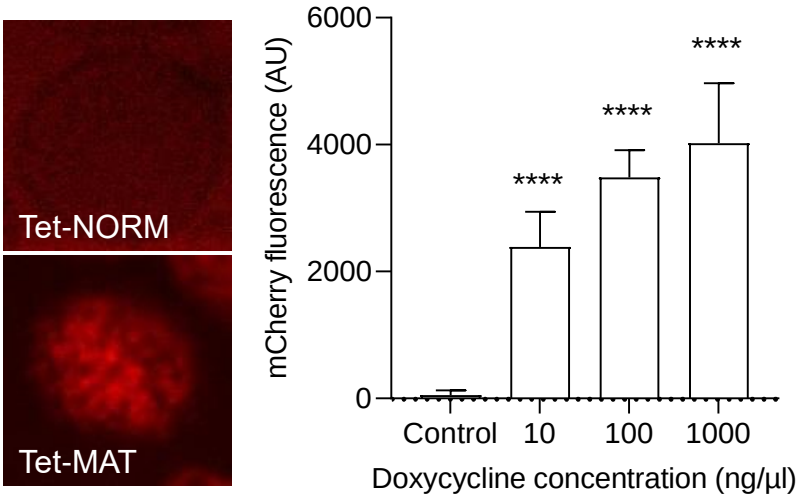

Figure 5-4 | Confirmation of mCherry expression in Tet-MAT islets after exposure to dox. (Left) Confocal images of mCherry fluorescence in islets from Tet-NORM animals (Top) and Tet-MAT animals (Bottom). (Right) Bar graph of background-corrected mCherry fluorescence in Tet-MAT islets treated with vehicle alone or 10, 100 or 1000 ng/µl dox *in vitro* for 48-hours. Error bars are SD. Statistical analyses were performed using one-way ANOVA (n = 32 islets from 3 mice).

5.3.1.2 Tet-MAT islets show increased beta cell maturity marker gene expression and protein synthesis

mRNA was extracted from islets treated with dox *in vitro* for two days, then converted into cDNA, and gene expression was quantified using RT-qPCR. There was a robust upregulation of *Pdx1* mRNA expression in Tet-MAT compared with control. There were smaller but still significant increases in mRNA expression for both *Mafa* and *Ngn3* in Tet-MAT islets treated with dox (Figure 5-5 A). This is in line with the order of genes on the polycistronic construct.

To confirm that this increase in mRNA was related to increased protein synthesis, whole islets from Tet-NORM and Tet-MAT mice were fixed after 48-hours dox treatment *in vitro*. They were stained with a PDX1 antibody and

imaged using confocal microscopy. Fluorescence intensity was measured for each beta cell and binned according to fluorescence intensity before the distribution of these groups were plotted to compare Tet-NORM and Tet-MAT PDX1 protein content (Figure 5-5 B). The shift towards a higher PDX1 state demonstrated a loss of immature beta cells, but PDX1 levels in Tet-MAT islets were never greater than the maximum level in any beta cell in wild type islets.

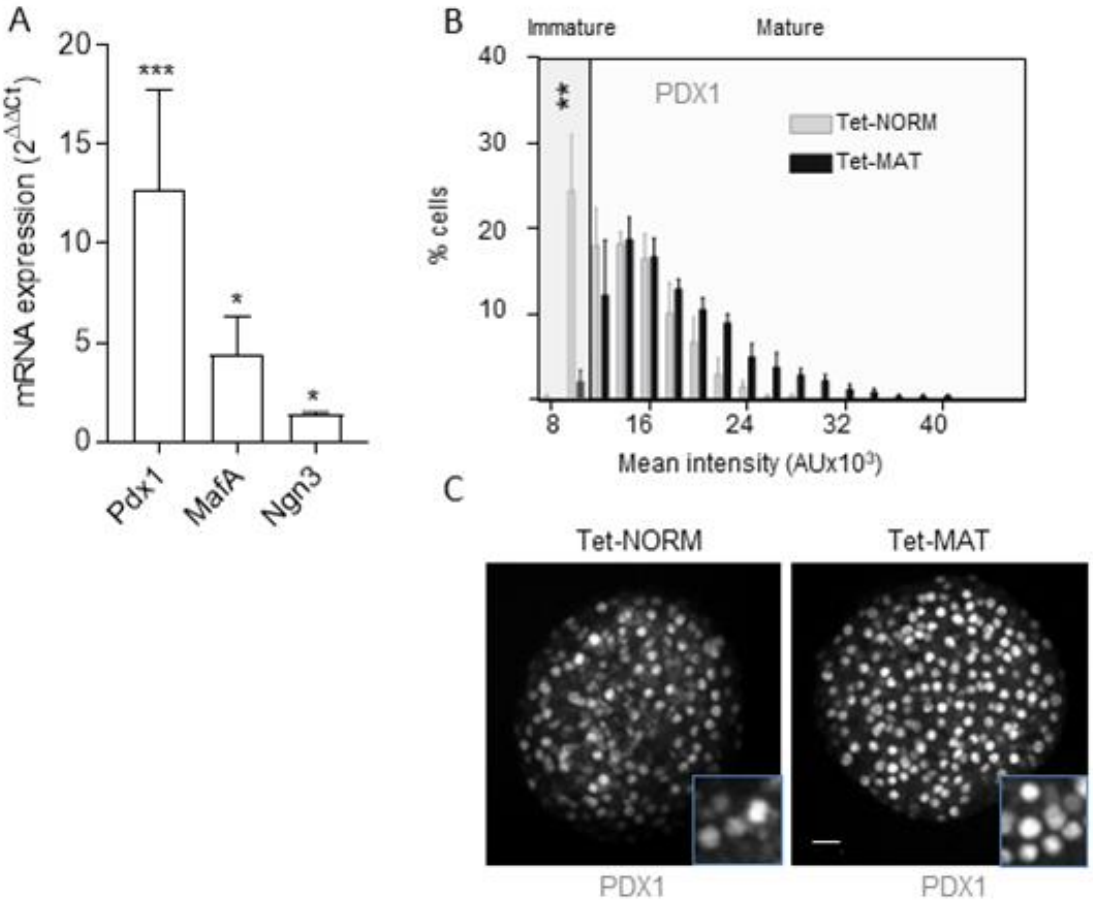

Figure 5-5 | mRNA and protein levels of beta cell maturity markers are upregulated in Tet-MAT mouse islets relative to Tet-NORM islets after treatment with dox. (A) mRNA expression of *Pdx1*, *Mafa* and *Ngn3* in Tet-MAT islets is increased relative to Tet-NORM islets using the $2^{\Delta\Delta Ct}$ method. *β-actin* used as the housekeeping gene ($2^{\Delta\Delta Ct}$ = 1, not shown). Error bars are SD (n= 3-7 replicates from 3 mice). (B) Histogram of frequency of cells binned by PDX1 fluorescence (n =6 islets from 3 mice). Analyses using two-way ANOVA; error bars are SD. (C) Representative images of PDX1 staining showing increased PDX1 protein quantified in B.

5.3.1.3 Forced overexpression of beta cell identity markers impair Ca^{2+} fluxes

To assess the functional effects of *Pdx1*, *Mafa* and *Ngn3* overexpression in islets from Tet-MAT mice, Ca^{2+} fluxes in beta cells in response to glucose and potassium chloride were measured using fluo-8. Islets were isolated from Tet-MAT and Tet-NORM mice and treated with dox for 48-hours prior to imaging on a spinning disk confocal microscope. Changes in fluo-8 fluorescence, a marker for intracellular Ca^{2+} concentration, in response to both high glucose and KCl were blunted in Tet-MAT compared with Tet-NORM islets (Figure 5-6).

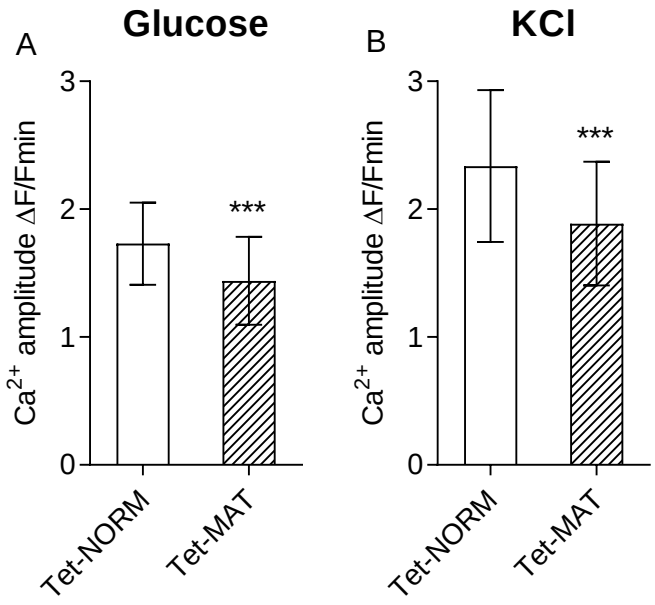

Figure 5-6 | Bar graph of Ca^{2+} responses to glucose in islets from Teto/M3C mice treated with dox 100 ng/µl for 48-hours. Ca^{2+} responses were measured in islets treated with 17 mM glucose (A) or 10mM KCl (B). Open bar = Tet-NORM; shaded bar = Tet-MAT. Error bars are SD (n= 33-37 islets from 3 mice).

5.3.1.4 Tet-MAT islets have normal gene expression in the absence of doxycycline

There have been reports of the effects of TetOn constructs on beta cell function (Jouvet and Estall, 2021). In these studies, all mice possessed one copy of the TetOn to control for this unintended feature. However, to confirm that Teto/M3C construct did not affect gene expression in the absence of dox, islets from Tet-NORM and Tet-MAT mice were isolated and *Pdx1* and *Mafa* mRNA was quantified. In the absence of dox, there was no significant difference between Tet-MAT and Tet-NORM gene expression (Figure 5-7).

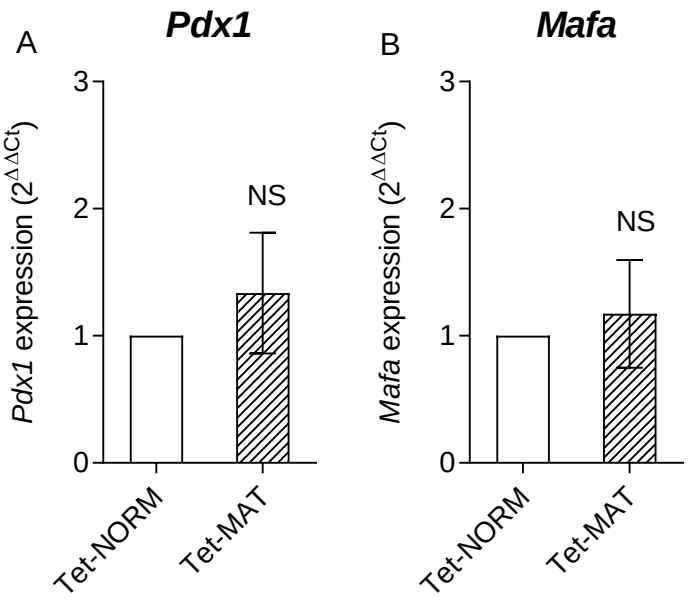

Figure 5-7 | Gene expression of key beta cell maturity markers are unchanged in Tet-MAT islets compared with Tet-NORM islets in the absence of dox. RT-qPCR data showing comparable levels of *Pdx1* (A) and *Mafa* (B) mRNA expression in islets from Tet-NORM (open bar) and Tet-MAT (shaded bar) mice in the absence of dox. Error bars are SD (n= 4 replicates from 2 mice).

5.3.2 RNA-seq identifies changes in genes related to beta cell identity, as well as glucose and carbohydrate metabolism

To understand how loss of immature beta cells influences the transcriptome across the beta cell compartment, RNA-seq was performed on doxycycline-treated islets from Tet-NORM and Tet-MAT mice. Differential gene expression (DGE) analysis revealed 83 genes with an adjusted p-value below 0.05 in Tet-MAT islets vs Tet-NORM (Figure 5-8 A). A full list of these genes is available in the APPENDIX. Gene ontology analysis showed that, of the genes most differentially expressed, a high proportion of them related to peptide hormone secretion and transport (Figure 5-8 B). Gene set enrichment analysis (GSEA) identified upregulation of genes involved in beta cell identity, as well as carbohydrate and glucose metabolism (Figure 5-8 C). Genes of interest were selected based on the literature, and changes in gene expression between Tet-MAT vs Tet-NORM islets were confirmed by RT-qPCR, namely *Ucn3, G6pc2*, *Cox6a2*, *Rgs4* and *Pkib*. Of these genes assayed, only *G6pc2*, *Cox6a2* and *Rgs4* were found to be significantly increased in Tet-MAT islets. However, both *Ucn3 and Pkib* showed a trend towards increase but were not found to be significant (Figure 5-8 D).

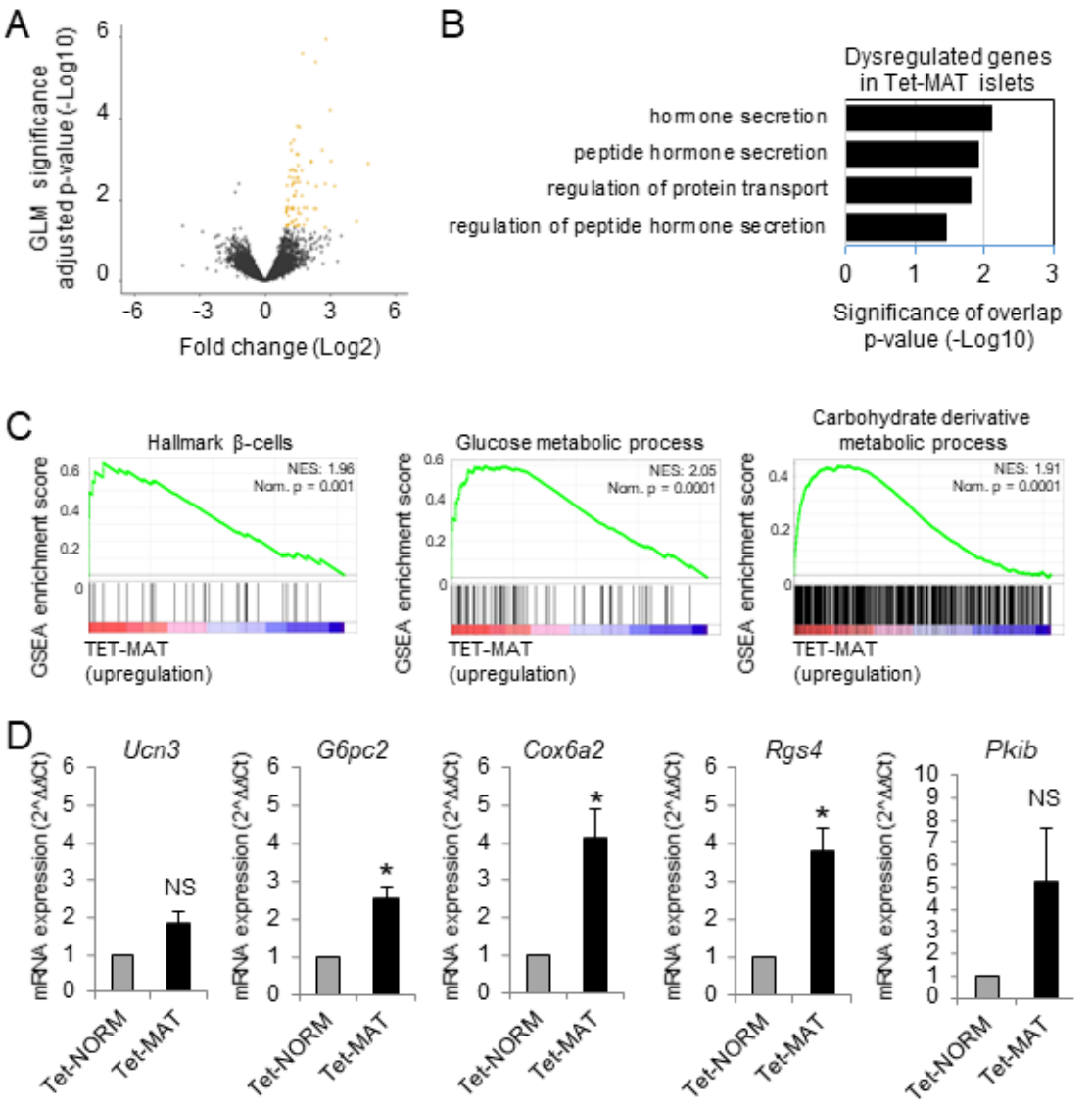

Figure 5-8 | RNA sequencing of Tet-MAT and Tet-NORM islets treated with dox for 48 hours. (A) Volcano plot of Log2 fold change vs significance. Significant data points are in yellow. (B) Gene ontology analysis of differentially regulated genes in Tet-MAT islets. (C) Gene set enrichment analysis (GSEA) suggests that genes belonging to the gene set "hallmark β-cells" are upregulated in Tet-MAT islets. Enrichment of genes belonging to glucose and carbohydrate derivative metabolic processes are also amongst the upregulated genes in Tet-MAT islets. (n=5 samples per condition from 5 mice). (D) RT-qPCR analyses confirming upregulation of *Ucn3*, *G6pc2*, *Cox6a2*, *Rgs4* and *Pkib* in Tet-MAT islets. Bar graphs and traces show the mean mRNA expression ($2^{\Delta\Delta Ct}$); error bars are SD. (n=3-4 replicates from 3 mice).

5.3.3 Tet-MAT mice fed doxycycline diet have increased basal insulin secretion and improved glucose tolerance

To determine if the defects detected *in vitro* were also seen *in vivo*, Tet-NORM and Tet-MAT mice were fed a dox diet starting from 8 weeks of age. Their glucose tolerance was assessed by intraperitoneal glucose tolerance test (IPGTT) at two days and two weeks post-dox diet administration. After this time, islets were removed, and glucose-stimulated insulin secretion (GSIS) measured.

5.3.3.1 Glucose-stimulated insulin secretion is normal in Tet-MAT islets.

When expressed as a percentage of total insulin, GSIS in Teto-MAT islets treated with dox was unchanged compared with that of Tet-NORM islets. However, there was a trend towards improved GSIS and higher basal secretion ($p=0.0931$ for 17 mM glucose plus 20 nm exendin 4 (Figure 5-9 A)). However, when GSIS was plotted as fold change compared to 3 mM glucose, there was a significant decrease in GSIS of Tet-MAT islets treated with 17 mM glucose plus exendin 4 compared to that of Tet-NORM islets (Figure 5-9 B).

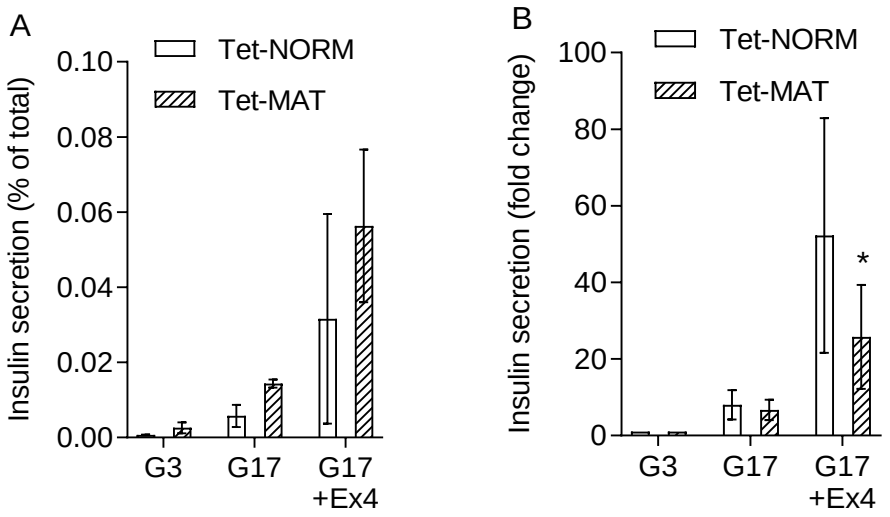

Figure 5-9 | Glucose- and exendin-4- stimulated insulin secretion from islets isolated from Tet-NORM and Tet-MAT mice fed a dox diet for 2 weeks. (A) Insulin secretion as a percentage of total insulin. (B) Insulin secretion expressed as fold change compared to G3. Error bars are SD (n=3-4).

5.3.3.2 Glucose tolerance is improved in Tet-MAT mice fed a doxycycline diet.

The metabolic phenotypes of Tet-NORM and Tet-MAT mice were assessed by IPGTT; the results of which are shown in Figure 5-10. Before treatment with dox, there was no significant difference in glucose tolerance between Tet-NORM and Tet-MAT (Figure 5-10 A). However, after two days of dox diet, there is a significant increase in glucose clearance at 30-, 60- and 90-minutes post glucose bolus in the Tet-MAT compared with Tet-NORM animals (Figure 5-10 B). This improvement is further enhanced after two weeks of dox diet, leading to significant decreases in blood glucose at all time-points (Figure 5-10 C). Significance was determined by two-way ANOVA with multiple comparisons.

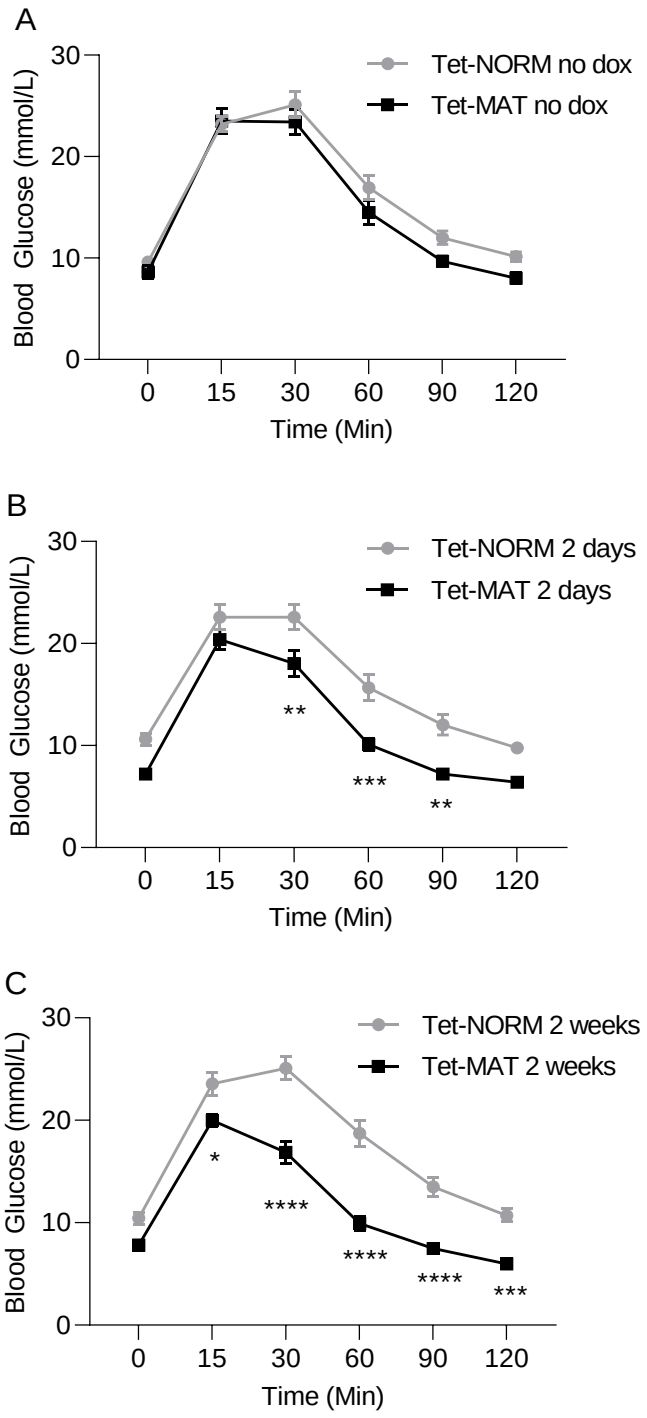

Figure 5-10 | Glucose tolerance in Tet-MAT mice before administration of dox is comparable to that of Tet-NORM mice, but improved after treatment with dox. A) IPGTT of Tet-NORM (grey lines) and Tet-MAT (black lines) mice on normal chow shows no change in glucose tolerance. (n=5-11 mice). B) IPGTT after treatment with dox for two days shows significant improvement in glucose tolerance at 30, 60 and 90 minutes in Tet-MAT mice. (n=9-11 mice). C) IPGTT after two weeks of dox diet administration shows further improvements in glucose tolerance in Tet-MAT mice vs Tet-NORM mice at all time-points post-injection. (n= 10-12 mice).

The change in glucose tolerance can be better seen in Figure 5-11, which plots IPGTTs in either the Tet-NORM mice or the Tet-MAT mice over time. There is no significant change in glucose tolerance over time in Tet-NORM mice (Figure 5-11 A). Conversely, Tet-MAT show improved glucose tolerance after 48 hr and 2 weeks of dox diet (Figure 5-11 B)

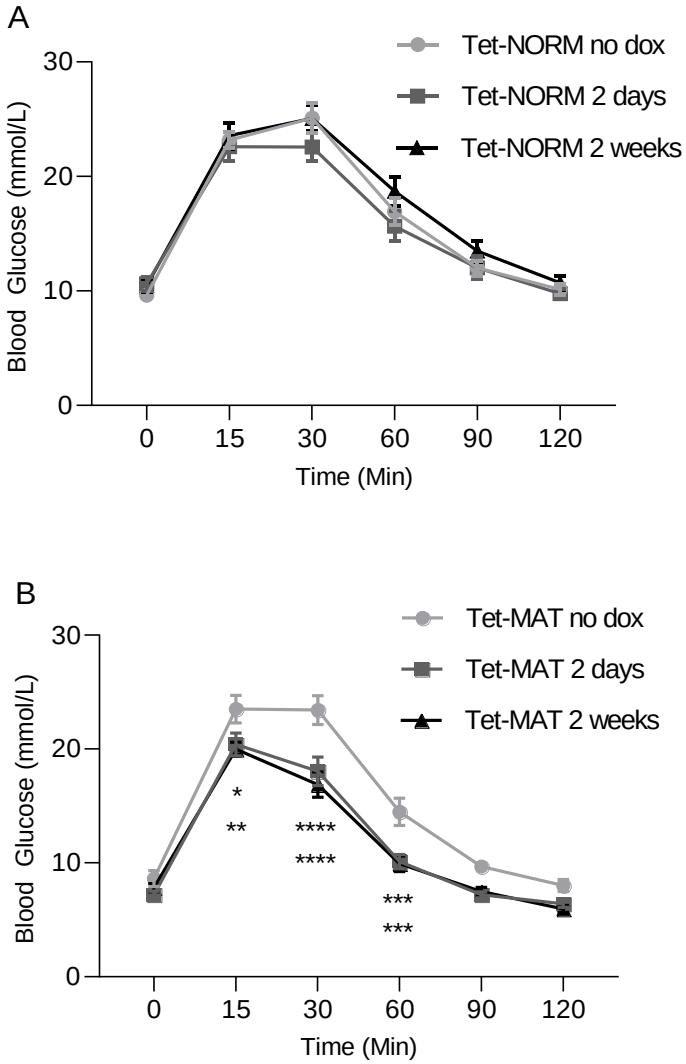

Figure 5-11 | Intraperitoneal glucose tolerance tests conducted on Tet-MAT and Tet-NORM mice, comparing before treatment, two days treatment, and two weeks treatment with dox diet. A) Tet-NORM mice show no chance in glucose tolerance after two days or two weeks on dox diet. (n= 11, 11 and 10 mice respectively). B) IPGTT of Tet-MAT mice before and after two days or two weeks of dox. (n= 5, 9 and 12 mice respectively).

5.3.3.3 Oral glucose tolerance test corroborates the IPGTT data.

Tet-NORM and Tet-MAT mice showed no differences in glucose tolerance when assessed by oral glucose tolerance test before treatment with dox (Figure 5-12 A). However, after four weeks on a dox diet, there is a significant improvement in glucose tolerance at all time-points (Figure 5-12 B).

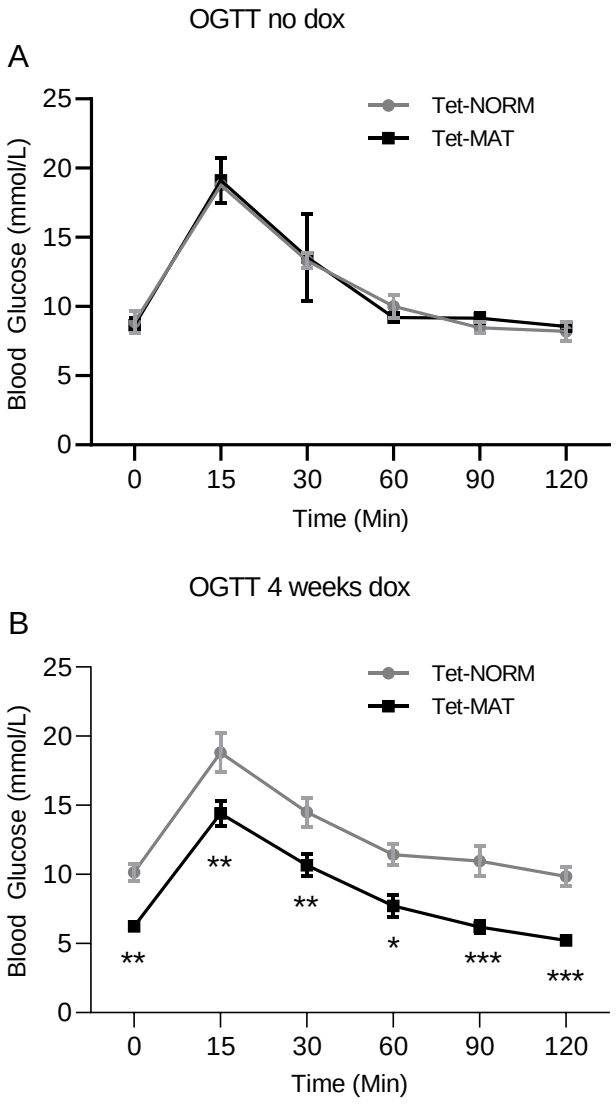

Figure 5-12 | Oral glucose tolerance tests show an improvement in glucose tolerance in Tet-Mat mice after 4 weeks dox diet but are comparable to that of Tet-NORM prior to dox diet. Blood glucose levels at different time points in Tet-NORM (grey lines) and Tet-Mat mice (black lines) before dox treatment (Top) and 4 weeks (Bottom) post dox diet treatment. Error bars are SEM (Tet-NORM n= 2-3 and Tet-MAT n= 4-5 mice).

5.4 Discussion

Recent evidence shows that levels of transcription factors associated with beta cell maturity can be used to define unique populations of beta cells which have subtle but important effects on insulin secretion and overall islet function (Pipeleers, 1992; Farack *et al.*, 2019). However, very little work has looked at the functional effects of altering the proportion of these beta cell populations. This is especially important considering that these populations are generally considered to be less functionally competent than mature beta cells which make up the majority of the pancreatic islet. Therefore, these studies set out to further interrogate the role of heterogeneity within the mouse islet by forcing it into a more uniform state via the upregulation of key transcription factors for beta cell identity. To do this, MAFA, NGN3 and PDX1 were chosen as targets to act as surrogates of beta cell maturity. We hypothesised that, without the support of immature subpopulations of beta cell (such as 'hubs'), the islet would be unable to maintain normal function, even with an increase in normal secretory mature beta cells (Johnston *et al.*, 2016).

5.4.1 A conditional mouse model of loss of heterogeneity

We were able to successfully cross white Teto/M3C mice (Zhou *et al.*, 2008) with those harbouring the RIP7rtTA transgene (Gossen *et al.*, 1995), producing Teto/M3CxRIP7rtTA mice on a C57BL6 background after 4-6 rounds of breeding. This generated a conditional mouse model overexpressing *Pdx1*, *MafA* and *Ngn3* in beta cells in the presence of dox (Figure 5-4 and Figure 5-5). Islets from these mice have impaired Ca^{2+} fluxes (Figure 5-6), consistent with

both our hypothesis and previously generated data using an adenovirus to overexpress *Pdx1*, *Ngn3* and *Mafa* (Nasteska *et al.*, 2021). Tet-MAT islets demonstrated normal gene expression in the absence of dox, indicating that the transgene was inactive under normal conditions (Figure 5-7). This normal gene expression in the absence of dox also alleviates any fears of the construct leaking, potentially causing anomalous errors in our control population of mice.

5.4.2 RNA-seq analysis found changes in genes related to metabolism and hormone secretion

Unsurprisingly, RNA-seq analysis revealed that numerous genes were upregulated in Tet-MAT islets, including those known to be related to beta cell identity and function, as well as metabolic processes (Figure 5-8 A-C). This correlates with our understanding of *Pdx1, Mafa and Ngn3* as transcriptional regulators, as an increase in one or all of these genes is likely to lead to changes in other genes that can be linked by these gene ontologies.

Upregulation of *Ucn3* in beta cells has been shown to be a key marker of transition from a population defined as “virgin” beta cells into mature beta cells (van der Meulen *et al.*, 2017). In these studies, RNA-seq demonstrated a 75% increase in *Ucn3* expression in Tet-MAT compared with Tet-NORM islets (see Table 6). Validation of the RNA-seq data using RT-qPCR does not support this increase ($p=0.75$); however, this modest increase may not be detected due to insufficiently powered experiments (Figure 5-8 D).

One other gene of interest upregulated by forced overexpression of these beta cell markers was C2CD4B, a candidate gene linked with the single nucleotide polymorphism rs7163757 which has been identified by GWAS studies as being associated with altered risk of T2D in a Danish population (Grarup *et al.*, 2011). This region of the genome which harbours this SNP has been identified as a stretch enhancer, as it is able to modulate expression of nearby genes such as *C2cd4b* (Mehta *et al.*, 2016; Kycia *et al.*, 2018). Knock out of *C2cd4b* in female mice has since been shown to lead to impaired glucose tolerance, assessed by IPGTT, after 20 weeks of age when maintained on a high fat diet (Mousavy Gharavy *et al.*, 2021).

Interestingly, there was a significant increase in somatostatin gene expression in Tet-MAT islets versus Tet-NORM, log fold change of 1.2 with an adjusted p-value of 0.0004 (see APPENDIX). There are mixed reports of the effect of insulin on somatostatin secretion (Huising *et al.*, 2018), but under these experimental conditions, upregulation of *Pdx1*, *Mafa* and *Ngn3* in beta cells lead to a robust upregulation in somatostatin expression. This may be due to the potent paracrine effects of insulin on delta cell identity and function (Arrojo e Drigo *et al.*, 2019). This warrants further investigation and is evaluated in the discussion chapter (6.5).

5.4.3 *In vivo* studies indicate the importance of whole-body effects on experimental outcomes

To investigate the effects of increased beta cell maturity in the context of the whole mouse, Tet-NORM and Tet-MAT mice were fed a dox diet for 48 hours. Isolated islets from Tet-MAT mice exhibited the same impairments in calcium fluxes seen in the *in vitro* dox-treated islets. Surprisingly, when glucose- and incretin- stimulated insulin secretion was assayed, a mild improvement was observed in Tet-MAT islets compared with Tet-NORM islets (Figure 5-9 A). Basal insulin secretion was also raised in Tet-MAT islets and, when stimulated insulin secretion is expressed as fold-change compared to basal, there was a significant decrease in insulin secretion at high glucose concentration (Figure 5-9 B). Changes in basal insulin secretion are often seen during metabolic stress and can be characteristic of islet failure (Taylor, 2013). In this case, it may be due to the loss of synchronicity in calcium fluxes throughout the islet, since cell-cell communication reduces fasting basal insulin secretion and amplifies glucose-stimulated insulin secretion in healthy islets (Konstantinova *et al.*, 2007).

While on normal chow, Tet-MAT mice showed normal glucose tolerance (Figure 5-10 A), demonstrating little to no leak from either the TetOn or M3C constructs. However, when the Tet-MAT mice were subjected to dox diet, the mice showed an improved response to glucose. This may be due to an increase in beta cell proliferation, which would not have been seen in isolated islets. However, *in vivo,* beta cells are much more proliferation-competent, and we may have

triggered this in the Tet-MAT mice. Future studies would be needed to assess beta cell mass in these mice, but the SARS-CoV-2 pandemic curtailed our ability to continue past this point due to UK university and animal facility closures. Alternatively, it could be an effect of fluorophore overexpression, as seen in Johnston *et al.*, 2016. Interestingly, there was no change in glucose tolerance between 48 hrs and 2 weeks of dox diet in Tet-MAT mice, and no change in Tet-NORM mice after dox diet, showing that neither dox nor time is a factor in these experiments (Figure 5-11 A&B).

OGTT tests demonstrated that, while on normal chow, both Tet-MAT and Tet-NORM mice have almost identical glucose responses after an oral bolus of glucose. However, after four weeks of dox diet, Tet-MAT mice had a profoundly improved glucose tolerance, as well as reduced fasting blood glucose levels (Figure 5-12). This fasting hypoglycaemia mirrors the increased basal insulin secretion seen in *in vitro* GSIS experiments using islets from these mice (Figure 5-9 A).

These perturbations in glucose sensing and insulin secretion in islets with reduced diversity in maturity states could be due to reduced numbers of hubs, therefore impairing the cell-cell communication needed to coordinate glucose responsiveness. This state is mirrored in experiments using obese mice (Ravier, Sehlin and Henquin, 2002), or mice lacking the *Cx36* gene (MA *et al.*, 2005; Speier *et al.*, 2007; WS *et al.*, 2012), as well as studies in which hubs are identified and silenced (Johnston *et al.*, 2016). Paracrine effects may also be involved, with mature beta cells exerting increased influence on somatostatin secreting cells, which inhibits beta cell function (Rorsman and Huising, 2018).

5.4.4 Conclusion

In summary, heterogeneity is important for normal beta cell function, and loss of that heterogeneity may account, at least in part, to the failure of the pancreatic islet in type 2 diabetes mellitus. Further investigation is warranted to elucidate the roles of immature subpopulations of beta cells, with the possible aim of manipulating them for therapeutic strategies.

6 DISCUSSION

Type 2 diabetes mellitus affects millions of people worldwide, and its prevalence is increasing more rapidly in low- and middle-income countries. Co-morbidities include kidney damage, impaired vision, heart attack and stroke, thus resulting in huge personal and financial burden. While ultra-low-calorie diets are able to reduce the severity of the disease for some (Lim *et al.*, 2011; Rehackova *et al.*, 2017), greater understanding of the processes that cause the disease is required to produce treatments that will improve the lives of people with diabetes.

This thesis set out to investigate the role of either glucocorticoid excess, or an increase in expression of genes responsible for beta cell identity, on beta cell function. Glucocorticoids are steroid hormones which are vital for normal glucose metabolism, prompting an increase in glucose synthesis in times of stress, however, in conditions in which it is produced inappropriately, such as Cushing's disease, beta cell function becomes impaired, leading to glucose intolerance (Boscaro *et al.*, 2001). Previous studies have shown that, while beta cells are glucocorticoid sensitive, concentration at the islet level are boosted by enzymatic activation and reactivation of the steroid by HSD11B1 present in the alpha cell (Swali *et al.*, 2008). This highlights the importance of different cell types within the pancreatic islet working in a coordinated fashion. However, in addition to different cell types (*e.g.*, alpha, beta, delta), there are differences seen within these cell types (Johnston *et al.*, 2016). The importance of these subpopulations are less well characterised. Therefore, human and mouse islets were treated with endogenous GCs in order to mimic a moderate excess to elucidate the mechanisms behind GC induced beta cell function. Furthermore, a

mouse model of beta cell overexpression of *Pdx1*, *Mafa* and *Ngn3* was utilised to mimic a beta cell population lacking the normal variation in identity. Both these lines of investigation have given us deeper insights into the mechanisms through with the pancreatic islet functions normally, and in the face of a perturbed internal or external environment. These findings provide future avenues for clinical applications, such as the Mouse islets are resistant to glucocorticoid treatment

6.1 Mouse islets are resistant to glucocorticoid treatment

As discussed in chapter 3, GCs are naturally occurring steroid hormones which control glucose metabolism and stress responses. However, conditions that are characterised by GC excess, such as Cushing's syndrome, or treatment with exogenous GCs for inflammatory disorders, are known to lead to glucose intolerance. This chapter demonstrated that, while GCs have profound effects on ionic fluxes, a parallel amplifying pathway, mediated by cAMP, exists and is able to compensate for impaired Ca^{2+} fluxes. While previous studies have shown an impairment in beta cell Ca^{2+} fluxes and secretion in conditions of GC excess, these studies often use whole body systems, or use synthetic GC such as Dexamethasone, providing a more confounding system, or incredibly high potencies of GC, respectively (Swali *et al.*, 2008). Swali *et al.* used dexamethasone over a short, two-hour, period which may not be long enough for the compensatory cAMP mechanism to counteract more short-term effects on Ca^{2+} signalling seen in this work.

GCs impair VDCC function but improve cAMP generation by upregulating *Adcy1* expression. Increased cAMP leads to a larger readily releasable pool of insulin granules through PKA, enabling the beta cell to maintain normal secretory function in the face of impaired Ca^{2+} responses to glucose (Shibasaki *et al.*, 2007; Kaihara *et al.*, 2013). Since this work was completed, it has been demonstrated that glucocorticoids can upregulate cAMP in lung through non-genomic pathways, such as $G_{\alpha s}$ (Nuñez *et al.*, 2020). This may account for some of the increased cAMP seen in these studies; however, given that we treated islets for 48 hours, genomic effects are more likely. Conversion of 11-DHC into cort is facilitated by HSD11B1 in a paracrine manner via alpha cells (Swali *et al.*, 2008; Fine *et al.*, 2018).

Mouse islets treated with GCs showed an approximately 50% reduction in glucose-stimulated Ca^{2+} rises which would normally result in impaired insulin secretion (Figure 3-1). Surprisingly, these islets showed normal insulin secretion *in-vitro* (Figure 3-4). These islets had normal levels of insulin and VDCC subunit mRNA expression but there were changes in VDCC conductance which would normally indicate deranged stimulus-secretion coupling, according to patch-clamp analyses performed by our collaborators at Vanderbilt University (Figure 3-5).

When cAMP responses to glucose were assayed using a luciferase-based kit, or via live cell imaging employing the cAMP sensor epac2-camps, they were found to be significantly increased. Gene expression of *Adcy1* was found to be significantly upregulated in both 11-DHC and corticosterone treated islets, providing a mechanism for enhanced cAMP production. Super-resolution

microscopy revealed an increased pool of readily releasable insulin granules at the cell membrane, which could be explained by an increase in cAMP activity and would help maintain normal insulin secretion. It would be interesting to subject this system to some perifusion experiments to interrogate insulin secretion dynamics over time and see if there is an increase in the contribution of the second phase to total insulin secretion (Georgiadou *et al.*, 2020). In mouse islets, cAMP responses to glucose have been shown to be oscillatory at the cell membrane using TIRF microscopy (Tian *et al.*, 2015), while other studies that used epifluorescence techniques showed non-oscillatory cAMP increases in response to high glucose concentrations (Landa *et al.*, 2005). Thus, additional studies are required to investigate the impact of glucocorticoids on cAMP oscillations, which were not detectable at the resolutions used here.

The novel concept of cAMP-based compensation of insulin secretion was supported by experiments in which the fatty acid palmitate, a known inhibitor of PKA (a signalling molecule downstream of cAMP), led to impaired glucose-stimulated cAMP generation. In addition, Tian *et al.* showed that long term treatment of mouse and human islets with palmitate led to delayed and blunted calcium responses to glucose. They identified the mechanism through which palmitate impaired GSIS as decreased *Adcy1* expression which supports the results of chapter 3, (Tian *et al.*, 2015). Additional studies thus are warranted in glucocorticoid-treated *Adcy1*- and *Adcy9*- null islets, since ADYC chemical inhibitors are poorly sub-type specific. Upregulated cAMP signalling may represent a protective mechanism that is disrupted by free fatty acids to induce β-cell failure/decompensation in the face of excess glucocorticoid. Of note,

endogenous elevation of glucocorticoids leads to dyslipidaemia as a result of lipolysis, de novo fatty acid production/turnover, and hepatic fat accumulation (Arnaldi *et al.*, 2010).

We also established a clear role of HSD11B1, the enzyme responsible for activation and reactivation of 11-DHC into corticosterone (cortisone into cortisol in human), in these processes as whole body *Hsd11b1* knockout rescued the effects of 11-DHC on Ca^{2+} fluxes. However, calcium responses in knockout islets treated with cort were equivalent to those of the control treated knockout islets. This may be due to the lack of reactivation of corticosterone in the knockout islets in the absence of HSD11B1 (Figure 3-14).

HSD11B1 is also required for the effects of 11-DHC on glucose-stimulated cAMP generation (Figure 3-15). However, corticosterone was still able to increase cAMP in the knockout mouse islets, suggesting that lower levels of corticosterone are required for the increases in cAMP responses we see. Indeed, corticosterone was still able to upregulate *Adcy1* expression in the knockout mice while 11-DHC was not. To confirm that 11-DHC and cort were acting through the glucocorticoid receptor, chemical blockade was performed using the GR antagonist, RU486 (Mifepristone), which was able to rescue the effects of 11-DHC on calcium flux. Interestingly, corticosterone was still able to exert its effects, suggesting an alternate mechanism or incomplete blockade of the receptor. A diagrammatic overview can of the main findings of chapter 3 is contained within Figure 3-18 (Fine *et al.*, 2018).

An aspect of this work which has not been previously considered is how this might have a wider impact of glucose metabolism in normal conditions in a wider sense. While glucocorticoids are known as stress hormones, allowing the body to produce the fuel needed in survival situations, there are less of these situations day to day. What is seen, is a lower level, but much more prolonged stress, caused by our modern environment (work, relationships, rising energy bills). The human body has not had to deal with this chronic low level GC excess which, combined with our sedentary lifestyle leads to long-term derangement of glucose homeostasis.

6.2 Human islets are also resistant to glucocorticoid treatment

In chapter 4, we successfully demonstrated that the mouse data described in chapter 3 was transferable to humans. Human islets from multiple donors (Table 4) were treated with GCs and, as seen in chapter 3, while Ca^{2+} fluxes were impaired, cAMP was able to sensitise the islet sufficiently to maintain normal glucose-stimulated insulin secretion (Fine *et al.*, 2018).

Many studies which interrogate the role of glucocorticoid use the synthetic analogue, dexamethasone. Dexamethasone has a potency of approximately 100 times that of endogenous glucocorticoid, making the changes seen in these experiments unrepresentative of the physiological role of glucocorticoid. As a result, the consensus in the literature is that GCs cause an impairment in beta cell function. However, endogenous GCs are in fact critical for beta cell function (Swali *et al.*, 2008). The translational relevance of using dexamethasone is also

unclear, since the GC is generally used in the oncology settings. Most individuals with inflammatory disease/allergy, who are the major subset to develop GC-induced T2D, would be treated with prednisolone (pred). That being said, few studies have look at endogenous GC, which is not only important for understanding how dex/pred-induced changes in adrenal function might contribute to beta cell function, but also for understanding how our endogenous stress response might contribute to T2D risk. Lastly, it is difficult to understand how dex/pred influence beta cell function without firstly understanding how endogenous steroids do the same.

6.3 Human and mouse islets show similar responses to glucocorticoids

Despite the differences in species, the time between isolation and experimentation, and the diverse nature of human islets compared to an inbred population of mice, the results in human islets perfectly mirrored those seen in mouse islets. This demonstrates that the mechanisms described in the first two results chapters are highly conserved. This evolutionary conservation indicates the importance of this mechanism in maintaining normal function of the pancreatic islet.

6.4 Heterogeneity is required for normal islet function

Not only are there multiple cell types within the pancreas which interact in a paracrine manner, but there are also subpopulations within these cell types. For example, ‘hub’ cells are highly metabolic, less mature beta cells which

coordinate calcium fluxes across the pancreatic islet to improve insulin secretion (Johnston *et al.*, 2016). 'Extreme' beta cells might be responsible for basal secretion due to their high insulin mRNA, but low protein content, suggesting high levels of export (Farack *et al.*, 2019).Additionally, there is a population of immature beta cells identified by expression of *c-Myc*. These cells are capable of replicating and may be responsible for beta cell expansion (Puri *et al.*, 2018). Finally, *Fltp* acts as a reporter to distinguish between immature and mature beta cells. *Fltp* is only present in mature secretory beta cells (Bader *et al.*, 2016).

In chapter 5, we studied the effect of decreased heterogeneity within the beta cell population and how this might affect some of the signalling mechanisms previously identified. To achieve this, we chose three markers of beta cell identity to upregulate in a temporospatial manner using a mouse expressing the M3C cassette in addition to a TetOn construct: *Pdx1, Mafa* and *Ngn3.* This produced mice possessing fewer beta cells with a $PDX^{low,}MAFA^{low}$ phenotype. Doxycycline-treated islets from these mice had impaired glucose-stimulated calcium fluxes and reduced GSIS, while RNA-seq showed upregulation of genes relating to carbohydrate metabolism, such as glucose-6-phosphatase 2 and Monocarboxylate transporter 7. Conversely, when these mice were treated with doxycycline, they showed improved glucose tolerance by OGTT and IPGTT, possibly due to an expansion in beta cell mass (Nasteska *et al.*, 2021).

While a decrease in *c-Myc* expression was seen in the RNA-seq data, this difference was not significant (data not shown), suggesting there may be other forces driving *c-Myc* expression despite decreased heterogeneity. Additionally,

there was no change in *Fltp* expression, despite *Wnt4* being significantly downregulated*, Wnt4* being highly expressed in *Fltp* positive cells. *Wnt4* has been shown to be a driver of PDX1 and NKX6.1 protein expression (Bader *et al.*, 2016). This downregulation may be a result of negative feedback due to the increased levels of PDX1 being driven by our construct.

6.5 Critical evaluation & future direction

In this section, the thesis is looked at with a critical eye, with a view to interrogate the methods, experimental design, and power of the data. It then suggests steps that could be taken to address these concerns if future work was to be completed.

All of the calcium imaging presented in this thesis was conducted using the non-ratio-metric dye Fluo8. However, one potential complication with using a non-ratio-metric calcium indicator is that any differential effects on pH caused by treatment conditions can lead to misleading changes in $F/F_{min.}$ These concerns could be assuaged by using a ratio-metric dye, such as Fura2 (Grynkiewicz, Poenie and Tsien, 1985). However, the use of Fura2 adds additional confounding variables due to the harmful effects of UV light on cells.

Another potential confounding factor is the use of 10 mM KCl to elicit a maximal calcium response, as this may not be enough to fully open the voltage dependent calcium channels. However, experiments described here used 10 mM KCl in the presence of high glucose concentrations, so amplifying mechanisms should already have been upregulated. Nevertheless, further work

employing higher potassium chloride concentrations (30 mM) could be undertaken to confirm the effect of glucocorticoids on calcium signalling.

While using isolated islets is beneficial since the three-dimensional structure of the islet and normal proportion of different cell types is maintained, one drawback is that the larger whole-body context is lost. The loss of endocrine signals contained in the blood supply, neuronal input, and circadian and ultradian rhythms will have countless effects on the function of the islet (Walker *et al.*, 2012). This is demonstrated by the *in vivo* work in the final chapter of this thesis, in which Tet-MAT mice had a completely different phenotype when compared with the *in vitro* work over the same time period using isolated islets from the same mice. Additional experiments looking at beta cell mass in Tet-MAT mice fed a dox diet would rule out a role beta cell expansion in the decreased basal glucose levels and improved glucose tolerance in these mice.

RNA-seq was conducted using a QuantSeq library kit, which uses 3' polyA sequences to identify and count mRNA only. As a result, QuantSeq may be less able to detect changes in the expression of genes with lower expression levels compared to traditional RNA-seq. This may have resulted in the loss of some interesting DGEs due to the reduced sensitivity (Jarvis *et al.*, 2020). Additionally, due to the low yield and/or RIN from some islet samples, n numbers could have been higher to ensure more samples with optimal RINs.

The more than 2-fold increase in somatostatin mRNA expression caused by overexpression of beta cell maturity markers mentioned in 5.4.2 could be further investigated. One potential method to analyse the effects of somatostatin is to

generate a mouse expressing DREADD receptors on delta cells, allowing them to be silenced in real time using specific designer drugs (Zhu and Roth, 2014; Roth, 2016). This was originally planned but due to closures caused to the pandemic, never came to fruition.

Another interesting avenue of investigation would be to use models in which islets are transplanted into the anterior eye chamber, which would allow the effects of doxycycline induction on these islets to be interrogated without influencing the wider pancreatic function (Tun *et al.*, 2020).

The role of fed and fasting state in relation to the described effects of glucocorticoids on beta cell function should be further investigated. The effects of fasting and diabetes act through the HPA axis and GCs to alter brain chemistry, such as Neuropeptide Y, which is responsible for satiety (Makimura *et al.*, 2003). Whereas in a fed state, in which increase insulin action should act on the liver and skeletal muscle to reduce lipogenesis and increase glycogen synthesis, GC excess might lead to impairment of these processes. Since the studies described in this thesis solely use isolated islets, we are currently unable to ascertain any potential effects of fed versus fasted state; however, this is an interesting avenue for further work.

The studies involving glucocorticoids are difficult to translate into a physiological system due to the nature of working with isolated islets. In addition, measurements of local levels of glucocorticoid within the islet in a whole animal model would be impractical. However, I would estimate the levels of

glucocorticoid used in these studies to be comparable to those seen in people with Cushing's.

One of the flaws in this work is its discordant nature, investigating both the effects of endogenous glucocorticoids, and overexpression of *Pdx1* and *Mafa*, on beta cell function. This lack of throughline makes it difficult to tie the results together neatly. However, it should be noted that the thesis was affected by the SARS-CoV-2 and closure of the lab and animal facilities, the latter lasting almost a year. Therefore, work that I had performed for other projects, which would not normally have been included in the thesis, needed to be instead used. It was not possible therefore to backwards engineer the work, since we had to cull all of our animal colonies, with mice only just becoming available again mid-2021. Having said that, if we were to repeat these studies, we would go back and look at the effects of GC on Tet-NORM and Tet-MAT islets.

6.6 Clinical applications

Perhaps therapeutic interventions which target these natural compensatory mechanisms observed in this thesis, such as cAMP or beta cell proliferation, can be developed to boost pancreatic function and improve the lives of patients with impaired glucose tolerance or overt diabetes.

Unpicking the GC based amplification mechanisms seen in chapters 3 and 4 might identify novel therapeutic targets. Given that endogenous GC boosts cAMP to maintain insulin secretion in the face of perturbed Ca2+ fluxes, we can predict that patients with steroid-induced diabetes would benefit more from

GLP1R agonists. Indeed, GLP1R agonists lead to a large increase in cAMP that would be expected to restore insulin secretion in these patients.

Conversely, we could think to harness the cAMP-amplifying effects of cortisol by conjugating it to GLP1R to make a unimolecular agonist targeted to beta cells. A similar dexamethasone-exendin4 conjugate was shown to target steroid to brain regions that become 'inflamed' during obesity (Quarta *et al.*, 2017).

There may be some aspect of the GC transcription factor pathway that would allow an appropriate upregulation of the cAMP pathway without the negative effects on ionic fluxes to improve glucose secretion. This might have a similar effect to that of GLP1R agonists without the negative neural side-effects such as headache, nausea, and GI disorders (Drucker, 2013). One potential drawback of treatments targeting these pathways is that they would be less beneficial, or even harmful, in patients with obesity (who would have high circulating levels of fatty acids which impair adenylate cyclase activity), a condition which is commonly associated with T2D. However, this could be ameliorated using drugs which lower fatty acids, such as fenofibrate.

A more technically challenging approach which might make use of the information gleaned from chapter 5 would be to use gene therapy to address the increase in beta cell differentiation seen in T2D. This may provide more immature beta cells to act as a proliferative pool, or coordinating hubs, to support the already stressed mature beta cell population. This immature population might even be generated by trans-differentiation of other endocrine pancreatic cells into beta cells.

6.7 Concluding statements

While the beta cell is responsible for the secretion of insulin, and therefore the prevention of hyperglycaemia, the pancreatic islet requires a range of signalling events that occur across the cell population. As such, cell types and subpopulations of those cells need to function optimally. This thesis demonstrates that, while glucocorticoid excess has profound effects on calcium signalling in islets, compensatory mechanisms which upregulate *Adcy1* are able to maintain normal glucose-stimulated insulin secretion in both mouse and humans (Fine *et al.*, 2018). Also, when the ability for beta cells to communicate via specialised hub cells is perturbed by upregulating beta cell identity markers, they find an alternative route to maintain glucose secretion via expansion of the beta cell population *in vivo*, although not *in vitro* (Nasteska *et al.*, 2021). These novel findings indicate that the pancreatic islet is somewhat resistant to perturbation, via adaptation to ensure normoglycaemia and, therefore, the ongoing survival of the organism.

7 REFERENCES

Adriaenssens, A. E. *et al.* (2016) ‘Transcriptomic profiling of pancreatic alpha, beta and delta cell populations identifies delta cells as a principal target for ghrelin in mouse islets’, *Diabetologia*. Springer Verlag, 59(10), pp. 2156–2165. doi: 10.1007/s00125-016-4033-1.

Agarwal, A. K. *et al.* (2002) ‘AGPAT2 is mutated in congenital generalized lipodystrophy linked to chromosome 9q34’, *Nature Genetics*. Nat Genet, 31(1), pp. 21–23. doi: 10.1038/ng880.

Alberts, B. *et al.* (2008) *Molecular biology of the cell, 5th edition by B. Alberts, A. Johnson, J. Lewis, M. Raff, K. Roberts, and P. Walter*, *Biochemistry and Molecular Biology Education*. John Wiley & Sons, Ltd. doi: 10.1002/BMB.20192.

Ämmälä, C., Ashcroft, F. M. and Rorsman, P. (1993) ‘Calcium-independent potentiation of insulin release by cyclic AMP in single β-cells’, *Nature*. Nature, 363(6427), pp. 356–358. doi: 10.1038/363356a0.

Andrea, M. M., Natascia, S. and Iorgi, D. (2012) *Disorders of the Posterior Pituitary*. Berlin: Springer. doi: 10.1007/978-3-642-02202-9_385.

Andrews, R. C. and Walker, B. R. (1999) ‘Glucocorticoids and insulin resistance: Old hormones, new targets’, *Clinical Science*, pp. 513–523. doi: 10.1042/CS19980388.

Anik, A. *et al.* (2015) ‘Maturity-onset diabetes of the young (MODY): An update’, *Journal of Pediatric Endocrinology and Metabolism*. Walter de Gruyter GmbH, pp. 251–263. doi: 10.1515/jpem-2014-0384.

Ariyachet, C. *et al.* (2016) ‘Reprogrammed Stomach Tissue as a Renewable Source of Functional β Cells for Blood Glucose Regulation’, *Cell Stem Cell*. Elsevier Inc., 18(3), pp. 410–421. doi: 10.1016/j.stem.2016.01.003.

Arnaldi, G. *et al.* (2010) ‘Pathophysiology of dyslipidemia in Cushing’s syndrome’, in *Neuroendocrinology*. Karger Publishers, pp. 86–90. doi: 10.1159/000314213.

Arrojo e Drigo, R. *et al.* (2019) ‘Structural basis for delta cell paracrine regulation in pancreatic islets’, *Nature Communications*. Nature Publishing Group, 10(1). doi: 10.1038/s41467-019-11517-x.

Bader, E. *et al.* (2016) ‘Identification of proliferative and mature β-cells in the islets of langerhans’, *Nature*. Nature Publishing Group, 535(7612), pp. 430–434. doi: 10.1038/nature18624.

Barbosa, R. M. *et al.* (1998) ‘Control of pulsatile 5-HT/insulin secretion from single mouse pancreatic islets by intracellular calcium dynamics’, *Journal of Physiology*. Wiley-Blackwell, 510(1), pp. 135–143. doi: 10.1111/j.1469-7793.1998.135bz.x.

Barroso, I. *et al.* (1999) ‘Dominant negative mutations in human PPARγ associated with severe insulin resistance, diabetes mellitus and hypertension’, *Nature*. Nature, 402(6764), pp. 880–883. doi: 10.1038/47254.

Basco, D. *et al.* (2018) ‘α-cell glucokinase suppresses glucose-regulated glucagon secretion’, *Nature Communications*. Nature Publishing Group, 9(1), pp. 1–9. doi: 10.1038/s41467-018-03034-0.

Benninger, R. K. P. and Hodson, D. J. (2018) ‘New understanding of β-cell heterogeneity and in situ islet function’, *Diabetes*. Diabetes, 67(4), pp. 537–547. doi: 10.2337/dbi17-0040.

Berg, J., Hung, Y. P. and Yellen, G. (2009) ‘A genetically encoded fluorescent reporter of ATP:ADP ratio’, *Nature Methods*, 6(2), pp. 161–166. doi: 10.1038/nmeth.1288.

Bonner-Weir, S., Sullivan, B. A. and Weir, G. C. (2015) ‘Human Islet Morphology Revisited: Human and Rodent Islets Are Not So Different After All’, *Journal of Histochemistry and Cytochemistry*. Histochemical Society Inc., 63(8), pp. 604–612. doi: 10.1369/0022155415570969.

Boscaro, M. *et al.* (2001) ‘Cushing’s syndrome’, in *Lancet*. Elsevier Limited, pp. 783–791. doi: 10.1016/S0140-6736(00)04172-6.

Bosco, D., Orci, L. and Meda, P. (1989) ‘Homologous but not heterologous contact increases the insulin secretion of individual pancreatic B-cells’, *Experimental Cell Research*. Academic Press, 184(1), pp. 72–80. doi: 10.1016/0014-4827(89)90365-0.

Bratanova-Tochkova, T. K. *et al.* (2002) ‘Triggering and augmentation mechanisms, granule pools, and biphasic insulin secretion’, in *Diabetes*. Diabetes. doi: 10.2337/diabetes.51.2007.s83.

Brissova, M. *et al.* (2005) ‘Assessment of human pancreatic islet architecture and composition by laser scanning confocal microscopy’, *Journal of Histochemistry and Cytochemistry*. SAGE PublicationsSage CA: Los Angeles,

CA, 53(9), pp. 1087–1097. doi: 10.1369/jhc.5C6684.2005.

Brown, J. C. *et al.* (1975) 'Identification and actions of gastric inhibitory polypeptide', *Recent Progress in Hormone Research*. Recent Prog Horm Res, pp. 487–532. doi: 10.1016/b978-0-12-571131-9.50017-7.

Bujalska, I. J., Kumar, S. and M Stewart, P. (1997) 'Does central obesity reflect 'Cushing's disease of the omentum '?', *Lancet*. Lancet Publishing Group, 349(9060), pp. 1210–1213. doi: 10.1016/S0140-6736(96)11222-8.

Butcher, M. J. *et al.* (2014) 'Association of proinflammatory cytokines and islet resident leucocytes with islet dysfunction in type 2 diabetes', *Diabetologia*. Diabetologia, 57(3), pp. 491–501. doi: 10.1007/s00125-013-3116-5.

Chen, C. W. *et al.* (2022) 'Adaptation to chronic ER stress enforces pancreatic β-cell plasticity', *Nature Communications*. Nature Publishing Group, 13(1), pp. 1–18. doi: 10.1038/s41467-022-32425-7.

Chen, M. *et al.* (1985) 'Pathogenesis of Age-Related Glucose Intolerance in Man: Insulin Resistance and Decreased β-Cell Function', *Journal of Clinical Endocrinology and Metabolism*, 60(1), pp. 13–20. doi: 10.1210/jcem-60-1-13.

Chowdhury, S. *et al.* (2015) 'Decreased 11β-hydroxysteroid dehydrogenase 1 level and activity in murine pancreatic islets caused by insulin-like growth factor i overexpression', *PLoS ONE*. Public Library of Science, 10(8). doi: 10.1371/journal.pone.0136656.

Cnop, M. *et al.* (2002) 'The concurrent accumulation of intra-abdominal and subcutaneous fat explains the association between insulin resistance and

plasma leptin concentrations: Distinct metabolic effects of two fat compartments', *Diabetes*, 51(4), pp. 1005–1015. doi: 10.2337/diabetes.51.4.1005.

Cooper, D. M. F. (2003) 'Regulation and organization of adenylyl cyclases and cAMP', *Biochemical Journal*. Portland Press Ltd, pp. 517–529. doi: 10.1042/BJ20031061.

Cooper, G. M. and Hausman, R. E. (2006) *The Cell: A Molecular Approach,4th ed*. 4th edn, *Sinauer Associates, Inc.* 4th edn.

Cooper, M. S. and Stewart, P. M. (2009) '11β-hydroxysteroid dehydrogenase type 1 and its role in the hypothalamus-pituitary-adrenal axis, metabolic syndrome, and inflammation', *Journal of Clinical Endocrinology and Metabolism*. Endocrine Society, pp. 4645–4654. doi: 10.1210/jc.2009-1412.

Crapo, L. (1979) 'Cushing's syndrome: A review of diagnostic tests', *Metabolism*. Metabolism, pp. 955–977. doi: 10.1016/0026-0495(79)90097-0.

Dallman, M. F. *et al.* (1993) 'Feast and famine: Critical role of glucocorticoids with insulin in daily energy flow', *Frontiers in Neuroendocrinology*. Academic Press, 14(4), pp. 303–347. doi: 10.1006/frne.1993.1010.

Davani, B. *et al.* (2000) 'Type 1 11β-hydroxysteroid dehydrogenase mediates glococorticoid activation and insulin release in pancreatic islets', *Journal of Biological Chemistry*. JBC Papers in Press, 275(45), pp. 34841–34844. doi: 10.1074/jbc.C000600200.

Davidson, H. W. and Hutton, J. C. (1987) 'The insulin-secretory-granule

carboxypeptidase H. Purification and demonstration of involvement in proinsulin processing.', *The Biochemical journal*, 245(2), pp. 575–582. doi: 10.1042/bj2450575.

Delaunay, F. *et al.* (1997) 'Pancreatic β cells are important targets for the diabetogenic effects of glucocorticoids', *Journal of Clinical Investigation*. American Society for Clinical Investigation, 100(8), pp. 2094–2098. doi: 10.1172/JCI119743.

Dhatariya, K. K. *et al.* (2019) 'The cost of treating diabetic ketoacidosis in an adolescent population in the UK: a national survey of hospital resource use', *Diabetic Medicine*. Blackwell Publishing Ltd, 36(8), pp. 982–987. doi: 10.1111/dme.13893.

Dickens, M. J. and Pawluski, J. L. (2018) 'The HPA axis during the perinatal period: Implications for perinatal depression', *Endocrinology*. Oxford University Press, pp. 3737–3746. doi: 10.1210/en.2018-00677.

DiGruccio, M. R. *et al.* (2016) 'Comprehensive alpha, beta and delta cell transcriptomes reveal that ghrelin selectively activates delta cells and promotes somatostatin release from pancreatic islets', *Molecular Metabolism*. Elsevier GmbH, 5(7), pp. 449–458. doi: 10.1016/j.molmet.2016.04.007.

Dovio, A. *et al.* (2001) 'Autocrine up-regulation of glucocorticoid receptors by interleukin-6 in human osteoblast-like cells', *Calcified Tissue International*. Springer New York, 69(5), pp. 293–298. doi: 10.1007/s00223-001-2024-8.

Draper, N. *et al.* (2003) 'Mutations in the genes encoding 11β-hydroxysteroid

dehydrogenase type 1 and hexose-6-phosphate dehydrogenase interact to cause cortisone reductase deficiency', *Nature Genetics*. Nature Publishing Group, 34(4), pp. 434–439. doi: 10.1038/ng1214.

Drucker, D. J. (2013) 'Incretin action in the pancreas: Potential promise, possible perils, and pathological pitfalls', *Diabetes*. American Diabetes Association, 62(10), pp. 3316–3323. doi: 10.2337/DB13-0822/-/DC1.

Dubé, J. J. *et al.* (2014) 'Effects of acute lipid overload on skeletal muscle insulin resistance, metabolic flexibility, and mitochondrial performance', *American Journal of Physiology - Endocrinology and Metabolism*. American Physiological Society, 307(12), pp. E1117–E1124. doi: 10.1152/ajpendo.00257.2014.

Dworken, H. J. (1982) 'A Survey of Gastrointestinal Hormonology', in *Gastroenterology*. Elsevier, pp. 23–35. doi: 10.1016/b978-0-409-95021-2.50007-8.

Ebina, Y. *et al.* (1985) 'The human insulin receptor cDNA: The structural basis for hormone-activated transmembrane signalling', *Cell*. Cell Press, 40(4), pp. 747–758. doi: 10.1016/0092-8674(85)90334-4.

Ertel, E. A. *et al.* (2000) 'Nomenclature of voltage-gated calcium channels', *Neuron*. Cell Press, pp. 533–535. doi: 10.1016/S0896-6273(00)81057-0.

Everett, B. M. *et al.* (2018) 'Anti-Inflammatory Therapy With Canakinumab for the Prevention and Management of Diabetes', *Journal of the American College of Cardiology*. Elsevier USA, 71(21), pp. 2392–2401. doi:

10.1016/j.jacc.2018.03.002.

Everett, K. L. and Cooper, D. M. F. (2013) ‘An Improved Targeted cAMP Sensor to Study the Regulation of Adenylyl Cyclase 8 by Ca2+ Entry through Voltage-Gated Channels’, *PLoS ONE*. Edited by R. Berdeaux. Public Library of Science, 8(9), p. e75942. doi: 10.1371/journal.pone.0075942.

Farack, L. *et al.* (2019) ‘Transcriptional Heterogeneity of Beta Cells in the Intact Pancreas’, *Developmental Cell*, 48(1), pp. 115-125.e4. doi: 10.1016/j.devcel.2018.11.001.

Farino, Z. J. *et al.* (2016) ‘Development of a rapid insulin assay by homogenous time-resolved fluorescence’, *PLoS ONE*. Edited by F. Dehghani. Public Library of Science, 11(2), p. e0148684. doi: 10.1371/journal.pone.0148684.

Feldman, E. L. *et al.* (2017) ‘New Horizons in Diabetic Neuropathy: Mechanisms, Bioenergetics, and Pain’, *Neuron*. Elsevier, pp. 1296–1313. doi: 10.1016/j.neuron.2017.02.005.

Fernyhough, P. (2015) ‘Mitochondrial Dysfunction in Diabetic Neuropathy: a Series of Unfortunate Metabolic Events’, *Current Diabetes Reports*. Current Medicine Group LLC 1, pp. 1–10. doi: 10.1007/s11892-015-0671-9.

Ferrannini, E. *et al.* (1996) ‘Insulin action and age’, *Diabetes*, 45(3 SUPPL.), pp. 947–953. doi: 10.2337/diab.45.7.947.

Fiedorek, F. T. and Permutt, M. A. (1989) ‘Proinsulin mRNA levels in fasting and fed ADX rats: evidence for an indirect effect of glucocorticoids.’, *The American Journal of Physiology*, 256(2 Pt 1), pp. E303-8. doi:

10.1152/AJPENDO.1989.256.2.E303.

Fine, N. H. F. *et al.* (2018) ‘Glucocorticoids reprogram b-cell signaling to preserve insulin secretion’, *Diabetes*. American Diabetes Association Inc., 67(2), pp. 278–290. doi: 10.2337/db16-1356.

Froguel, P. *et al.* (1992) ‘Close linkage of glucokinase locus on chromosome 7p to early-onset non-insulin-dependent diabetes mellitus’, *Nature*. Macmillan Magazines Ltd, 356(6365), pp. 162–164. doi: 10.1038/356162a0.

Funder, J. W. *et al.* (1988) ‘Mineralocorticoid action: Target tissue specificity is enzyme, not receptor, mediated’, *Science*. American Association for the Advancement of Science, 242(4878), pp. 583–585. doi: 10.1126/science.2845584.

Gathercole, L. L. *et al.* (2011) ‘Regulation of lipogenesis by glucocorticoids and insulin in human adipose tissue’, *PLoS ONE*, 6(10). doi: 10.1371/journal.pone.0026223.

Geberhiwot, T. *et al.* (2021) ‘Relative adipose tissue failure in alström syndrome drives obesity-induced insulin resistance’, *Diabetes*. Diabetes, 70(2), pp. 364–376. doi: 10.2337/db20-0647.

Gembal, M., Gilon, P. and Henquin, J. C. (1992) ‘Evidence that glucose can control insulin release independently from its action on ATP-sensitive K+ channels in mouse B cells’, *Journal of Clinical Investigation*. The American Society for Clinical Investigation, 89(4), pp. 1288–1295. doi: 10.1172/JCI115714.

Georgiadou, E. *et al.* (2020) ‘The pore-forming subunit MCU of the mitochondrial Ca(2+) uniporter is required for normal glucose-stimulated insulin secretion in vitro and in vivo in mice.’, *Diabetologia*. Diabetologia, 63(7), pp. 1368–1381. doi: 10.1007/s00125-020-05148-x.

Geraldes, P. and King, G. L. (2010) ‘Activation of protein kinase C isoforms and its impact on diabetic complications’, *Circulation Research*. Lippincott Williams & Wilkins, pp. 1319–1331. doi: 10.1161/CIRCRESAHA.110.217117.

Gesina, E. *et al.* (2004) ‘Dissecting the role of glucocorticoids on pancreas development’, *Diabetes*. American Diabetes Association, 53(9), pp. 2322–2329. doi: 10.2337/diabetes.53.9.2322.

Goodpaster, B. H. and Sparks, L. M. (2017) ‘Metabolic Flexibility in Health and Disease’, *Cell Metabolism*. Elsevier, pp. 1027–1036. doi: 10.1016/j.cmet.2017.04.015.

Gossen, M. *et al.* (1995) ‘Transcriptional activation by tetracyclines in mammalian cells’, *Science*. American Association for the Advancement of Science, 268(5218), pp. 1766–1769. doi: 10.1126/science.7792603.

Grarup, N. *et al.* (2011) ‘The diabetogenic VPS13C/C2CD4A/C2CD4B rs7172432 variant impairs glucose-stimulated insulin response in 5,722 non-diabetic Danish individuals’, *Diabetologia*. Diabetologia, 54(4), pp. 789–794. doi: 10.1007/s00125-010-2031-2.

Graves, T. K. and Hinkle, P. M. (2003) ‘Ca2+-induced Ca2+ release in the pancreatic β-cell: Direct evidence of endoplasmic reticulum Ca2+ release’,

Endocrinology, 144(8), pp. 3565–3574. doi: 10.1210/en.2002-0104.

Gremlich, S., Roduit, R. and Thorens, B. (1997) 'Dexamethasone Induces Posttranslational Degradation of GLUT2 and Inhibition of Insulin Secretion in Isolated Pancreatic β Cells', *Journal of Biological Chemistry*, 272(6), pp. 3216–3222. doi: 10.1074/jbc.272.6.3216.

Gromada, J., Chabosseau, P. and Rutter, G. A. (2018) 'The α-cell in diabetes mellitus', *Nature Reviews Endocrinology*. Nature Publishing Group, pp. 694–704. doi: 10.1038/s41574-018-0097-y.

Grynkiewicz, G., Poenie, M. and Tsien, R. Y. (1985) 'A new generation of Ca2+ indicators with greatly improved fluorescence properties', *Journal of Biological Chemistry*, pp. 3440–3450. doi: 10.1016/s0021-9258(19)83641-4.

Guariguata, L. *et al.* (2014) 'Global estimates of the prevalence of hyperglycaemia in pregnancy', *Diabetes Research and Clinical Practice*, 103(2), pp. 176–185. doi: 10.1016/j.diabres.2013.11.003.

Guillam, M. T. *et al.* (1997) 'Early diabetes and abnormal postnatal pancreatic islet development in mice lacking Glut-2', *Nature Genetics*. Nature Publishing Group, 17(3), pp. 327–330. doi: 10.1038/ng1197-327.

Guo, S. *et al.* (2013) 'Inactivation of specific β cell transcription factors in type 2 diabetes', *Journal of Clinical Investigation*. American Society for Clinical Investigation, 123(8), pp. 3305–3316. doi: 10.1172/JCI65390.

Haeusler, R. A., McGraw, T. E. and Accili, D. (2018) 'Metabolic Signalling: Biochemical and cellular properties of insulin receptor signalling', *Nature*

Reviews Molecular Cell Biology. Nature Publishing Group, pp. 31–44. doi: 10.1038/nrm.2017.89.

Halban, P. A. *et al.* (1982) 'The possible importance of contact between pancreatic islet cells for the control of insulin release', *Endocrinology*, 111(1), pp. 86–94. doi: 10.1210/endo-111-1-86.

Hanoune, J. and Defer, N. (2001) 'Regulation and role of adenylyl cyclase isoforms', *Annual Review of Pharmacology and Toxicology*, pp. 145–174. doi: 10.1146/annurev.pharmtox.41.1.145.

Hebrok, M., Kim, S. K. and Melton, D. A. (1998) 'Notochord repression of endodermal sonic hedgehog permits pancreas development', *Genes and Development*. Cold Spring Harbor Laboratory Press, 12(11), pp. 1705–1713. doi: 10.1101/gad.12.11.1705.

Henning, R. J. (2018) 'Type-2 diabetes mellitus and cardiovascular disease', *Future Cardiology*. Future Medicine Ltd., pp. 491–509. doi: 10.2217/fca-2018-0045.

Henquin, J. C. (2000) 'Triggering and amplifying pathways of regulation of insulin secretion by glucose', *Diabetes*. American Diabetes Association Inc., pp. 1751–1760. doi: 10.2337/diabetes.49.11.1751.

Hotamisligil, G. S. and Davis, R. J. (2016) 'Cell signaling and stress responses', *Cold Spring Harbor Perspectives in Biology*. Cold Spring Harb Perspect Biol, 8(10). doi: 10.1101/cshperspect.a006072.

Huising, M. O. *et al.* (2018) 'The difference δ-cells make in glucose control',

Physiology. American Physiological Society, 33(6), pp. 403–411. doi: 10.1152/physiol.00029.2018.

Hwang, J. L. and Weiss, R. E. (2014) 'Steroid-induced diabetes: a clinical and molecular approach to understanding and treatment', *Diabetes/Metabolism Research and Reviews*. John Wiley & Sons, Ltd, 30(2), pp. 96–102. doi: https://doi.org/10.1002/dmrr.2486.

Inagaki, N. *et al.* (1995) 'Reconstitution of IKATP: An inward rectifier subunit plus the sulfonylurea receptor', *Science*. American Association for the Advancement of Science, 270(5239), pp. 1166–1170. doi: 10.1126/science.270.5239.1166.

Ishihara, H. *et al.* (1994) 'Overexpression of hexokinase I but not GLUT1 glucose transporter alters concentration dependence of glucose-stimulated insulin secretion in pancreatic β-cell line MIN6', *Journal of Biological Chemistry*. J Biol Chem, 269(4), pp. 3081–3087. doi: 10.1016/s0021-9258(17)42050-3.

Ishihara, H. *et al.* (1999) 'Overexpression of monocarboxylate transporter and lactate dehydrogenase alters insulin secretory responses to pyruvate and lactate in β cells', *Journal of Clinical Investigation*. The American Society for Clinical Investigation, 104(11), pp. 1621–1629. doi: 10.1172/JCI7515.

Jacobson, D. A. *et al.* (2010) 'Calcium-activated and voltage-gated potassium channels of the pancreatic islet impart distinct and complementary roles during secretagogue induced electrical responses', *Journal of Physiology*. J Physiol, 588(18), pp. 3525–3537. doi: 10.1113/jphysiol.2010.190207.

James, D. E. *et al.* (1988) ‘Insulin-regulatable tissues express a unique insulin-sensitive glucose transport protein’, *Nature*, 333(6169), pp. 183–185. doi: 10.1038/333183a0.

Jarvis, S. *et al.* (2020) ‘A Comparison of Low Read Depth QuantSeq 3′ Sequencing to Total RNA-Seq in FUS Mutant Mice’, *Frontiers in Genetics*. Frontiers Media S.A., 11, p. 1412. doi: 10.3389/FGENE.2020.562445/BIBTEX.

Jennings, R. E. *et al.* (2015) ‘Human pancreas development’, *Development (Cambridge)*, 142(18), pp. 3126–3137. doi: 10.1242/dev.120063.

Jewell, J. L., Oh, E. and Thurmond, D. C. (2010) ‘Exocytosis mechanisms underlying insulin release and glucose uptake: conserved roles for Munc18c and syntaxin 4.’, *American journal of physiology. Regulatory, integrative and comparative physiology*, 298(3), pp. R517-31. doi: 10.1152/ajpregu.00597.2009.

Jing, X. *et al.* (2005) ‘CaV2.3 calcium channels control second-phase insulin release’, *Journal of Clinical Investigation*. American Society for Clinical Investigation, 115(1), pp. 146–154. doi: 10.1172/jci22518.

Johnston, N. R. *et al.* (2016) ‘Beta Cell Hubs Dictate Pancreatic Islet Responses to Glucose’, *Cell Metabolism*. Cell Press, 24(3), pp. 389–401. doi: 10.1016/j.cmet.2016.06.020.

Jouvet, N. and Estall, J. (2021) ‘Expression of a tetracycline-controlled transactivator (Tet-On/Off system) in beta cells reduces insulin expression and secretion in mice’, *bioRxiv*. Cold Spring Harbor Laboratory, p.

2021.02.10.430692. doi: 10.1101/2021.02.10.430692.

Kahn, S. E. (2003) ‘The relative contributions of insulin resistance and beta-cell dysfunction to the pathophysiology of Type 2 diabetes’, *Diabetologia*, 46(1), pp. 3–19. doi: 10.1007/s00125-002-1009-0.

Kaihara, K. A. *et al.* (2013) ‘β-cell-specific protein kinase A activation enhances the efficiency of glucose control by increasing acute-phase insulin secretion’, *Diabetes*. Diabetes, 62(5), pp. 1527–1536. doi: 10.2337/db12-1013.

Kaprio, J. *et al.* (1992) ‘Concordance for Type 1 (insulin-dependent) and Type 2 (non-insulin-dependent) diabetes mellitus in a population-based cohort of twins in Finland’, *Diabetologia*, 35(11), pp. 1060–1067. doi: 10.1007/BF02221682.

Keahey, H. H. *et al.* (1989) ‘Characterization of voltage-dependent Ca2+ channels in β-cell line’, *Diabetes*. American Diabetes Association, 38(2), pp. 188–193. doi: 10.2337/diab.38.2.188.

Kitaguchi, T. *et al.* (2013) ‘Extracellular calcium influx activates adenylate cyclase 1 and potentiates insulin secretion in MIN6 cells’, *Biochemical Journal*. Portland Press Ltd, 450(2), pp. 365–373. doi: 10.1042/BJ20121022.

Klip, A., McGraw, T. E. and James, D. E. (2019) ‘Thirty sweet years of GLUT4’, *Journal of Biological Chemistry*, 294(30), pp. 11369–11381. doi: 10.1074/jbc.REV119.008351.

de Kloet, E. R. *et al.* (2019) ‘Top-down and bottom-up control of stress-coping’, *Journal of Neuroendocrinology*. Blackwell Publishing Ltd, 31(3), p. e12675. doi: 10.1111/jne.12675.

Kohn, A. D., Kovacina, K. S. and Roth, R. A. (1995) ‘Insulin stimulates the kinase activity of RAC-PK, a pleckstrin homology domain containing ser/thr kinase.’, *The EMBO Journal*. Wiley, 14(17), pp. 4288–4295. doi: 10.1002/j.1460-2075.1995.tb00103.x.

Kohrt, W. M. *et al.* (1993) ‘Insulin resistance in aging is related to abdominal obesity’, *Diabetes*, 42(2), pp. 273–281. doi: 10.2337/diab.42.2.273.

Koizumi, M. and Yada, T. (2008) ‘Sub-chronic stimulation of glucocorticoid receptor impairs and mineralocorticoid receptor protects cytosolic Ca2+ responses to glucose in pancreatic β-cells’, *Journal of Endocrinology*, 197(2), pp. 221–229. doi: 10.1677/JOE-07-0462.

Kojima, M. *et al.* (1999) ‘Ghrelin is a growth-hormone-releasing acylated peptide from stomach’, *Nature*. Nature Publishing Group, 402(6762), pp. 656–660. doi: 10.1038/45230.

Konstantinova, I. *et al.* (2007) ‘EphA-Ephrin-A-Mediated β Cell Communication Regulates Insulin Secretion from Pancreatic Islets’, *Cell*. Cell Press, 129(2), pp. 359–370. doi: 10.1016/j.cell.2007.02.044.

Koprulu, M. *et al.* (2022) ‘Identification of Rare Loss-of-Function Genetic Variation Regulating Body Fat Distribution’, *Journal of Clinical Endocrinology and Metabolism*. J Clin Endocrinol Metab, 107(4), pp. 1065–1077. doi: 10.1210/clinem/dgab877.

Kotelevtsev, Y. *et al.* (1997) ‘11β-Hydroxysteroid dehydrogenase type 1 knockout mice show attenuated glucocorticoid-inducible responses and resist

hyperglycemia on obesity or stress', *Proceedings of the National Academy of Sciences of the United States of America*. National Academy of Sciences, 94(26), pp. 14924–14929. doi: 10.1073/pnas.94.26.14924.

Kreymann, B. *et al.* (1987) 'GLUCAGON-LIKE PEPTIDE-1 7-36: A PHYSIOLOGICAL INCRETIN IN MAN', *The Lancet*, 330(8571), pp. 1300–1304. doi: 10.1016/S0140-6736(87)91194-9.

Kulkarni, R. R. N. R. R. N. *et al.* (1999) '… in Pancreatic Cells Creates an Insulin Secretory Defect Similar to that in Type 2 Diabetes', *Cell-Cambridge Ma-*, 96, pp. 329–339. doi: 10.1016/S0092-8674(00)80546-2.

Kycia, I. *et al.* (2018) 'A Common Type 2 Diabetes Risk Variant Potentiates Activity of an Evolutionarily Conserved Islet Stretch Enhancer and Increases C2CD4A and C2CD4B Expression', *American Journal of Human Genetics*, 102(4), pp. 620–635. doi: 10.1016/j.ajhg.2018.02.020.

Lakhtakia, R. (2013) *The history of diabetes mellitus*, *Sultan Qaboos University Medical Journal*. Sultan Qaboos University. doi: 10.12816/0003257.

Lambillotte, C., Gilon, P. and Henquin, J. C. (1997) 'Direct glucocorticoid inhibition of insulin secretion: An in vitro study of dexamethasone effects in mouse islets', *Journal of Clinical Investigation*. American Society for Clinical Investigation, 99(3), pp. 414–423. doi: 10.1172/JCI119175.

Landa, L. R. J. *et al.* (2005) 'Interplay of Ca2+ and cAMP signaling in the insulin-secreting MIN6 beta-cell line.', *The Journal of biological chemistry*, 280(35), pp. 31294–31302. doi: 10.1074/jbc.M505657200.Interplay.

Larsson, L. I. *et al.* (1979) ‘Somatostatin cell processes as pathways for paracrine secretion’, *Science*. Science, 205(4413), pp. 1393–1395. doi: 10.1126/science.382360.

Lim, E. L. *et al.* (2011) ‘Reversal of type 2 diabetes: Normalisation of beta cell function in association with decreased pancreas and liver triacylglycerol’, *Diabetologia*, 54(10), pp. 2506–2514. doi: 10.1007/s00125-011-2204-7.

Lindquist, C. *et al.* (2019) ‘A mitochondria-targeted fatty acid analogue influences hepatic glucose metabolism and reduces the plasma insulin/glucose ratio in male Wistar rats’, *PLoS ONE*. Public Library of Science, 14(9). doi: 10.1371/JOURNAL.PONE.0222558.

Liu, Y. J. *et al.* (1996) ‘Crosstalk between the cAMP and inositol trisphosphate-signalling pathways in pancreatic β-cells’, *Archives of Biochemistry and Biophysics*. Academic Press Inc., 334(2), pp. 295–302. doi: 10.1006/abbi.1996.0458.

Lu, N. Z. and Cidlowski, J. A. (2005) ‘Translational regulatory mechanisms generate N-terminal glucocorticoid receptor isoforms with unique transcriptional target genes’, *Molecular Cell*. Elsevier, 18(3), pp. 331–342. doi: 10.1016/j.molcel.2005.03.025.

Luger, A. L. *et al.* (2018) ‘Doxycycline impairs mitochondrial function and protects human glioma cells from hypoxia-induced cell death: Implications of using tet-inducible systems’, *International Journal of Molecular Sciences*. Int J Mol Sci, 19(5). doi: 10.3390/ijms19051504.

MA, R. *et al.* (2005) ‘Loss of connexin36 channels alters beta-cell coupling, islet synchronization of glucose-induced Ca2+ and insulin oscillations, and basal insulin release’, *Diabetes*. Diabetes, 54(6), pp. 1798–1807. doi: 10.2337/DIABETES.54.6.1798.

MacDonald, P. E., Joseph, J. W. and Rorsman, P. (2005) ‘Glucose-sensing mechanisms in pancreatic β-cells’, *Philosophical Transactions of the Royal Society B: Biological Sciences*, 360(1464), pp. 2211–2225. doi: 10.1098/rstb.2005.1762.

Makimura, H. *et al.* (2003) ‘Role of glucocorticoids in mediating effects of fasting and diabetes on hypothalamic gene expression’, *BMC Physiology*. BioMed Central, 3(1), pp. 1–13. doi: 10.1186/1472-6793-3-1.

Malhotra, J. D. *et al.* (2008) ‘Antioxidants reduce endoplasmic reticulum stress and improve protein secretion’, *Proceedings of the National Academy of Sciences of the United States of America*, 105(47), pp. 18525–18530. doi: 10.1073/pnas.0809677105.

McCulloch, L. J. *et al.* (2011) ‘GLUT2 (SLC2A2) is not the principal glucose transporter in human pancreatic beta cells: Implications for understanding genetic association signals at this locus’, *Molecular Genetics and Metabolism*. Academic Press, 104(4), pp. 648–653. doi: 10.1016/j.ymgme.2011.08.026.

Mehta, Z. B. *et al.* (2016) ‘Changes in the expression of the type 2 diabetes-associated gene VPS13C in the β-cell are associated with glucose intolerance in humans and mice’, *American Journal of Physiology - Endocrinology and Metabolism*, 311(2), pp. E488–E507. doi: 10.1152/ajpendo.00074.2016.

Mergenthaler, P. *et al.* (2013) ‘Sugar for the brain: The role of glucose in physiological and pathological brain function’, *Trends in Neurosciences*, 36(10), pp. 587–597. doi: 10.1016/j.tins.2013.07.001.

Mertz, R. J. *et al.* (1996) ‘Activation of stimulus-secretion coupling in pancreatic β-cells by specific products of glucose metabolism: Evidence for privileged signaling by glycolysis’, *Journal of Biological Chemistry*. American Society for Biochemistry and Molecular Biology, 271(9), pp. 4838–4845. doi: 10.1074/jbc.271.9.4838.

van der Meulen, T. *et al.* (2017) ‘Virgin Beta Cells Persist throughout Life at a Neogenic Niche within Pancreatic Islets’, *Cell Metabolism*. Cell Press, 25(4), pp. 911-926.e6. doi: 10.1016/j.cmet.2017.03.017.

Milo-Landesman, D. *et al.* (2001) ‘Correction of hyperglycemia in diabetic mice transplanted with reversibly immortalized pancreatic β cells controlled by the tet-on regulatory system’, *Cell Transplantation*. Cognizant Communication Corporation, 10(7), pp. 645–650. doi: 10.3727/000000001783986422.

Mojsov, S., Weir, G. C. and Habener, J. F. (1987) ‘Insulinotropin: Glucagon-like peptide I (7-37) co-encoded in the glucagon gene is a potent stimulator of insulin release in the perfused rat pancreas’, *Journal of Clinical Investigation*, 79(2), pp. 616–619. doi: 10.1172/JCI112855.

Morgan, S. A. *et al.* (2014) ‘11β-HSD1 is the major regulator of the tissue-specific effects of circulating glucocorticoid excess’, *Proceedings of the National Academy of Sciences of the United States of America*, 111(24). doi: 10.1073/pnas.1323681111.

Mousavy Gharavy, S. N. *et al.* (2021) ‘Sexually dimorphic roles for the type 2 diabetes-associated C2cd4b gene in murine glucose homeostasis’, *Diabetologia*. Springer Science and Business Media Deutschland GmbH, 64(4), pp. 850–864. doi: 10.1007/s00125-020-05350-x.

Mühlemann, M. (2018) *Intestinal stem cells and the Na+-D-Glucose Transporter SGLT1: potential targets regarding future therapeutic strategies for diabetes*.

Munck, A. and Náray-Fejes-Tóth, A. (1992) ‘The ups and downs of glucocorticoid physiology Permissive and suppressive effects revisited’, *Molecular and Cellular Endocrinology*. Elsevier, 90(1), pp. C1–C4. doi: 10.1016/0303-7207(92)90091-J.

Murphy, M. P. (2013) ‘Mitochondrial dysfunction indirectly elevates ROS production by the endoplasmic reticulum’, *Cell Metabolism*. Cell Press, pp. 145–146. doi: 10.1016/j.cmet.2013.07.006.

Nasteska, D. *et al.* (2021) ‘PDX1LOW MAFALOW β-cells contribute to islet function and insulin release’, *Nature Communications*. Nature Research, 12(1). doi: 10.1038/s41467-020-20632-z.

Ng, J. M. *et al.* (2012) ‘PET imaging reveals distinctive roles for different regional adipose tissue depots in systemic glucose metabolism in nonobese humans’, *American Journal of Physiology - Endocrinology and Metabolism*. Am J Physiol Endocrinol Metab, 303(9). doi: 10.1152/ajpendo.00282.2012.

Nikolaev, V. O. *et al.* (2004) ‘Novel single chain cAMP sensors for receptor-induced signal propagation’, *Journal of Biological Chemistry*. American Society

for Biochemistry and Molecular Biology, 279(36), pp. 37215–37218. doi: 10.1074/jbc.C400302200.

Nuñez, F. J. *et al.* (2020) ‘Glucocorticoids rapidly activate cAMP production via Gαs to initiate non-genomic signaling that contributes to one-third of their canonical genomic effects’, *FASEB Journal*, 34(2), pp. 2882–2895. doi: 10.1096/fj.201902521R.

Oakley, R. H. and Cidlowski, J. A. (2011) ‘Cellular processing of the glucocorticoid receptor gene and protein: New mechanisms for generating tissue-specific actions of glucocorticoids’, *Journal of Biological Chemistry*. Elsevier, pp. 3177–3184. doi: 10.1074/jbc.R110.179325.

Oates, P. (2008) ‘Aldose Reductase, Still a Compelling Target for Diabetic Neuropathy’, *Current Drug Targets*, 9(1), pp. 14–36. doi: 10.2174/138945008783431781.

Offield, M. F. *et al.* (1996) ‘PDX-1 is required for pancreatic outgrowth and differentiation of the rostral duodenum’, *Development*, 122(3), pp. 983–995.

Ogawa, A. *et al.* (1992) ‘Roles of insulin resistance and β-cell dysfunction in dexamethasone- induced diabetes’, *Journal of Clinical Investigation*. American Society for Clinical Investigation, 90(2), pp. 497–504. doi: 10.1172/JCI115886.

Ohneda, A., Kobayashi, T. and Nihei, J. (1983) ‘Effects of Ca Antaǵonists, Nifedipine, Niludipine and Verapamil, on Endocrine Function of the Pancreas’, *Tohoku Journal of Experimental Medicine*. Tohoku J Exp Med, 140(2), pp. 153–159. doi: 10.1620/tjem.140.153.

Olofsson, C. S. *et al.* (2002) ‘Fast insulin secretion reflects exocytosis of docked granules in mouse pancreatic B-cells’, *Pflugers Archiv European Journal of Physiology*. Springer, 444(1–2), pp. 43–51. doi: 10.1007/s00424-002-0781-5.

Orci, L. *et al.* (1987) ‘Proteolytic maturation of insulin is a post-Golgi event which occurs in acidifying clathrin-coated secretory vesicles’, *Cell*. Cell Press, 49(6), pp. 865–868. doi: 10.1016/0092-8674(87)90624-6.

Ortsäter, H. *et al.* (2005) ‘Regulation of 11β-hydroxysteroid dehydrogenase type 1 and glucose-stimulated insulin secretion in pancreatic islets of langerhans’, *Diabetes/Metabolism Research and Reviews*, 21(4), pp. 359–366. doi: 10.1002/dmrr.525.

Patel, Y. C. (1999) ‘Somatostatin and its receptor family’, *Frontiers in Neuroendocrinology*. Academic Press Inc., 20(3), pp. 157–198. doi: 10.1006/frne.1999.0183.

Pemberton, P. A. *et al.* (1988) ‘Hormone binding globulins undergo serpin conformational change in inflammation’, *Nature*. Nature Publishing Group, 336(6196), pp. 257–258. doi: 10.1038/336257a0.

Phillips, D. I. W. *et al.* (1996) ‘Intramuscular triglyceride and muscle insulin sensitivity: Evidence for a relationship in nondiabetic subjects’, *Metabolism: Clinical and Experimental*. W.B. Saunders, 45(8), pp. 947–950. doi: 10.1016/S0026-0495(96)90260-7.

Pipeleers, D. G. (1992) ‘Heterogeneity in pancreatic β-cell population’, *Diabetes*. Diabetes, pp. 777–781. doi: 10.2337/diabetes.41.7.777.

Pradhan, A. D. *et al.* (2001) ‘C-reactive protein, interleukin 6, and risk of developing type 2 diabetes mellitus’, *Journal of the American Medical Association*. American Medical Association, 286(3), pp. 327–334. doi: 10.1001/jama.286.3.327.

Pullen, T. J. *et al.* (2012) ‘Overexpression of monocarboxylate transporter-1 (Slc16a1) in mouse pancreatic β-cells leads to relative hyperinsulinism during exercise’, *Diabetes*. Diabetes, 61(7), pp. 1719–1725. doi: 10.2337/db11-1531.

Pullen, T. J., Huising, M. O. and Rutter, G. A. (2017) ‘Analysis of purified pancreatic islet beta and alpha cell transcriptomes reveals 11β-hydroxysteroid dehydrogenase (Hsd11b1) as a novel disallowed gene’, *Frontiers in Genetics*. Frontiers Research Foundation, 8(APR), p. 41. doi: 10.3389/fgene.2017.00041.

Puri, S. *et al.* (2018) ‘Replication confers β cell immaturity’, *Nature Communications*. Springer US, 9(1). doi: 10.1038/s41467-018-02939-0.

Quarta, C. *et al.* (2017) ‘Molecular Integration of Incretin and Glucocorticoid Action Reverses Immunometabolic Dysfunction and Obesity’, *Cell Metabolism*. Cell Metab, 26(4), pp. 620-632.e6. doi: 10.1016/j.cmet.2017.08.023.

Quintens, R. *et al.* (2008) ‘Why expression of some genes is disallowed in β-cells’, in *Biochemical Society Transactions*. Biochem Soc Trans, pp. 300–305. doi: 10.1042/BST0360300.

Rafacho, A. *et al.* (2010) ‘Glucocorticoids in vivo induce both insulin hypersecretion and enhanced glucose sensitivity of stimulus-secretion coupling in isolated rat islets’, *Endocrinology*. Oxford Academic, 151(1), pp. 85–95. doi:

10.1210/en.2009-0704.

Ramamoorthy, S. and Cidlowski, J. A. (2016) ‘Corticosteroids. Mechanisms of Action in Health and Disease’, *Rheumatic Disease Clinics of North America*. W.B. Saunders, pp. 15–31. doi: 10.1016/j.rdc.2015.08.002.

Ravier, M., Sehlin, J. and Henquin, J. (2002) ‘Disorganization of cytoplasmic Ca2+ oscillations and pulsatile insulin secretion in islets from ob/ob mice’, *Diabetologia*. Diabetologia, 45(8), pp. 1154–1163. doi: 10.1007/s00125-002-0883-9.

Rehackova, L. *et al.* (2017) ‘Acceptability of a very-low-energy diet in Type 2 diabetes: patient experiences and behaviour regulation’, *Diabetic Medicine*. Blackwell Publishing Ltd, 34(11), pp. 1554–1567. doi: 10.1111/dme.13426.

Rodriguez-Diaz, R. *et al.* (2018) ‘Paracrine Interactions within the Pancreatic Islet Determine the Glycemic Set Point’, *Cell Metabolism*. Cell Press, 27(3), pp. 549-558.e4. doi: 10.1016/j.cmet.2018.01.015.

Rorsman, P. and Ashcroft, F. M. (2018) ‘Pancreatic β-cell electrical activity and insulin secretion: Of mice and men’, *Physiological Reviews*. American Physiological Society, 98(1), pp. 117–214. doi: 10.1152/physrev.00008.2017.

Rorsman, P. and Huising, M. O. (2018) ‘The somatostatin-secreting pancreatic δ-cell in health and disease’, *Nature Reviews Endocrinology*. Nature Publishing Group, 14(7), pp. 404–414. doi: 10.1038/s41574-018-0020-6.

Roth, B. L. (2016) ‘DREADDs for Neuroscientists.’, *Neuron*, 89(4), pp. 683–694. doi: 10.1016/j.neuron.2016.01.040.

Saeedi, P. *et al.* (2019) ‘Global and regional diabetes prevalence estimates for 2019 and projections for 2030 and 2045: Results from the International Diabetes Federation Diabetes Atlas, 9th edition’, *Diabetes Research and Clinical Practice*, 157. doi: 10.1016/j.diabres.2019.107843.

Salehi, A. *et al.* (2007) ‘Pulses of somatostatin release are slightly delayed compared with insulin and antisynchronous to glucagon’, *Regulatory Peptides*, 144(1–3), pp. 43–49. doi: 10.1016/j.regpep.2007.06.003.

Salinno, C. *et al.* (2019) ‘β-Cell Maturation and Identity in Health and Disease’, *International Journal of Molecular Sciences*. Multidisciplinary Digital Publishing Institute (MDPI), 20(21). doi: 10.3390/ijms20215417.

Samols, E., Marri, G. and Marks, V. (1965) ‘Promotion of Insulin Secretion By Glucagon’, *The Lancet*, 286(7409), pp. 415–416. doi: 10.1016/S0140-6736(65)90761-0.

Sanger, F. (1959) ‘Chemistry of insulin’, *Science*. American Association for the Advancement of Science, 129(3359), pp. 1340–1344. doi: 10.1126/science.129.3359.1340.

Schiller, B. J. *et al.* (2014) ‘Glucocorticoid receptor binds half sites as a monomer and regulates specific target genes’, *Genome Biology*. BioMed Central Ltd., 15(7), p. 418. doi: 10.1186/s13059-014-0418-y.

Segerstolpe, Å. *et al.* (2016) ‘Single-Cell Transcriptome Profiling of Human Pancreatic Islets in Health and Type 2 Diabetes’, *Cell Metabolism*. Cell Press, 24(4), pp. 593–607. doi: 10.1016/j.cmet.2016.08.020.

Sharma, L., Lu, J. and Bai, Y. (2009) ‘Mitochondrial Respiratory Complex I: Structure, Function and Implication in Human Diseases’, *Current Medicinal Chemistry*. Bentham Science Publishers Ltd., 16(10), pp. 1266–1277. doi: 10.2174/092986709787846578.

Shen, C. N. *et al.* (2003) ‘Glucocorticoids suppress β-cell development and induce hepatic metaplasia in embryonic pancreas’, *Biochemical Journal*. Portland Press Ltd, 375(1), pp. 41–50. doi: 10.1042/BJ20030140.

Shibasaki, T. *et al.* (2007) ‘Essential role of Epac2/Rap1 signaling in regulation of insulin granule dynamics by cAMP’, *Proceedings of the National Academy of Sciences of the United States of America*. National Academy of Sciences, 104(49), pp. 19333–19338. doi: 10.1073/pnas.0707054104.

Shulman, G. I. (2000) ‘Cellular mechanisms of insulin resistance’, *Journal of Clinical Investigation*, pp. 171–176. doi: 10.1172/JCI10583.

Smith, S. *et al.* (2022) ‘Prevention and Management Strategies for Diabetic Neuropathy’, *Life 2022, Vol. 12, Page 1185*. Multidisciplinary Digital Publishing Institute, 12(8), p. 1185. doi: 10.3390/LIFE12081185.

Speier, S. *et al.* (2007) ‘Cx36-mediated coupling reduces β-cell heterogeneity, confines the stimulating glucose concentration range, and affects insulin release kinetics’, *Diabetes*, 56(4), pp. 1078–1086. doi: 10.2337/db06-0232.

Stamateris, R. E. *et al.* (2013) ‘Adaptive β-cell proliferation increases early in high-fat feeding in mice, concurrent with metabolic changes, with induction of islet cyclin D2 expression’, *American Journal of Physiology - Endocrinology and*

Metabolism. American Physiological Society, 305(1), p. E149. doi: 10.1152/ajpendo.00040.2013.

Steiner, D. F. *et al.* (1967) 'Insulin biosynthesis: Evidence for a precursor', *Science*. American Association for the Advancement of Science, 157(3789), pp. 697–700. doi: 10.1126/science.157.3789.697.

Steiner, D. F. and Oyer, P. E. (1967) *the Biosynthesis of Insulin and a Probable Precursor of Insulin By a Human Islet Cell Adenoma*, *Proceedings of the National Academy of Sciences*. doi: 10.1073/pnas.57.2.473.

Steiner, D. J. *et al.* (2010) 'Pancreatic islet plasticity: Interspecies comparison of islet architecture and composition', *Islets*. Landes Bioscience, p. 135. doi: 10.4161/isl.2.3.11815.

Sun, Z.-Y. *et al.* (2021) 'Functional maturation of immature β cells: A roadblock for stem cell therapy for type 1 diabetes.', *World journal of stem cells*, 13(3), pp. 193–207. doi: 10.4252/wjsc.v13.i3.193.

Swali, A. *et al.* (2008) '11β-Hydroxysteroid dehydrogenase type 1 regulates insulin and glucagon secretion in pancreatic islets', *Diabetologia*, 51(11), pp. 2003–2011. doi: 10.1007/s00125-008-1137-2.

Talchai, C. *et al.* (2012) 'Pancreatic β cell dedifferentiation as a mechanism of diabetic β cell failure', *Cell*. Elsevier B.V., 150(6), pp. 1223–1234. doi: 10.1016/j.cell.2012.07.029.

Taylor, R. (2013) 'Type 2 diabetes: Etiology and reversibility', *Diabetes Care*. Diabetes Care, pp. 1047–1055. doi: 10.2337/dc12-1805.

Thomas, M. K. *et al.* (2021) ‘Dual GIP and GLP-1 Receptor Agonist Tirzepatide Improves Beta-cell Function and Insulin Sensitivity in Type 2 Diabetes’, *Journal of Clinical Endocrinology and Metabolism*. J Clin Endocrinol Metab, 106(2), pp. 388–396. doi: 10.1210/clinem/dgaa863.

Thorens, B. *et al.* (1988) *Cloning and Functional Expression in Bacteria of a Novel Glucose Transporter Present in Liver, Intestine, Kidney, and P-Pancreatic Islet Cells*, *Cell*.

Thorrez, L. *et al.* (2011) ‘Tissue-specific disallowance of housekeeping genes: The other face of cell differentiation’, *Genome Research*. Genome Res, 21(1), pp. 95–105. doi: 10.1101/gr.109173.110.

Tian, G. *et al.* (2015) ‘Impaired cAMP generation contributes to defective glucose-stimulated insulin secretion after long-term exposure to palmitate’, *Diabetes*. American Diabetes Association Inc., 64(3), pp. 904–915. doi: 10.2337/db14-1036.

Tomita, T. *et al.* (1989) ‘Protein meal-stimulated pancreatic polypeptide secretion in prader-willi syndrome of adults’, *Pancreas*, 4(4), pp. 395–400. doi: 10.1097/00006676-198908000-00001.

Tomlinson, J. W., Walker, E. A., *et al.* (2004) ‘11β-Hydroxysteroid dehydrogenase type 1: A tissue-specific regulator of glucocorticoid response’, *Endocrine Reviews*. Oxford Academic, pp. 831–866. doi: 10.1210/er.2003-0031.

Tomlinson, J. W., Moore, J. S., *et al.* (2004) ‘Weight loss increases 11β-

hydroxysteroid dehydrogenase type 1 expression in human adipose tissue', in *Journal of Clinical Endocrinology and Metabolism*. J Clin Endocrinol Metab, pp. 2711–2716. doi: 10.1210/jc.2003-031376.

Tun, S. B. B. *et al.* (2020) 'Islet Transplantation to the Anterior Chamber of the Eye—A Future Treatment Option for Insulin-Deficient Type-2 Diabetics? A Case Report from a Nonhuman Type-2 Diabetic Primate', *Cell Transplantation*, 29, pp. 1–9. doi: 10.1177/0963689720913256.

Turban, S. *et al.* (2012) 'Optimal elevation of β-cell 11β-hydroxysteroid dehydrogenase type 1 is a compensatory mechanism that prevents high-fat diet-induced β-cell failure', *Diabetes*. American Diabetes Association, 61(3), pp. 642–652. doi: 10.2337/db11-1054.

Ullrich, A. *et al.* (1985) 'Human insulin receptor and its relationship to the tyrosine kinase family of oncogenes', *Nature*. Nature, 313(6005), pp. 756–761. doi: 10.1038/313756a0.

Valdeolmillos, M. *et al.* (1989) 'Glucose-induced oscillations of intracellular Ca2+ concentration resembling bursting electrical activity in single mouse islets of Langerhans', *FEBS Letters*, 259(1), pp. 19–23. doi: 10.1016/0014-5793(89)81484-X.

Villamayor, L. *et al.* (2018) 'GATA6 controls insulin biosynthesis and secretion in adult β-cells', *Diabetes*. American Diabetes Association Inc., 67(3), pp. 448–460. doi: 10.2337/db17-0364.

Walker, J. J. *et al.* (2012) 'The origin of glucocorticoid hormone oscillations',

PLoS Biology. Edited by A. J. Vidal-Puig. Public Library of Science, 10(6), p. e1001341. doi: 10.1371/journal.pbio.1001341.

Wang, Z. *et al.* (1995) 'Glucagon-like peptide-1 is a physiological incretin in rat', *Journal of Clinical Investigation*, 95(1), pp. 417–421. doi: 10.1172/jci117671.

Weiss, M. A. *et al.* (1990) 'NMR and Photo-CIDNP Studies of Human Proinsulin and Prohormone Processing Intermediates with Application to Endopeptidase Recognition', *Biochemistry*. American Chemical Society, 29(36), pp. 8389–8401. doi: 10.1021/bi00488a028.

Williams, R. *et al.* (2020) 'Global and regional estimates and projections of diabetes-related health expenditure: Results from the International Diabetes Federation Diabetes Atlas, 9th edition', *Diabetes Research and Clinical Practice*, p. 108072. doi: 10.1016/j.diabres.2020.108072.

Wollheim, C. B. and Maechler, P. (2015) 'Beta cell glutamate receptor antagonists: novel oral antidiabetic drugs?', *Nature Medicine 2015 21:4*. Nature Publishing Group, 21(4), pp. 310–311. doi: 10.1038/nm.3835.

Wollheim, C. B. and Sharp, G. W. G. (1981) *Regulation of Insulin Release by Calcium*, *PHYSIOLOGICAL REVIEWS*.

WS, H. *et al.* (2012) 'Connexin-36 gap junctions regulate in vivo first- and second-phase insulin secretion dynamics and glucose tolerance in the conscious mouse', *Diabetes*. Diabetes, 61(7), pp. 1700–1707. doi: 10.2337/DB11-1312.

Yada, T. *et al.* (2014) 'Ghrelin signalling in β-cells regulates insulin secretion

and blood glucose', *Diabetes, Obesity and Metabolism*. Blackwell Publishing Ltd, pp. 111–117. doi: 10.1111/dom.12344.

Yang, S. N. and Berggren, P. O. (2006) 'The role of voltage-gated calcium channels in pancreatic β-cell physiology and pathophysiology', *Endocrine Reviews*. Endocr Rev, pp. 621–676. doi: 10.1210/er.2005-0888.

Ying, W. *et al.* (2019) 'Expansion of Islet-Resident Macrophages Leads to Inflammation Affecting β Cell Proliferation and Function in Obesity', *Cell Metabolism*. Cell Press, 29(2), pp. 457-474.e5. doi: 10.1016/j.cmet.2018.12.003.

Zhou, Q. *et al.* (2008) 'In vivo reprogramming of adult pancreatic exocrine cells to β-cells', *Nature*. Nature Publishing Group, 455(7213), pp. 627–632. doi: 10.1038/nature07314.

Zhu, H. and Roth, B. L. (2014) 'Silencing Synapses with DREADDs', *Neuron*, 82(4), pp. 723–725. doi: https://doi.org/10.1016/j.neuron.2014.05.002.

Zhu, L. *et al.* (2017) 'β-Arrestin-2 is an essential regulator of pancreatic β-cell function under physiological and pathophysiological conditions', *Nature Communications*. Nature Publishing Group, 8. doi: 10.1038/ncomms14295.

Zhu, Y. and Zhang, C. (2016) 'Prevalence of Gestational Diabetes and Risk of Progression to Type 2 Diabetes: a Global Perspective', *Current Diabetes Reports*. Current Medicine Group LLC 1, pp. 1–11. doi: 10.1007/s11892-015-0699-x.

Zinselmeyer, B. H. *et al.* (2018) 'The resident macrophages in murine

pancreatic islets are constantly probing their local environment, capturing beta cell granules and blood particles', *Diabetologia*. Springer Verlag, 61(6), pp. 1374–1383. doi: 10.1007/s00125-018-4592-4.

8 APPENDIX

Tet-NORM	Tet-MAT	FC	padj	Gene ID	Description
0.000	149.336	9.582	0.0000000	Igfbpl1	insulin-like growth factor binding protein-like 1
21.363	300.484	3.867	0.0000000	Crybb3	crystallin, beta B3
75.852	384.846	2.257	0.0000000	Cox6a2	cytochrome c oxidase subunit 6A2
145.553	523.844	1.878	0.0000000	Aldh5a1	aldhehyde dehydrogenase family 5, subfamily A1
0.000	53.321	7.926	0.0000000	Tspan2os	tetraspanin 2, opposite strand
147.221	485.934	1.736	0.0000001	P2ry1	purinergic receptor P2Y, G-protein coupled 1
3.341	59.511	4.103	0.0000005	Mt3	metallothionein 3
19.793	116.694	2.792	0.0000011	Mlph	melanophilin
372.265	1221.851	1.729	0.0000025	Dhrs4	dehydrogenase/reductase (SDR family) member 4
16.708	87.171	2.346	0.0000041	Rsad2	radical S-adenosyl methionine domain containing 2
8.451	57.327	3.012	0.0000611	Gm2861	predicted gene 2861
652.165	1980.477	1.500	0.0001638	Psmd13	proteasome (prosome, macropain) 26S subunit, non-ATPase, 13
80.790	254.292	1.605	0.0001661	Nefm	neurofilament, medium polypeptide
344.965	856.874	1.331	0.0003425	Gmppb	GDP-mannose pyrophosphorylase B
8545.191	19481.212	1.201	0.0004233	Sst	somatostatin
13.446	67.682	2.641	0.0006026	Ly6h	lymphocyte antigen 6 complex, locus H
124.764	287.122	1.221	0.0006026	Smpd3	sphingomyelin phosphodiesterase 3, neutral
79.627	214.369	1.470	0.0007900	Rasgrf2	RAS protein-specific guanine nucleotide-releasing factor 2
140.929	426.084	1.540	0.0007900	Pdx1	pancreatic and duodenal homeobox 1
27.932	102.994	2.112	0.0011140	Th	tyrosine hydroxylase
4.847	36.749	3.027	0.0011408	Fmo1	flavin containing monooxygenase 1
49.302	251.438	2.123	0.0011658	Nnat	neuronatin
1.017	20.307	4.742	0.0012875	4933440M02Rik	RIKEN cDNA 4933440M02 gene
53.357	148.417	1.521	0.0014136	Spock1	sparc/osteonectin, cwcv and kazal-like domains proteoglycan 1
318.493	733.132	1.253	0.0018560	Spink10	serine peptidase inhibitor, Kazal type 10
217.197	499.695	1.155	0.0019039	Etv1	ets variant 1
37.527	113.519	1.675	0.0019039	Vps8	VPS8 CORVET complex subunit
123.983	320.818	1.350	0.0019039	Tubb2b	tubulin, beta 2B class IIB
130.782	340.200	1.429	0.0019662	Fam210b	family with sequence similarity 210, member B
955.564	1962.744	1.110	0.0027824	G6pc2	glucose-6-phosphatase, catalytic, 2
77.857	228.693	1.518	0.0029392	Rgs4	regulator of G-protein signaling 4

793.078	1947.714	1.277	0.0029392	Snhg9	small nucleolar RNA host gene 9
83.209	212.354	1.450	0.0029518	Mir5136	microRNA 5136
73.873	183.412	1.313	0.0037659	Cdkn1a	cyclin-dependent kinase inhibitor 1A (P21)
28.844	84.601	1.587	0.0038127	Dapp1	dual adaptor for phosphotyrosine and 3-phosphoinositides 1
48.822	122.902	1.456	0.0038127	Msln	Mesothelin
12.469	47.365	1.977	0.0039190	Dtx2	deltex 2, E3 ubiquitin ligase
137.193	304.315	1.302	0.0040239	Gsdma	gasdermin A
6.722	43.916	2.783	0.0040239	Gm19202	predicted gene, 19202
490.239	209.990	-1.183	0.0040239	Wnt4	wingless-type MMTV integration site family, member 4
235.245	540.486	1.248	0.0044927	Tmed3	transmembrane p24 trafficking protein 3
181.721	365.431	1.031	0.0045954	Cyb5r1	cytochrome b5 reductase 1
18.676	81.743	2.376	0.0047299	Rassf10	Ras association (RalGDS/AF-6) domain family (N-terminal) member 10
2.704	23.060	3.216	0.0047947	Pemt	phosphatidylethanolamine N-methyltransferase
2471.865	6421.197	1.411	0.0061581	Swi5	SWI5 recombination repair homolog (yeast)
336.002	125.701	-1.377	0.0066751	Mlxipl	MLX interacting protein-like
123.597	320.079	1.392	0.0080329	Trpm5	transient receptor potential cation channel, subfamily M, member 5
133.964	304.855	1.334	0.0080329	C2cd4b	C2 calcium-dependent domain containing 4B
30.694	95.863	1.677	0.0081263	Mpi	mannose phosphate isomerase
226.739	461.703	1.048	0.0101066	Banp	BTG3 associated nuclear protein
409.818	839.345	1.047	0.0146244	Gm26917	predicted gene, 26917
35.579	87.006	1.285	0.0157297	Adam32	a disintegrin and metallopeptidase domain 32
87.353	271.965	1.941	0.0157297	mt-Tv	mitochondrially encoded tRNA valine
172.236	550.966	1.806	0.0157297	mt-Tc	mitochondrially encoded tRNA cysteine
59.779	146.072	1.265	0.0157297	Lyrm9	LYR motif containing 9
673.315	1391.515	0.997	0.0157297	Slc48a1	solute carrier family 48 (heme transporter), member 1
77.326	182.594	1.204	0.0160034	Exoc7	exocyst complex component 7
199.484	529.332	1.512	0.0164206	Gm10073	predicted pseudogene 10073
10.043	60.678	2.349	0.0164206	mt-Tr	mitochondrially encoded tRNA arginine
24.339	79.602	2.265	0.0164206	Gm22748	predicted gene, 22748
2783.963	5884.072	1.034	0.0170638	Atp6ap1	ATPase, H+ transporting, lysosomal accessory protein 1
127.719	307.517	1.301	0.0171802	Fmc1	formation of mitochondrial complex V assembly factor 1
808.056	1503.041	0.989	0.0189495	Tmem215	transmembrane protein 215
257.111	495.452	0.977	0.0205957	Dad1	defender against cell death 1
21.655	62.267	1.526	0.0205957	B3galt2	UDP-Gal:betaGlcNAc beta 1,3-galactosyltransferase, polypeptide 2
15.685	47.636	1.628	0.0221830	Pkib	protein kinase inhibitor beta, cAMP dependent, testis specific
68.948	147.713	1.092	0.0255509	Gpx2	glutathione peroxidase 2

26.922	71.538	1.428	0.0311195	Glce	glucuronyl C5-epimerase
14.034	48.035	1.923	0.0320085	Ints1	integrator complex subunit 1
110.022	279.503	1.291	0.0355380	Hspbp1	HSPA (heat shock 70kDa) binding protein, cytoplasmic cochaperone 1
6.632	16.698	4.213	0.0355380	Med9os	mediator complex subunit 9, opposite strand
149.413	336.917	1.206	0.0373843	Slc16a6	solute carrier family 16 (monocarboxylic acid transporters), member 6
3475.861	6905.859	1.079	0.0418726	Rplp1	ribosomal protein, large, P1
80.524	161.817	1.072	0.0428565	Sdccag8	serologically defined colon cancer antigen 8
29.927	79.273	1.523	0.0428565	Pim2	proviral integration site 2
18.187	54.734	1.806	0.0428565	Trp53cor1	tumor protein p53 pathway corepressor 1
26.812	89.225	1.571	0.0433382	Gm30606	predicted gene, 30606
61.043	154.451	1.334	0.0442443	Psat1	phosphoserine aminotransferase 1
17.354	6.458	-3.796	0.0442443	Gm44126	predicted gene, 44126
232.824	440.542	0.972	0.0444508	Smdt1	single-pass membrane protein with aspartate rich tail 1
310.217	594.452	0.994	0.0446930	Vti1b	vesicle transport through interaction with t-SNAREs 1B
46.631	118.776	1.431	0.0475728	Dlgap1	DLG associated protein 1
6.523	31.410	2.783	0.0498757	Pde11a	phosphodiesterase 11A

Table 6 | Table of differential gene expression data showing 83 genes with a significant change in Tet-MAT vs Tet-NORM. Normalised counts displayed in the first two columns. padj = adjusted p-value. FC = fold-change. Genes of interest or those mentioned in this thesis are highlighted in blue. A positive FC indicates an upregulation in gene expression in islets from Tet-MAT mice vs those from Tet-NORM mice, whereas a negative FC suggests a downregulation.

9 PUBLICATIONS

Nasteska D, **Fine NHF**, Ashford FB, Cuozzo F, Viloria K, Smith G, Dahir A, Dawson PWJ, Lai YC, Bastidas-Ponce A, Bakhti M, Rutter GA, Fiancette R, Nano R, Piemonti L, Lickert H, Zhou Q, Akerman I, Hodson DJ. *PDX1^{LOW}MAFA^{LOW} β-cells contribute to islet function and insulin release*. Nat Commun. 2021 Jan 29;12(1):674. doi: 10.1038/s41467-020-20632-z. Erratum in: Nat Commun. 2021 Jul 20;12(1):4521. PMID: 33514698; PMCID: PMC7846747.

Mousavy Gharavy SN, Owen BM, Millership SJ, Chabosseau P, Pizza G, Martinez-Sanchez A, Tasoez E, Georgiadou E, Hu M, **Fine NHF**, Jacobson DA, Dickerson MT, Idevall-Hagren O, Montoya A, Kramer H, Mehta Z, Withers DJ, Ninov N, Gadue PJ, Cardenas-Diaz FL, Cruciani-Guglielmacci C, Magnan C, Ibberson M, Leclerc I, Voz M, Rutter GA. *Sexually dimorphic roles for the type 2 diabetes-associated C2cd4b gene in murine glucose homeostasis*. Diabetologia. 2021 Apr;64(4):850-864. doi: 10.1007/s00125-020-05350-x. Epub 2021 Jan 25. PMID: 33492421; PMCID: PMC7829492.

Viloria K, Nasteska D, Briant LJB, Heising S, Larner DP, **Fine NHF**, Ashford FB, da Silva Xavier G, Ramos MJ, Hasib A, Cuozzo F, Manning Fox JE, MacDonald PE, Akerman I, Lavery GG, Flaxman C, Morgan NG, Richardson SJ, Hewison M, Hodson DJ. *Vitamin-D-Binding Protein Contributes to the Maintenance of α Cell Function and Glucagon Secretion*. Cell Rep. 2020 Jun 16;31(11):107761. doi: 10.1016/j.celrep.2020.107761. PMID: 32553153; PMCID: PMC7302426.

Seabright AP, **Fine NHF**, Barlow JP, Lord SO, Musa I, Gray A, Bryant JA, Banzhaf M, Lavery GG, Hardie DG, Hodson DJ, Philp A, Lai YC. *AMPK activation induces mitophagy and promotes mitochondrial fission while activating TBK1 in a PINK1-Parkin independent manner*. FASEB J. 2020 May;34(5):6284-6301. doi: 10.1096/fj.201903051R. Epub 2020 Mar 22. PMID: 32201986; PMCID: PMC7212019.

Ast J, Arvaniti A, **Fine NHF**, Nasteska D, Ashford FB, Stamataki Z, Koszegi Z, Bacon A, Jones BJ, Lucey MA, Sasaki S, Brierley DI, Hastoy B, Tomas A, D'Agostino G, Reimann F, Lynn FC, Reissaus CA, Linnemann AK, D'Este E, Calebiro D, Trapp S, Johnsson K, Podewin T, Broichhagen J, Hodson DJ. *Super-resolution microscopy compatible fluorescent probes reveal endogenous glucagon-like peptide-1 receptor distribution and dynamics*. Nat Commun. 2020 Jan 24;11(1):467. doi: 10.1038/s41467-020-14309-w. Erratum in: Nat Commun. 2020 Oct 9;11(1):5160. PMID: 31980626; PMCID: PMC6981144.

Sayers SR, Beavil RL, **Fine NHF**, Huang GC, Choudhary P, Pacholarz KJ, Barran PE, Butterworth S, Mills CE, Cruickshank JK, Silvestre MP, Poppitt SD, McGill AT, Lavery GG, Hodson DJ, Caton PW. *Structure-functional changes in eNAMPT at high concentrations mediate mouse and human beta cell dysfunction in type 2 diabetes*. Diabetologia. 2020 Feb;63(2):313-323. doi: 10.1007/s00125-019-05029-y. Epub 2019 Nov 15. PMID: 31732790; PMCID: PMC6946736.

Thompson RJ, Fletcher A, Brookes K, Nieto H, Alshahrani MM, Mueller JW, Fine NHF, Hodson DJ, Boelaert K, Read ML, Smith VE, McCabe CJ.

Dimerization of the Sodium/Iodide Symporter. Thyroid. 2019 Oct;29(10):1485-1498. doi: 10.1089/thy.2019.0034. Epub 2019 Aug 30. PMID: 31310151; PMCID: PMC6797079.

Fehrentz T, Huber FME, Hartrampf N, Bruegmann T, Frank JA, **Fine NHF**, Malan D, Danzl JG, Tikhonov DB, Sumser M, Sasse P, Hodson DJ, Zhorov BS, Klöcker N, Trauner D. *Optical control of L-type Ca^{2+} channels using a diltiazem photoswitch*. Nat Chem Biol. 2018 Aug;14(8):764-767. doi: 10.1038/s41589-018-0090-8. Epub 2018 Jul 16. Erratum in Nat Chem Biol. 2021 Mar;17(3):360. PMID: 30013061.

Frank JA, Yushchenko DA, **Fine NHF**, Duca M, Citir M, Broichhagen J, Hodson DJ, Schultz C, Trauner D. *Optical control of GPR40 signalling in pancreatic β-cells*. Chem Sci. 2017 Nov 1;8(11):7604-7610. doi: 10.1039/c7sc01475a. Epub 2017 Aug 30. PMID: 29568424; PMCID: PMC5848828.

Podewin T, Ast J, Broichhagen J, **Fine NHF**, Nasteska D, Leippe P, Gailer M, Buenaventura T, Kanda N, Jones BJ, M'Kadmi C, Baneres JL, Marie J, Tomas A, Trauner D, Hoffmann-Röder A, Hodson DJ. *Conditional and Reversible Activation of Class A and B G Protein-Coupled Receptors Using Tethered Pharmacology*. ACS Cent Sci. 2018 Feb 28;4(2):166-179. doi: 10.1021/acscentsci.7b00237. Epub 2018 Jan 16. PMID: 29532016; PMCID: PMC5832994.

Fine NHF, Doig CL, Elhassan YS, Vierra NC, Marchetti P, Bugliani M, Nano R, Piemonti L, Rutter GA, Jacobson DA, Lavery GG, Hodson DJ. *Glucocorticoids Reprogram β-Cell Signaling to Preserve Insulin Secretion*. Diabetes. 2018

Feb;67(2):278-290. doi: 10.2337/db16-1356. Epub 2017 Dec 4. PMID: 29203512; PMCID: PMC5780059.

Podewin T, Broichhagen J, Frost C, Groneberg D, Ast J, Meyer-Berg H, Fine NHF, Friebe A, Zacharias M, Hodson DJ, Trauner D, Hoffmann-Röder A. *Optical control of a receptor-linked guanylyl cyclase using a photoswitchable peptidic hormone*. Chem Sci. 2017 Jun 1;8(6):4644-4653. doi: 10.1039/c6sc05044a. Epub 2017 Apr 19. PMID: 28626572; PMCID: PMC5471452.